

UCSF

UC San Francisco Electronic Theses and Dissertations

Title

The Molecular Mechanism of White-Opaque Switching in *Candida albicans*

Permalink

<https://escholarship.org/uc/item/5kr5b3vg>

Author

Zordan, Rebecca

Publication Date

2008-09-08

Peer reviewed|Thesis/dissertation

The Molecular Mechanism of White-Opaque Switching in *Candida albicans*

by

Rebecca E. Zordan

DISSERTATION

Submitted in partial satisfaction of the requirements for the degree of

DOCTOR OF PHILOSOPHY

in

BIOCHEMISTRY AND MOLECULAR BIOLOGY

in the

GRADUATE DIVISION

of the

UNIVERSITY OF CALIFORNIA, SAN FRANCISCO

Copyright 2008
by
Rebecca E. Zordan

Acknowledgments

I wish I had a profound reason to explain why I wanted to go to grad school. Really, it boils down to the fact that I like science, and I *really* like pathogenesis. The ability for microbes to wreak havoc on our bodies amazes me. Rather than become a doctor and treat people with nasty infectious diseases, I decided to go the less-nauseating route and study the pathogens in the lab. As it turns out, even though I studied a fungal pathogen, my research was far removed from pathogenesis research. Thankfully, I also really enjoy genetics, so it all worked out in the end.

I have to start by thanking my advisor, Sandy Johnson. Sandy has been an amazingly supportive mentor, both scientifically and professionally. He always had an open door and was more than willing to chat about my project. He gave me great opportunities to speak at conferences, and somehow kept trusting me with rotation students, though none of them joined the lab. Sandy also has many interests beyond the lab (squash, opera, hiking...) and actively supports the lab members taking time to pursue outside activities. I am extremely thankful for his generosity of time, resources, and opportunity during my graduate school years.

Anita Sil and Hiten Madhani were the other faculty members on my thesis committee. Their combined knowledge of yeast literature is staggering, and they have been very supportive of my research. I honestly and truly looked forward to having my thesis committee meeting every year.

Next, I have to thank the members of the Johnson Lab for making it such a great place to be. Over the years, we have all helped each other with thoughtful discussions and technical help, so I'm not going to belabor that here. The combination of

personalities and interests has generated a fun atmosphere which made the long hours in lab much more enjoyable. Matt Miller was the best rotation mentor I could have asked for – enthusiastic, knowledgeable, organized, and patient with all of my questions. Also, Matt and I enjoyed frequent impromptu sing-a-longs, though I can't vouch for how much the rest of the lab liked our singing. Sarah Green was a fellow critic of TV shows and movies, and she made a valiant effort towards trying to toughen me up. Dave Galgoczy was a great (if repetitive) story-teller, which helped pass the time. Along with Matt, Richard Bennett, Annie Tsong, Aaron Hernday, Matt Lohse, Chris Cain, and Lauren Booth are members of the mating affinity meeting, past and present. We've had many valuable brainstorming sessions over the years, and I'm glad to see many Worl-related projects will carry on. Brian Tuch, my bioinformatics and computer go-to guy, and Oliver, my white-board artwork partner, have survived my perkiness over the years. Chris Baker has been a delight to sit near because is in a perpetually good mood – there is never any drama with him. Sarah Elson and I have traveled through grad school together, and she is one of the most thoughtful people I know. In addition to being a patient cross-country ski teacher, she is also a master cake-baker. Brad Green has a wealth of random knowledge, which we put to good use on our pub trivia team. Sudarsi Desta and Jorge Mendoza are the engines that keep our lab running – grad school would have taken twice as long without them. There are other lab members, past and present, who I haven't listed here, but they also contributed to the warm environment in lab, and for that I am thankful.

I would not have survived graduate school without the company of my friends. Terri O'Brien is one of the most energetic and motivated people I know, and she has

welcomed me into her circle of local friends and family. We have had a lot of good times together, whether hiking in Chile or sitting around watching movies. Rachael Hanby Webster was the most enthusiastic cheerleader I have ever had, and I treasure the time we've spent together. I will miss our walks in the park, horribly cheesy movies, and endless hours chatting. Rachael and Dale have also fed me well over the years, and for this I am grateful. I also have to repeat my thanks to Sarah Green and Jeff Ubersax. Sarah was my brunch buddy and chick-flick companion, and she was great sounding-board when I needed to vent my frustrations. Sarah and Jeff also pseudo-adopted me, taking me in for holiday dinners and getting me into museums on their family membership. I will miss exploring the city with them. I realize the descriptions above make it sound like my social activities solely consist of eating and watching movies.... which isn't too far from the truth. But really, it's all about the company you keep, and I will miss these friends dearly.

Finally, I have to thank my family, though I don't have the words to express my gratitude to them. My parents, Barbara and Thomas Zordan, have had the greatest influence on my success in life. They taught me always to live up to my own standards and that I was capable of anything I wanted to do, with the possible exception of driving a zamboni. My brothers, Chris and David, have helped make me what I am today. They took their role as older brothers quite seriously, and though I sometimes bristle at unsolicited advice, I know that they will always be ready with a helping hand. My family is the reason I'm the science-loving, beer-drinking, music-loving, pie-baking, hockey fan that I am. I love them all.

The work described in Chapter 2 was originally published with open access as “Epigenetic properties of white–opaque switching in *Candida albicans* are based on a self-sustaining transcriptional feedback loop” Rebecca E. Zordan, David J. Galgoczy, and Alexander D. Johnson (2006) *Proceedings of the National Academy of Sciences*, 103(34): 12807-12812. © 2006 by The National Academy of Sciences. Authors need not obtain specific permission to reprint their work for inclusion in thesis dissertations. All work described was performed by Rebecca Zordan, with the exception of the chromatin immunoprecipitation experiments performed by David Galgoczy. Alexander Johnson oversaw the work.

The research described in Chapter 3 is slightly modified from its original format, where it was originally published with open access as “Interlocking transcriptional feedback loops control white-opaque switching in *Candida albicans*” Rebecca E. Zordan, Mathew G. Miller, David J. Galgoczy, Brian B. Tuch, and Alexander D. Johnson (2007) *PLoS Biology*, 5(10):e256. PLoS publications are freely available through the Creative Commons Attributions License, which allows reprints so long as the original source and authors are cited. Rebecca Zordan and Mathew Miller constructed strains, performed switching assays, and designed and tested genetic models for white-opaque switching. David Galgoczy performed the full genome chromatin immunoprecipitation experiments. Brian Tuch designed the *C. albicans* tiling microarrays used to analyze the chromatin immunoprecipitation studies. Alexander Johnson oversaw the work.

A portion of the work described in Chapter 4 was performed by Kristin Cook and Bentley Lim, two rotation students that I supervised.

The Molecular Mechanism of White-Opaque Switching

in *Candida albicans*

Rebecca E. Zordan

Abstract

White-opaque switching is a process by which the opportunistic fungal pathogen *Candida albicans* reversibly alternates between two growth states, named “white” and “opaque”. The white-opaque switch regulates over 400 genes transcriptionally, and cells in each state have different morphology, virulence properties, metabolism, and mating competency. At the time I started my work, there was minimal molecular understanding of the white-opaque switch, and my goal was to identify the genes responsible for generating the opaque state. My work identified a gene, which we named White-Opaque Regulator 1 (*WOR1*), as the master regulator of the white-opaque switch. This gene is necessary for opaque formation and ectopic expression of *WOR1* can drive cells to the opaque state, as verified through an examination of morphology, expression profiling, and behavioral tests. Northern analysis and chromatin immunoprecipitation (ChIP) assays revealed that Wor1 binds its own promoter and upregulates its own expression, forming a self-sustaining positive feedback loop.

Subsequent work sought to understand Wor1 in the context of other transcriptional regulators with known effects on white-opaque switching (*CZF1*, *EFG1*, and *WOR2*). Mutants of *CZF1*, *EFG1*, and *WOR2* were analyzed in combination with *WOR1* to define genetic epistasis relationships. This genetic analysis was combined with ChIP experiments to analyze where Wor1 was associated with chromatin across the entire

C. albicans genome. Wor1 was found to associate with the DNA upstream of each of the other regulators. Using the genetic relationships and ChIP data together, we defined a “circuit” of interlocking regulatory feedback loops that are modeled to reinforce Wor1 expression during initiation of the switch to the opaque state.

Unpublished work found that increased osmotic pressure or contact with solid surfaces can increase the frequency of white-to-opaque switching. Ongoing research focuses on purifying Wor1 for use in assays to determine if it can directly bind DNA. Together these studies enriched our understanding of the molecular control of the white-opaque switch.

Table of contents

Chapter 1.	Introduction.....	1
Chapter 2.	Epigenetic Properties of White–Opaque Switching in <i>Candida albicans</i> are Based on a Self-Sustaining Transcriptional Feedback Loop.....	9
Chapter 3.	Interlocking Transcriptional Feedback Loops Control White- Opaque Switching in <i>Candida albicans</i>	43
Chapter 4.	White-Opaque Switching in Response to Osmolites and Surface Contact.....	102
Chapter 5.	Conclusions and Future Directions.....	138
Appendix 1.	Epistasis Between Efg1 and Wor2.....	144
Appendix 2.	Strategy for Cloning and Purifying Wor1 and Wor2.....	157

List of Tables

Chapter 1. Introduction – no tables

Chapter 2. Epigenetic Properties of White–Opaque Switching in *Candida albicans* are Based on a Self-Sustaining Transcriptional Feedback Loop

Table 1. Transient ectopic expression of <i>WOR1</i> forms stable opaque colonies in a strains containing the endogenous <i>WOR1</i> genes	38
Table 2. Strains used in this study	41
Table 3. Primers used in this study	42

Chapter 3. Interlocking Transcriptional Feedback Loops Control White-Opaque Switching in *Candida albicans*

Table 1. White-opaque switching frequency in mutants lacking putative opaque-enriched transcriptional regulators.....	78
Table 2. White-to-opaque switching frequencies in strains ectopically expressing <i>CZF1</i> , <i>WOR1</i> , or <i>WOR2</i>	79
Table 3. Stability of the opaque state when ectopic expression of <i>WOR1</i> is repressed	81
Table 4. Epistasis among <i>EFG1</i> , <i>CZF1</i> , and <i>WOR2</i> in the regulation of white-opaque switching.....	82
Table S1. ORFs with Wor1 bound at the intergenic DNA upstream of their coding sequences	88
Table S2. Strains used in this study	95

Table S3. Primers used in this study	97
--	----

Chapter 4. White-Opaque Switching in Response to Osmolites and Surface Contact

Table 1. White-to-opaque switching in response to osmolites in solid media....	129
--	-----

Table 2. White-to-opaque switching after prolonged exposure to osmolites in liquid media	132
---	-----

Table 3. White-to-opaque switching on solid media with different agar concentrations	133
---	-----

Chapter 5: Conclusions and Future Directions – no tables

Appendix 1: Epistasis between Efg1 and Wor2 – no tables

Appendix 2: Strategy for Cloning and Purifying Wor1 and Wor2

Table 1. Primers used in this study	165
---	-----

Table 2. Explanation of shorthand code used to identify Wor1 and Wor2 expression constructs	166
--	-----

Table 3. Wor1 constructs in the pCR-BluntII backbone.....	168
---	-----

Table 4. Wor1 constructs in expression backbones.....	170
---	-----

Table 5. Wor2 constructs in the pCR-BluntII backbone.....	173
---	-----

Table 6. Wor2 constructs in expression backbones.....	174
---	-----

List of Figures

Chapter 1. Introduction - no figures

Chapter 2. Epigenetic Properties of White–Opaque Switching in *Candida albicans* are Based on a Self-Sustaining Transcriptional Feedback Loop

Figure 1. Alignment of Wor1 homologs across fungal species.....	33
Figure 2. Ectopic expression of <i>WOR1</i> in white cells drives the cells to the opaque phase.....	34
Figure 3. Northern and Western analysis of <i>WOR1</i> expression.....	36
Figure 4. Wor1 protein is bound to the region upstream of its gene	37
Figure 5. Ectopic expression of <i>WOR1</i> in a/α cells induces opaque-like characteristics.....	39
Figure 6. A model for a positive Wor1 feedback loop in regulation of white-opaque switching.....	40

Chapter 3. Interlocking Transcriptional Feedback Loops Control White-Opaque Switching in *Candida albicans*

Figure 1. Ectopic expression of <i>WOR1</i> drives opaque formation in <i>czf1</i> Δ / <i>czf1</i> Δ or <i>wor2</i> Δ / <i>wor2</i> Δ strains.....	80
Figure 2. Verification of mating type in <i>efg1</i> Δ / <i>efg1</i> Δ strains.....	83
Figure 3. Wor1 binds upstream of the <i>CZF1</i> , <i>WOR2</i> , <i>EFG1</i> , and <i>WOR1</i> genes.....	84
Figure 4. Model of the genetic network regulating the white-opaque switch	86

Figure 5. Activity of the white-opaque genetic regulatory network in different cell types.....	87
Figure S1. Oligo probe spacing across the <i>C. albicans</i> genome.....	99
Figure S2. Uniqueness of the probe set	100
Figure S3. GC content of the probe set.....	101

Chapter 4. White-Opaque Switching in Response to Osmolites and Surface Contact

Figure 1. White-to-opaque switching in response to osmolites in solid media ..	128
Figure 2. White-to-opaque switching in response to osmolites in liquid media: pilot.....	130
Figure 3. White-to-opaque switching after prolonged exposure to osmolites in liquid media	131
Figure 4. Colony morphology on plates with varied agar and osmolites	134
Figure 5. White-opaque switching on agarose plates	135
Figure 6. White-to-opaque switching assays in response to agarose and SD concentrations	136
Figure 7. White-to-opaque switching is dependent on calcium availability and signaling in response to contact	137

Chapter 5: Conclusions and Future Directions - no figures

Appendix 1: Epistasis between Efg1 and Wor2

Figure 1. Model of the genetic network regulating the white-opaque switch	152
Figure 2. White-to-opaque switching assays with <i>WOR2</i> ectopic expression in <i>efg1Δ/efg1Δ</i> switching strains	153
Figure 3. Colony morphology in white-opaque switching assays with <i>efg1Δ/efg1Δ</i> strains	154
Figure 4. Updated model of the genetic network regulating white-opaque switching	155
Figure 5. Activity of the white-opaque genetic regulatory network in different cell types	156

Appendix 2: Strategy for Cloning and Purifying Wor1 and Wor2

Figure 1. Cloning <i>WOR1</i> full-length and truncated alleles for expression in <i>E. coli</i>	167
Figure 2. Cloning <i>WOR2</i> full-length and truncated alleles for expression in <i>E. coli</i>	171

Chapter 1

Introduction

The Johnson Lab studies the white-opaque switch, a process by which the opportunistic fungal pathogen *C. albicans* cells can reversibly switch between two genetically identical cell types, designated “white” and “opaque”. Cells in each state can be distinguished by their cellular and colony morphology. White cells are typical round budding yeast cells, and they form white, shiny, domed colonies when grown on agar plates. In contrast, opaque cells are elongated and form darker, flatter, and duller colonies than white cells. The two states are heritable for many generations, though cells will stochastically switch between the states at a rate of one switch in every $\sim 10^3$ - 10^4 cell generations [1].

The white-opaque switch is an example of phenotypic switching, where one genome can give rise to two different cell types. This is reminiscent of tissue differentiation in higher eukaryotes, where one progenitor cell may become many different specialized tissues. In *C. albicans*, we have an advantage studying such a process, as it is a single-cell organism and genetic manipulations are comparatively easier.

Opaque cells were first observed in the clinical *C. albicans* strain WO-1 [2], and were found to have a number of different properties as compared to white cells. Electron microscopy revealed that the cell surface of opaques is covered with “pimples” or areas where a break in the cell wall enables the cell membrane to contact the environment. Early work also revealed that white and opaque cells elevated expression of certain transcripts, and monitoring the expression of *WH11* and *OP4* could aid in distinguishing white and opaque cells, respectively. Deletion and ectopic expression studies revealed that neither of these genes regulated the white-opaque switch, but they served as useful

markers for white- and opaque- transcription and began the field of transcriptional studies comparing white and opaque cells [3]. Studies also found that environmental factors could influence whether *C. albicans* grew in the white or opaque state; elevated temperatures (>30°C) drove cells to the white state, whereas oxidative stress drove cells to the opaque state [2,4].

In *C. albicans*, white and opaque cells have been shown to have different virulence properties, which may contribute to its success as an opportunistic pathogen. Many bacterial and parasitic pathogens regularly alter the proteins exposed on their surface as a way to evade the host immune system. White cells are thought to be more virulent in systemic models of infection, whereas opaque cells are more virulent than whites when grown on skin [5,6]. Also, white (but not opaque) cells release a chemical that attracts polymorphonuclear leukocytes, and host macrophage more efficiently recognize and phagocytose white cells [7,8]. Thus, the switching the opaque state may serve as a route to escape recognition by host immune cells, which has important implications in *C. albicans* virulence studies. *Candida spp.* are commensal organisms in 80% of the population and are becoming a considerable public health concern as opportunistic infections become more common. *Candida spp.* cause a variety of mucosal and invasive diseases, depending on the particular defect in the host's immune system. Candidiasis is the 4th leading cause of hospital-acquired blood stream infections (BSIs), with *C. albicans* accounting for over 60% of those infections ([9], and references therein). *Candida* BSIs are a serious concern, as they have a 34% mortality rate and patients have greater risk of contracting BSIs as the use of indwelling medical devices, such as intravenous catheters, becomes more common.

When studies of white-opaque switching began, the ability to switch was limited to a few clinical isolates, excluding the standard laboratory strain, SC5314, which was unable to form opaque cells. For many years, the molecular basis underlying this restriction was unknown. Work by Miller and Johnson [10] revealed that the ability to undergo white-opaque switching controlled by genes encoded at the mating type locus in *C. albicans*. Similar to *Saccharomyces cerevisiae*, the two mating types in *C. albicans* are designated “**a**” and “**α**” [11]. *Candida albicans* is a diploid organism, and the vast majority of clinical strains, as well as the standard lab strain, are **a/α** heterozygous at the mating type locus (MTL). The **a1-α2** heterodimer, encoded at the MTL in **a/α** cells, locks cells in the white state [10,12]. Mutating either the *a1* or *α2* genes results in cells that are able to switch to the opaque state. Opaque cells are, in fact, the mating-competent form of *C. albicans*. Each mating partner (one **a** and one **α** cell) must first switch to the opaque state before responding to mating pheromone and fusing with its partner [10,13,14]. The mating products are **a/α** tetraploid cells, which lose chromosomes in order to return to 2n chromosome number, as a part of a parasexual cycle [15,16]. Prior to understanding the MTL-based control of white-opaque switching, it had been noted that mating products could be isolated from the kidneys during a mouse model of disseminated infection; this implies that a conditions within the mouse may stimulate white-opaque switching to allow the *C. albicans* cells to mate successfully [17].

Previous hints that white and opaque cells had different transcriptional profiles, and the fact that the **a1-α2** heterodimer functions as a transcriptional repressor [11], motivated genome-wide expression studies comparing white and opaque cells. Original studies observed that roughly 400 genes were differentially transcribed between the two

cell types, though recent repetitions of these experiments have found the number to be closer to 250 genes ([18,19], personal communication with Aaron Hernday).

At the point I began my graduate work, the role of the $\alpha 1$ - $\alpha 2$ heterodimer blocking white-opaque switching and the large transcriptional changes between white and opaque cells were the few molecular clues we had towards understanding how white-opaque switching was controlled. I was interested in identifying the core genes responsible for the white-opaque switch in order to understand how such a large transcriptional change is regulated and coordinated. The work I accomplished, in collaboration with other students in the lab, is represented in Chapters 2 and 3 and Appendix 1. Additionally, I was interested in understanding molecularly how environmental stimuli are sensed and transmitted to the core switching machinery to influence white-opaque switching in response to environmental conditions; this work is described in Chapter 4. Relevant details of the background information are elaborated in the introduction to each chapter.

Ultimately, my studies identified a master regulator of white-opaque switching, which was named White-Opaque Regulator 1 (*WOR1*). *WOR1* expression is necessary for opaque formation and maintenance of *Wor1* expression (and the heritability of the opaque state) relies on a self-sustaining feedback loop, where *WOR1* reinforces its own expression. Further studies placed *WOR1* at the center of a set of nested and interlocking feedback loops with other transcriptional regulators. This work defined a naturally-occurring transcriptional network that regulates bistability in a eukaryote. Further work found that certain osmotic stimuli drive cells to the opaque state, and that known components of the osmotic signaling cascade are responsible for some, but not all of these responses. Additionally, we found that the white-opaque switch is responsive to

contact with solid surfaces, which could have implications for switching in the context of mammalian hosts.

REFERENCES

1. Rikkerink EH, Magee BB, Magee PT (1988) Opaque-white phenotype transition: a programmed morphological transition in *Candida albicans*. *J Bacteriol* 170: 895-899.
2. Slutsky B, Staebell M, Anderson J, Risen L, Pfaller M, et al. (1987) "White-opaque transition": a second high-frequency switching system in *Candida albicans*. *J Bacteriol* 169: 189-197.
3. Park YN, Strauss A, Morschhauser J (2004) The white-phase-specific gene WH11 is not required for white-opaque switching in *Candida albicans*. *Mol Genet Genomics* 272: 88-97.
4. Kolotila MP, Diamond RD (1990) Effects of neutrophils and in vitro oxidants on survival and phenotypic switching of *Candida albicans* WO-1. *Infect Immun* 58: 1174-1179.
5. Kvaal C, Lachke SA, Srikantha T, Daniels K, McCoy J, et al. (1999) Misexpression of the opaque-phase-specific gene PEP1 (SAP1) in the white phase of *Candida albicans* confers increased virulence in a mouse model of cutaneous infection. *Infect Immun* 67: 6652-6662.

6. Kvaal CA, Srikantha T, Soll DR (1997) Misexpression of the white-phase-specific gene WH11 in the opaque phase of *Candida albicans* affects switching and virulence. *Infect Immun* 65: 4468-4475.
7. Geiger J, Wessels D, Lockhart SR, Soll DR (2004) Release of a potent polymorphonuclear leukocyte chemoattractant is regulated by white-opaque switching in *Candida albicans*. *Infect Immun* 72: 667-677.
8. Lohse MB, Johnson AD (2008) Differential phagocytosis of white versus opaque *Candida albicans* by *Drosophila* and mouse phagocytes. *PLoS ONE* 3: e1473.
9. Pfaller MA, Diekema DJ (2007) Epidemiology of invasive candidiasis: a persistent public health problem. *Clin Microbiol Rev* 20: 133-163.
10. Miller MG, Johnson AD (2002) White-opaque switching in *Candida albicans* is controlled by mating-type locus homeodomain proteins and allows efficient mating. *Cell* 110: 293-302.
11. Hull CM, Johnson AD (1999) Identification of a mating type-like locus in the asexual pathogenic yeast *Candida albicans*. *Science* 285: 1271-1275.
12. Lockhart SR, Pujol C, Daniels KJ, Miller MG, Johnson AD, et al. (2002) In *Candida albicans*, white-opaque switchers are homozygous for mating type. *Genetics* 162: 737-745.
13. Bennett RJ, Uhl MA, Miller MG, Johnson AD (2003) Identification and characterization of a *Candida albicans* mating pheromone. *Mol Cell Biol* 23: 8189-8201.

14. Lockhart SR, Zhao R, Daniels KJ, Soll DR (2003) Alpha-pheromone-induced "shmooing" and gene regulation require white-opaque switching during *Candida albicans* mating. *Eukaryot Cell* 2: 847-855.
15. Bennett RJ, Johnson AD (2003) Completion of a parasexual cycle in *Candida albicans* by induced chromosome loss in tetraploid strains. *Embo J* 22: 2505-2515.
16. Magee BB, Magee PT (2000) Induction of mating in *Candida albicans* by construction of MTL α and MTL α strains. *Science* 289: 310-313.
17. Hull CM, Raisner RM, Johnson AD (2000) Evidence for mating of the "asexual" yeast *Candida albicans* in a mammalian host. *Science* 289: 307-310.
18. Tsong AE, Miller MG, Raisner RM, Johnson AD (2003) Evolution of a combinatorial transcriptional circuit: a case study in yeasts. *Cell* 115: 389-399.
19. Lan CY, Newport G, Murillo LA, Jones T, Scherer S, et al. (2002) Metabolic specialization associated with phenotypic switching in *Candida albicans*. *Proc Natl Acad Sci U S A* 99: 14907-14912.

Chapter 2

Epigenetic properties of white-opaque switching in
Candida albicans are based on a self-sustaining
transcriptional feedback loop

Epigenetic properties of white-opaque switching in *Candida albicans* are based on a self-sustaining transcriptional feedback loop

Rebecca E. Zordan^{*}, David J. Galgoczy^{*}, and Alexander D. Johnson^{*†}

^{*}Departments of Biochemistry and Biophysics and [†]Microbiology and Immunology,
University of California, 600 16th Street, San Francisco, CA 94158-2517

ABSTRACT

White-opaque switching in the human fungal pathogen *Candida albicans* is an alternation between two distinct types of cells, white and opaque. White and opaque cells differ in their appearance under the microscope, in the genes they express, in their mating behaviors, and in the host tissues for which they are best suited. Each state is heritable for many generations, and switching between states occurs stochastically, at low frequency. In this paper, we identify a master regulator of white-opaque switching (Wor1), and we show that this protein is a transcriptional regulator that is needed to both establish and maintain the opaque state. We show that in opaque cells, Wor1 forms a positive feedback loop: it binds its own DNA regulatory region and activates its own transcription leading to the accumulation of high levels of Wor1. We further show that this feedback loop is self-sustaining—once activated it persists for many generations—and we propose that this Wor1 feedback loop accounts, at least in part, for the heritability of the opaque state. In contrast, white cells (and their descendents) lack appreciable

levels of Wor1 and the feedback loop remains inactive. Thus, this simple model can account for both the heritability of the white and opaque states as well as the stochastic nature of the switching between them.

INTRODUCTION

In this paper, we examine the interconversion between two distinctive types of cells in the human fungal pathogen *Candida albicans*. This interconversion, which plays important roles in both pathogenesis and mating, exemplifies two characteristics shared by many examples of cell differentiation: the conversion from one cellular state to another is stochastic, and each state, once formed, is heritable for many generations.

The property of *C. albicans* we investigate is called white-opaque switching, and it refers to an alternation between two distinctive types of cells, white and opaque (1). White cells generally give rise to white cell progeny, but approximately every 10,000 generations, a white cell spontaneously switches to the opaque form, which will then produce opaque cell progeny for many generations (2) (3). Conversely, an opaque cell can spontaneously switch back to the white form, and the progeny of this cell will remain in the white form for many generations. Any molecular mechanism for white-opaque switching must therefore account for the ability of each state to stochastically convert to the other as well as the heritability of each state, once formed.

White and opaque cells of *C. albicans* differ in many features (for reviews, see (4) (5) (6)). They are easily distinguished under the microscope, with white cells appearing nearly spherical and opaque cells appearing larger and more elongated. When grown on agar plates, white cells form white, dome-shaped colonies whereas opaque colonies are

darker and lie flatter against the agar. Many, if not all, of the differences between white and opaque cells are due to differences in gene expression: for example, mRNAs from approximately 400 genes (~7% of the genome) are present in significantly different levels in white compared to opaque cells (7) (8). These genes cover a wide range of functions including adhesion, drug resistance, metabolism, virulence, and mating.

Although the full range of biological roles for white-opaque switching are only beginning to be appreciated, a few specific examples are well-documented. *C. albicans* can colonize many different niches in the mammalian host, and white and opaque cells differ significantly in this regard. While white cells are more suited for bloodstream infections, opaque cells are better at colonizing skin surfaces (9) (10) (11). Thus white-opaque switching provides *C. albicans* with two distinctive types of cells that interact differently with the host. White-opaque switching also has a key role in the mating of *C. albicans*. White cells mate poorly (if at all) whereas opaque cells mate with high efficiency (12). The key role of white-opaque switching in mating is also reflected by the fact that the mating-type locus of *C. albicans* controls white-opaque switching: while **a** and α cells (the mating forms) are permissive for switching, **a**/ α cells cannot switch and remain locked in the white form. This block to white-opaque switching in **a**/ α cells is mediated through the a1- α 2 heterodimer, a transcriptional repressor (12) (13).

In this paper, we investigate the molecular mechanism of white-opaque switching. We begin by identifying a master regulator of white-opaque switching, the *WOR1* gene. We show that strains deleted for *WOR1* are locked in the white form and that ectopic expression *WOR1* in white cells converts the population *en masse* to opaque cells. Ectopic *WOR1* expression can also override, at least partially, the a1- α 2 block to white-

opaque switching. We show that Wor1 protein is normally present at very low levels in white cells but accumulates to high levels in opaque cells through the action of a positive feedback loop: Wor1 binds to its own promoter and activates its own synthesis. Finally, we show that a pulse of ectopically expressed Wor1 in white cells converts the entire population to opaque cells, and that these opaque cells continue to give rise to opaque progeny for many generations after the ectopic construct has been turned off. Based on these results, we propose a simple model – a self-sustaining transcriptional feedback loop present in opaque but not white cells – that can account for the stochastic nature of white-opaque switching and for the heritability of each of the two states.

RESULTS

Identification of *WOR1* as a regulator of white-opaque switching.

In order to identify genes controlling white-opaque switching, we based our strategy on the observation that the $\alpha 1$ - $\alpha 2$ heterodimer blocks white-opaque switching (12). We therefore considered all genes repressed by $\alpha 1$ - $\alpha 2$ in white cells as candidate regulators of white-opaque switching. Six $\alpha 1$ - $\alpha 2$ repressed genes (*CEK2* (orf19.460), *STE2* (orf19.696), *FGR23* (orf19.1616), *FAR1* (orf19.7105), *CAG1* (orf19.4015), *WOR1* (orf19.4884)) were identified in our previous microarray analysis (8), and we constructed two independent knockout strains for each gene in an **a** cell background. All of the mutant strains underwent white-to-opaque switching at normal frequencies (14), as monitored by sectored colony formation (typically 2-5% of colonies show opaque sectors), except for the two strains deleted for the *WOR1* gene (based on the work in this

paper, *WOR1* was named as White-Opaque Regulator 1). These strains failed to switch; that is, they appeared locked in the white phase. In the course of this work, we examined over 6000 colonies of the *wor1Δ* strains and never observed an opaque colony or sector. Note that *C. albicans* is diploid and that construction of a knockout strain requires sequential disruption of both gene copies. For convenience, we will denote strains deleted for both copies of the *WOR1* gene simply as *wor1Δ* mutants.

WOR1 codes for a class of conserved fungal proteins that have been implicated in several biological processes but whose precise biochemical function is not known (Figure 1). For example, *Schizosaccharomyces pombe* has two proteins closely related to *WOR1*: *GTII* regulates alternative sugar uptake (15) and *PAC2* regulates sexual development (16). The *C. albicans* *WOR1* gene was previously identified (as *EAP2*) by its ability to enhance adhesiveness to polystyrene when introduced into *Saccharomyces cerevisiae*, but the basis of this effect has not been investigated (17). We show in this paper that *Wor1* is a transcriptional regulator, a result strongly suggesting that all members of this protein class share this function.

Ectopic Expression of *WOR1* converts an entire population of white cells to opaque cells.

As described in the Introduction, white **a** or α cells typically switch to the opaque form approximately once every 10,000 generations. When a copy of the *WOR1* coding region was placed under control of the *MET3* promoter (18) and its expression was induced in white **a** cells, the entire population of white cells was converted to opaque cells (Figure 2). We identify these cells as *bona fide* opaque cells by four criteria: they

have the cell shape characteristic of opaque cells (Figure 2A, 2B), they form colonies with the highly characteristic morphology of those formed by normal opaque cells (not shown), they up-regulate transcription of opaque-specific genes and down-regulate white-specific genes (Figure 2C), and they respond to mating pheromone in the way that only opaque cells do—by forming highly characteristic mating projections (14) (Figure 2D). Control experiments demonstrate that the *pMET3-WOR1* construct has no significant effect on white-opaque switching unless it is induced (Figure 2A); in addition, the nutritional conditions used to regulate the *MET3* promoter have no effect on white-opaque switching in cells that lack the *pMET3-WOR1* construct (not shown). We considered the possibility that Wor1 could also regulate hyphal growth in *C. albicans*, thereby confusing our identification of opaque cells by their increased length-to-width ratios. To test this possibility, we monitored hyphal growth in the *wor1Δ* strains on spider medium and on *YEPD* + 10% serum and found it to be normal (not shown). Thus *WOR1* is necessary for opaque cell formation but not for hyphal cell formation.

Wor1 activates its own transcription and binds to its own promoter.

When *WOR1* is expressed ectopically in white cells, transcription from the endogenous copies of *WOR1* is strongly induced, demonstrating that Wor1 activates its own transcription (Figure 3A). As indicated in the figure, the endogenous transcript is considerably larger than that produced from the *pMET3-WOR1* construct and is easily distinguished from it.

The simplest model for Wor1 activating its own transcription predicts that Wor1 binds to its own DNA regulatory region. Inspection of the Wor1 amino acid sequence

indicated that it lacks all of the conventional motifs associated with sequence-specific DNA binding or other aspects of transcriptional regulation. We therefore experimentally tested the idea that Wor1 is a transcriptional regulator of its own gene by chromatin immunoprecipitation (ChIP). Protein-DNA complexes were crosslinked in opaque cells, sheared, and precipitated using affinity-purified antibodies directed against an Wor1 peptide. As shown in Figure 4, the Wor1 protein specifically occupies several discrete positions upstream of its gene. For this experiment, all values for immunoprecipitated DNA were normalized to an *ADE2* control; the peaks of Wor1 occupancy are approximately 10-fold above both the *ADE2* values and those of the “troughs” in the *WOR1* upstream region. Control experiments demonstrate that no significant precipitation of the *WOR1* control region is observed in white **a**, **a/α**, or **a wor1Δ** cells (Figure 4).

Although we have not formally shown that Wor1 binds DNA directly, this seems likely given the multiple discrete sites of occupancy in the *WOR1* upstream region. If true, this would mean that Wor1 exemplifies a new motif for sequence-specific DNA recognition.

Wor1 Protein Accumulates to high levels in opaque cells.

The results of the ChIP experiments described above demonstrate that Wor1 occupies its own DNA regulatory region in opaque but not in white cells of the same genotype (Figure 4). A simple explanation for this finding is that Wor1 is present at much higher concentration in opaque cells than in white cells, thereby driving its DNA occupancy. As shown in Figure 3A, the *WOR1* transcript is present at higher levels in

opaque cells than white cells, a result also consistent with previous microarray experiments (7) (8). In the experiment of Figure 3B, we monitored levels of Wor1 protein by Western analysis of crude extracts prepared from a variety of white and opaque strains. Consistent with the mRNA regulation, the results clearly show that the Wor1 protein is present in much higher concentrations in opaque cells compared to white cells. The immunoblot also shows that, when induced, the *pMET3-WOR1* construct does not grossly under- or over-express the Wor1 protein. This experiment also includes a series of control experiments that unambiguously establish that the antibodies specifically recognize the Wor1 protein; these same antibodies were used in the ChIP experiments of Figure 4.

A pulse of *WOR1* expression is sufficient to stably convert white cells to opaque cells.

Our results indicate that Wor1 turns on its own transcription resulting in high levels of the protein in opaque cells. In contrast, the protein is expressed at very low levels in white cells. These observations suggest a simple model for white-opaque switching based on a positive feedback loop: in white cells, levels of Wor1 protein are below the threshold needed to activate its own synthesis; switching to opaque cells occurs when this threshold is exceeded and the feedback loop is activated. According to this model, the positive feedback loop should be self-sustaining; that is, once excited, it should persist for many generations. In this regard, the model makes two important predictions, which we test in turn.

First, if the model is correct, ectopic expression of *WOR1* in white cells should be needed only transiently to convert the population to stable opaque cells. In other words,

ectopic expression of *WOR1* should be needed to initially excite the feedback loop but its continued expression should not be required to maintain it. This prediction was borne out by the experiment of Table 1 (lines 1&2). Here, ectopic expression of *WOR1* was induced in white cells for several generations, converting the population to opaque cells, and then shut off. Many generations later (enough to form a colony from a single cell), these cells were still in the opaque form and they continued to give rise to opaque progeny cells. Thus, the cells retained a memory of the pulse of ectopic *WOR1* expression, faithfully maintaining the opaque state for many generations after the original stimulus had been removed.

A second prediction of the feedback loop model is that continued expression of *Wor1* should be needed to maintain the opaque state; that is, *Wor1* should be needed not only to establish but also to maintain the opaque state. To test this prediction, we deleted the endogenous copies of *WOR1* and introduced the *pMET3-WOR1* construct. When the construct was induced in white cells, the population converted to a mix of cells types, with many resembling true opaque cells, but others showing a less elongated shape. However, when the *pMET3-WOR1* construct was turned off, all the cells – including those resembling true opaques – reverted to white cells as judged by both cell appearance and colony morphology (Table 1, lines 3&4). This experiment shows that, unless the endogenous copies of *WOR1* are present, a pulse of *Wor1* expression from the ectopic construct is not sufficient to generate a heritable opaque state. Thus, *Wor1* is necessary for both the establishment and the maintenance of the opaque state.

Ectopic Expression of *WOR1* can override the $\mathbf{a1-\alpha2}$ block to white-opaque switching.

As discussed in the Introduction, white-opaque switching can occur in **a** cells and α cells, but is blocked in **a**/ α cells by the transcriptional repressor $\mathbf{a1-\alpha2}$. We present four lines of evidence that argue that the **a**/ α block to white-opaque switching is due to repression of *WOR1* transcription by $\mathbf{a1-\alpha2}$. First, as discussed above, *WOR1* is absolutely required for white-opaque switching, hence its repression would be sufficient to block switching. Second, our previous work showed that *WOR1* transcription is indeed repressed by $\mathbf{a1-\alpha2}$ (8). Third, $\mathbf{a1-\alpha2}$ binding sites are highly conserved between *C. albicans* and *S. cerevisiae* (19), and we found a close match (TTGATGTGATTTTAAACACG) to the composite consensus sequence in the *WOR1* upstream region. To provide a fourth test of the idea that the **a**/ α block to white-opaque switching is due to repression of *WOR1*, we introduced the *pMET3-WOR1* construct into **a**/ α cells and induced expression of *WOR1*. We observed conversion *en masse* of the population to an opaque-like form: many, but not all, of the cells resembled true opaque cells under the microscope (Figure 5A), the colonies resembled, but were not identical to, those formed by true opaque cells (not shown), and opaque-specific genes were induced and white specific genes were repressed (Figure 5B). As for the case of the *wor1* Δ strain, continued expression of the *pMET3-WOR1* construct was required to maintain this state: when the construct was turned off in the **a**/ α strain, the cells reverted to the white form (Table 1, lines 5&6). This experiment shows that ectopic expression of *WOR1* can partially override the **a**/ α block to white opaque switching and, in combination with the other observations cited above, demonstrates that repression of *WOR1* by $\mathbf{a1-\alpha2}$ is

sufficient to explain why \mathbf{a}/α cells cannot undergo white-opaque switching. The experiment also confirms that expression of the endogenous copies of *WOR1* is necessary to maintain the heritability of the opaque state once the ectopic construction is turned off.

DISCUSSION

Discovered nearly twenty years ago, white-opaque switching in *Candida albicans* is an interconversion between two different types of cells, white and opaque. As reviewed in the introduction, white and opaque cells differ in their appearances, in the genes they express, in the host tissues they are most suited for, and in their mating behavior. White-opaque switching in *C. albicans* embodies two critical features of gene expression that underlie numerous examples of cell differentiation. First, switching is stochastic, occurring on average once per 10,000 cell generations. Second, the two states are heritable; that is white cells give rise to white progeny and opaque cells to opaque progeny. This inheritance proceeds for many generations until a cell spontaneously switches to the other form.

In this paper we investigate the molecular mechanism of white-opaque switching. We first identify a master regulator of white-opaque switching, the *WOR1* gene. We show that this gene is required for white-opaque switching, and that, when ectopically expressed, it converts wholesale a population of white cells to opaque cells. We show that *WOR1* forms a positive feedback loop: the protein binds to its own promoter, activates its own transcription, and accumulates to high levels in opaque cells. We demonstrate that this feedback loop is self-sustaining by showing that a pulse of ectopic

WOR1 expression is sufficient to convert a whole population of white cells into opaque cells and that these cells continue to generate opaque cell progeny many generations after the pulse was ended. We also provide an explanation for the genetic block to white-opaque switching in **a**/ α cells: the $\alpha 1$ - $\alpha 2$ heterodimer represses *WOR1* expression. These results show that *WOR1* is a master regulator of white-opaque switching and that it is required both to establish and maintain the opaque state. We propose that it does so by forming a self-sustaining positive feedback loop, which produces high levels of the protein in the opaque state. It seems likely that, in addition to turning on its own expression, *Wor1* activates a set of opaque-specific genes, whose expression endows the opaque state with its specialized properties.

In its most succinct form, our model for white-opaque switching is given in Figure 6. **a**/ α cells cannot undergo white-opaque switching because *WOR1* transcription is repressed. In **a** and α white cells, *WOR1* is expressed at low levels, below the threshold necessary to excite the *WOR1* positive feedback loop. According to the model, the level of *WOR1* expression in white cells exhibits cell-to-cell variation (noise) and, in a population, the threshold level of *WOR1* will be exceeded in a small number of cells. In these rare cells, the feedback loop will be activated, *Wor1* levels will accumulate, and the cells will switch to the opaque form. A similar idea can explain the switch from opaque back to white: if the levels of *WOR1* expression drop below the threshold needed for self-activation, the feedback loop will be broken and cells will revert to the white form. The self-sustaining feedback loop model also explains the heritability of the two states. According to the model, white cells give rise to white cells because their progeny receive

only low levels of Wor1 protein. In contrast, opaque cell progeny would receive sufficiently high levels of Wor1 to maintain the feedback loop.

Although the simplified model of Figure 6 can in principle account for the critical features of white-opaque switching, the actual circuitry probably includes additional features that further stabilize the white and opaque states. For example, Wor1 binds to multiple positions in the *WOR1* upstream region, and cooperative effects may well sharpen the switch-like behavior of the white-opaque transition. It is also possible that *WOR1* levels in white α and α cells are kept low by a repressor, thereby ensuring a low (but observable) switching rate, and the production of this repressor is antagonized as Wor1 levels increase. It is also possible that the high levels of *WOR1* production in opaque cells are limited, perhaps by a negative feedback loop. The structure of the *WOR1* gene itself is consistent with additional regulatory inputs: its mRNA contains extensive untranslated regions and the DNA control region appears to be on the order of 8 kb in length.

In closing, we note that our experiments establish that white-opaque switching is almost certainly an epigenetic phenomenon; that is, switching creates a heritable change without altering the primary DNA sequence. (Technically, a small, reversible DNA rearrangement cannot be rigorously ruled out, but this idea seems highly unlikely in light of the experiments presented here.) In eukaryotes such as *C. albicans*, epigenetic changes are often attributed to heritable changes in chromatin structure, but we are proposing a very different type of model for white-opaque switching--the inheritance of a diffusible protein that directs its own production. This idea is reminiscent of the epigenetic alterations between the immune and anti-immune states of *E. coli* containing

derivatives of bacteriophage lambda (20). In this case, inheritance of the immune state is based on a diffusible protein (the lambda repressor) which activates its own synthesis.

Many challenges remain in understanding white-opaque switching in *C. albicans*. Given the apparent absence of this type of phenomenon in many other fungi including *S. cerevisiae*, it is possible that white-opaque switching co-evolved during *C. albicans*' long association with warm-blooded animals (21). Perhaps producing two distinct types of cells has enabled *C. albicans* to thrive in the hostile environment created by an evolving innate immune system. The simple mechanism we have proposed suggests that an epigenetic phenomenon like white-opaque switching could have easily evolved from more conventional (that is, non-heritable) types of transcriptional circuits.

MATERIALS AND METHODS

See Table 2 for a list of strains used in this study. PCR primers are listed in Supplemental Table 3.

Media

Standard laboratory media have been described (22). Synthetic complete medium + 2% glucose + 100 µg/ml uridine (SCD+Urd) was used to maintain strains in the white and opaque phases at room temperature (RT). Supplemented Lee's medium (1) was further supplemented with 70 µg/ml Arg, 81 µg/ml Ade, 0.023 µg/ml His, and 100 µg/ml Urd. For the *MET3* induction experiments (18), cells were grown in SCD+Urd lacking Met and Cys (SD-Met-Cys+Urd). To repress the *MET3* promoter, SCD+Urd was

supplemented with 2.5 mM each of Met and Cys (SD+Met+Cys+Urd). Strains were grown on solid media for 5-7 days at RT before inoculating liquid cultures used in the experiments described below.

Plasmids

To generate *pMET3-WOR1*, the *WOR1* ORF was amplified from SC5314 genomic DNA using primers containing BglII and AvaI restriction sites and was cloned into BamHI/BspEI-digested pCaEXP(18), creating plasmid pRZ25.

Strain construction

All strains were derived from SC5314. With the exception of the *cag1Δ* mutant, the **a** strains were generated by growth on sorbose-containing medium, as described previously (see (14) and references therein). Mating type was determined by PCR (12).

The *cag1Δ* mutant was derived from RM1000: Urablaster methods using pCH152 disrupted the *MTLa1* and *MTLa2* genes (23) (24), and the two alleles of *CAG1* were disrupted using *HIS1* and *URA3* markers (25). This strain also contains a maltose-inducible *STE3* construct, generated from pAU15 (26).

Deletions of *CEK2*, *FGR23*, *FAR1*, and *WOR1* were created from the parent strain RZY47 –an **a** derivative of SN87 (-His -Leu) generated by sorbose-selection (27). The target genes were disrupted using the fusion PCR strategy as described previously (27). For each target gene, at least two independent deletion mutants were generated from independent heterozygous mutants.

The fusion knockout strategy was also used to create a *wor1Δ* mutant in SN78 (**a/α** -His -Leu -Ura) (27). The strain was then transformed with linearized pRZ25 (containing *pMET3-WOR1*) to direct integration to the *RP10* locus (18). Proper integration was verified using PCR. This strain was sorbose-selected on media supplemented with 2.5 mM Met and Cys to generate **a** isolates.

The pRZ25 plasmid was also transformed into CAI4 (-Ura) or RZY9 (**a** derivative of CAI4). These strains are referenced as *pMET3-WOR1* (**a/α** or **a**) in the text. As controls, pCaEXP was introduced into CAI4 or RZY9 to create *pMET3* control (**a/α** or **a**) strains.

DNA sequences of *C. albicans* genes were obtained from the *Candida* Genome Database (<http://www.candidagenome.org>). Fungal protein sequences were obtained from Proteome Bioknowledge Library (<http://www.proteome.com>).

White-Opaque Switching Assays

White–opaque switching assays were performed as described previously (12), with the following modifications. Each strain was streaked onto supplemented Lee’s medium (described above) and grown for 5 days at 25°C. Cells were then plated onto SCD+Urd and grown for 7 days at RT, at which time the colonies were monitored for the presence of opaque colonies and sectors. At least two independent isolates of each mutant were used in this assay.

Ectopic expression of *WOR1* and cell measurements

Cells were grown on SD+Met+Cys+Urd (repressing) media at RT for 5 days. For each strain, 5-10 colonies were resuspended in sterile water and plated onto repressing or inducing media (SD-Met-Cys+Urd). After growth at RT for 5 days, colony phenotypes were recorded. Colonies were resuspended in sterile water and cells were examined using differential interference contrast (DIC) microscopy on a Zeiss Axiovert 200M microscope (Carl Zeiss, Germany). Cell dimensions were measured using Zeiss AxioVision software. Additional experiments with independent wildtype and mutant strains were nearly identical to those shown in Figures 2 and 6 (not shown). To test the effect of transient ectopic expression of *WOR1*, colonies grown on inducing media were replated on repressing media (or inducing, as a control). Plates were grown at RT for ~7 days and colony phenotypes were recorded.

Quantitative reverse transcription PCR (RT-PCR)

Cultures were grown in SD-Met-Cys+Urd at RT to mid-log phase, harvested by centrifugation, and frozen in liquid nitrogen. Total RNA was isolated from the cell pellets using buffered phenol extractions. Total RNA from each sample was linearly reverse-transcribed and cDNA was amplified by quantitative PCR, as monitored by Sybr Green fluorescence in a MJ Research Opticon instrument (Waltham, MA). Quantitative PCR was performed 3 times on the same cDNA preparation and the median value is shown in Figures 2 and 6. Signal for each gene is normalized to the median PAT1 transcript level in the corresponding strain.

Response to mating pheromone

Synthetic α -factor treatment was performed as previously described (14). Cells were fixed and observed by DIC microscopy after 4 hours of pheromone treatment.

Northern Blot Analysis

Five μ g of total RNA (isolated above) were analyzed by Northern blot analysis. Radio-labeled DNA probes were generated by PCR and purified using Probe Quant G50 Sephadex Columns (Amersham Biosciences, UK). Signal was detected using a Storm phosphorimager (Molecular Dynamics, Sunnyvale, CA).

Western Blot Analysis

C. albicans cultures were grown in repressing or inducing medium and harvested as described above. Whole cell extracts (WCE) were prepared in urea lysis buffer (28), and 5 μ g of WCE from each sample was separated SDS-PAGE and analyzed by Western blotting. α -Wor1 is an affinity-purified antibody generated against a peptide at the C-terminus of Wor1 (DDAVGNSSGSYYTGT) (Bethyl Laboratories, Montgomery, TX). As a loading control, the membrane was stripped and reprobed with rat α -Tub1, raised against *S. cerevisiae* Tub1 (#ab1616, Abcam, Cambridge, MA).

ChIP Experiments

Overnight cultures were grown in SCD+Urd for ~16h at 25°C to an OD₆₀₀ of 0.4. Cells were formaldehyde crosslinked and lysed by spheroplasting and osmotic lysis. Using 5 μ l α -Wor1 antibody (described above), immunoprecipitation (IP) was performed

as described (29), with modifications. After spheroplasting, micrococcal nuclease digestion was omitted, and spheroplasts were resuspended in lysis buffer (50 mM HEPES-KOH [pH 7.5], 140 mM NaCl, 1 mM EDTA, 1% Triton X-100, 0.1% sodium deoxycholate). DNA was sheared by sonication 10 times for 10s at power setting 2 on a Branson 450 sonicator, incubating on ice for 2 min between sonication pulses. Extracts were clarified by centrifugation.

PCR primers were designed at ~250bp intervals across the intergenic sequence upstream of the *WOR1* ORF. For each ChIP experiment, DNA derived from the WCE and IP eluate was analyzed by quantitative PCR (qPCR). For each primer pair, three independent pairs of WCE and IP qPCR reactions were run, and median IP/WCE quantity ratios across the three replicates were divided by median IP/WCE quantity ratios across three control reactions run in parallel using primers to the *ADE2* ORF. ChIP experiments using an *MTL α 1 Δ MTL α 2 Δ* opaque strain (not shown) had an enrichment profile that was virtually identical to the **a** opaque profile shown in Figure 4.

ACKNOWLEDGEMENTS

We thank Matt Miller, Richard Bennett, Brian Tuch, Annie Tsong, and other lab members for many valuable discussions and reagents. We also thank Marie Bao and Hiten Madhani for providing the α -Tub1 antibody. REZ was supported by ARCS Scholarship. DJG was supported by a NSF predoctoral fellowship. The work was supported by grants from the NIH (RO1 AI49187) and the Ellison Foundation to ADJ.

REFERENCES

1. Slutsky B, Staebell M, Anderson J, Risen L, Pfaller M, et al. (1987) "White-opaque transition": a second high-frequency switching system in *Candida albicans*. *J Bacteriol* 169: 189-197.
2. Bergen MS, Voss E, Soll DR (1990) Switching at the cellular level in the white-opaque transition of *Candida albicans*. *J Gen Microbiol* 136: 1925-1936.
3. Rikkerink EH, Magee BB, Magee PT (1988) Opaque-white phenotype transition: a programmed morphological transition in *Candida albicans*. *J Bacteriol* 170: 895-899.
4. Soll DR, Morrow B, Srikantha T (1993) High-frequency phenotypic switching in *Candida albicans*. *Trends Genet* 9: 61-65.
5. Lockhart SR, Daniels KJ, Zhao R, Wessels D, Soll DR (2003) Cell biology of mating in *Candida albicans*. *Eukaryot Cell* 2: 49-61.
6. Johnson A (2003) The biology of mating in *Candida albicans*. *Nat Rev Microbiol* 1: 106-116.
7. Lan CY, Newport G, Murillo LA, Jones T, Scherer S, et al. (2002) Metabolic specialization associated with phenotypic switching in *Candida albicans*. *Proc Natl Acad Sci U S A* 99: 14907-14912.
8. Tsong AE, Miller MG, Raisner RM, Johnson AD (2003) Evolution of a combinatorial transcriptional circuit: a case study in yeasts. *Cell* 115: 389-399.
9. Kvaal CA, Srikantha T, Soll DR (1997) Misexpression of the white-phase-specific gene WH11 in the opaque phase of *Candida albicans* affects switching and virulence. *Infect Immun* 65: 4468-4475.

10. Kvaal C, Lachke SA, Srikantha T, Daniels K, McCoy J, et al. (1999) Misexpression of the opaque-phase-specific gene PEP1 (SAP1) in the white phase of *Candida albicans* confers increased virulence in a mouse model of cutaneous infection. *Infect Immun* 67: 6652-6662.
11. Lachke SA, Lockhart SR, Daniels KJ, Soll DR (2003) Skin facilitates *Candida albicans* mating. *Infect Immun* 71: 4970-4976.
12. Miller MG, Johnson AD (2002) White-opaque switching in *Candida albicans* is controlled by mating-type locus homeodomain proteins and allows efficient mating. *Cell* 110: 293-302.
13. Lockhart SR, Pujol C, Daniels KJ, Miller MG, Johnson AD, et al. (2002) In *Candida albicans*, white-opaque switchers are homozygous for mating type. *Genetics* 162: 737-745.
14. Bennett RJ, Uhl MA, Miller MG, Johnson AD (2003) Identification and characterization of a *Candida albicans* mating pheromone. *Mol Cell Biol* 23: 8189-8201.
15. Caspari T (1997) Onset of gluconate-H⁺ symport in *Schizosaccharomyces pombe* is regulated by the kinases Wis1 and Pka1, and requires the *gti1+* gene product. *J Cell Sci* 110 (Pt 20): 2599-2608.
16. Kunitomo H, Sugimoto A, Wilkinson CR, Yamamoto M (1995) *Schizosaccharomyces pombe* *pac2+* controls the onset of sexual development via a pathway independent of the cAMP cascade. *Curr Genet* 28: 32-38.

17. Li F, Palecek SP (2005) Identification of *Candida albicans* genes that induce *Saccharomyces cerevisiae* cell adhesion and morphogenesis. *Biotechnol Prog* 21: 1601-1609.
18. Care RS, Trevethick J, Binley KM, Sudbery PE (1999) The MET3 promoter: a new tool for *Candida albicans* molecular genetics. *Mol Microbiol* 34: 792-798.
19. Hull CM, Raisner RM, Johnson AD (2000) Evidence for mating of the "asexual" yeast *Candida albicans* in a mammalian host. *Science* 289: 307-310.
20. Ptashne M (1994) *A Genetic Switch: Phage Lambda Revisited*. Cold Spring Harbor, NY: Cold Spring Harbor Laboratory Press.
21. Lott TJ, Fundyga RE, Kuykendall RJ, Arnold J (2005) The human commensal yeast, *Candida albicans*, has an ancient origin. *Fungal Genet Biol* 42: 444-451.
22. Guthrie C, and G. R. Fink (1991) *Guide to yeast genetics and molecular biology*. San Diego, CA: Academic Press.
23. Hull CM, Johnson AD (1999) Identification of a mating type-like locus in the asexual pathogenic yeast *Candida albicans*. *Science* 285: 1271-1275.
24. Fonzi WA, Irwin MY (1993) Isogenic strain construction and gene mapping in *Candida albicans*. *Genetics* 134: 717-728.
25. Wilson RB, Davis D, Enloe BM, Mitchell AP (2000) A recyclable *Candida albicans* URA3 cassette for PCR product-directed gene disruptions. *Yeast* 16: 65-70.
26. Uhl MA, Johnson AD (2001) Development of *Streptococcus thermophilus* lacZ as a reporter gene for *Candida albicans*. *Microbiology* 147: 1189-1195.

27. Noble SM, Johnson AD (2005) Strains and strategies for large-scale gene deletion studies of the diploid human fungal pathogen *Candida albicans*. *Eukaryot Cell* 4: 298-309.
28. Ubersax JA, Woodbury EL, Quang PN, Paraz M, Blethrow JD, et al. (2003) Targets of the cyclin-dependent kinase Cdk1. *Nature* 425: 859-864.
29. Liu CL, Kaplan T, Kim M, Buratowski S, Schreiber SL, et al. (2005) Single-nucleosome mapping of histone modifications in *S. cerevisiae*. *PLoS Biol* 3: e328.
30. Chenna R, Sugawara H, Koike T, Lopez R, Gibson TJ, et al. (2003) Multiple sequence alignment with the Clustal series of programs. *Nucleic Acids Res* 31: 3497-3500.

REFERENCES

Figure 1.

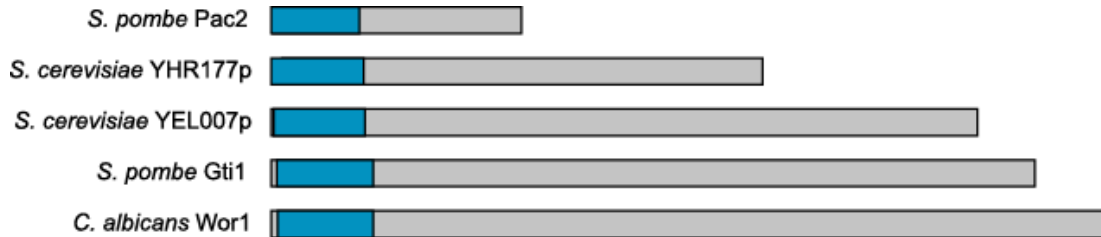


Figure 1. Alignment of Wor1 homologs across fungal species. Protein sequences were aligned using CLUSTALW (30), which identified a highly conserved region at the N-terminus of each protein (blue). For instance, *C. albicans* Wor1 and *S. pombe* Gti1 are 53% identical across the conserved region. *C. albicans* Wor1 protein is 785 amino acids in length, and the other proteins are drawn to scale.

Figure 2.

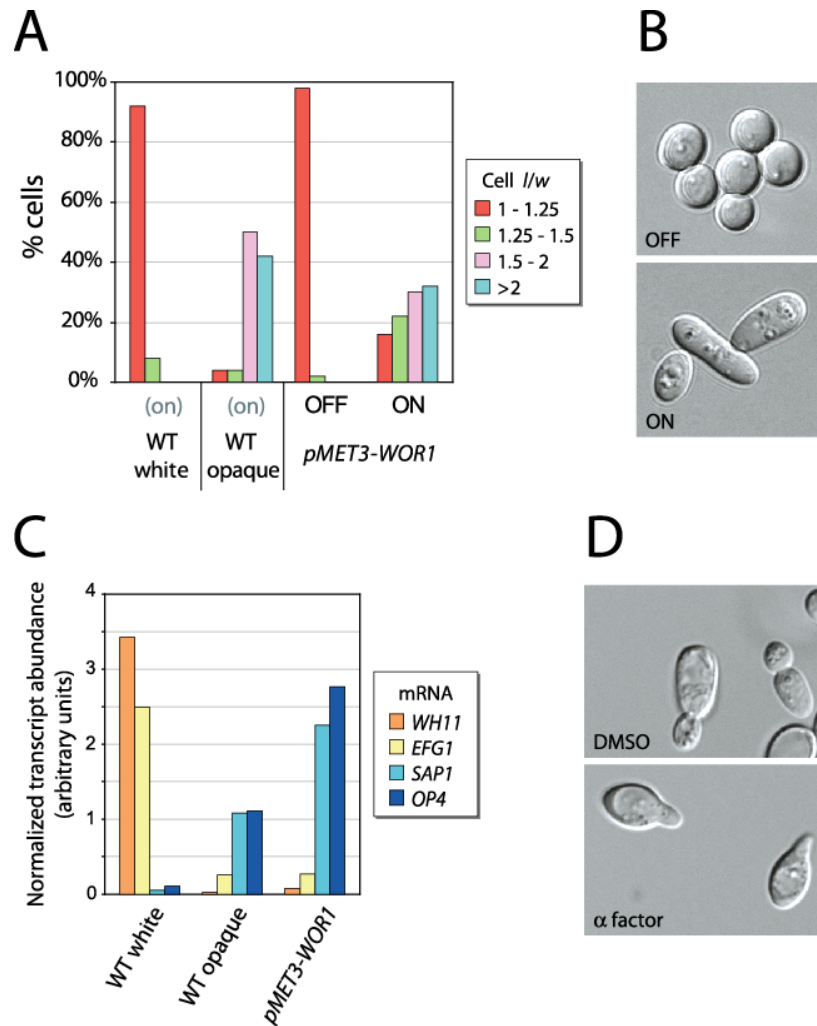


Figure 2. Ectopic expression of *WOR1* in white cells drives the cells to the opaque phase.

*Panels A and B: Ectopic expression of *WOR1* causes white cells to resemble opaque cells in appearance. Cell dimensions were measured in DIC images (panel B), and populations of cells were compared based on the distribution of length/width ratios for 50 cells/strain/condition (panel A). Panel C: Ectopic expression of *WOR1* in white cells causes them to express genes characteristic of opaque cells. Quantitative RT-PCR was*

used to monitor transcription of the white-specific genes *WH11* and *EFG1* and the opaque-specific genes *SAP1* and *OP4*. All values were normalized to *PAT1*, a transcript that is not regulated by white-opaque switching. *Panel D: Ectopic expression of *WOR1* in white cells renders them sensitive to the mating pheromone α -factor.* This specialized property of true opaque cells is visualized by the formation of mating projections on the ends of the cells (14). Cells were treated with α -factor (10 μ g/ml in DMSO) or an equivalent amount of DMSO as a control. In panels A and B, “ON” and “OFF” indicate the expression of the *pMET3-WOR1* construct, as controlled by media conditions. For strains that lack the *pMET3-WOR1* construct, media conditions are designated by “(on)” or “(off)”. For experiments shown in panels C and D, strains were grown in media that induces *pMET3-WOR1* expression. All strains are **a** strains.

Figure 3.

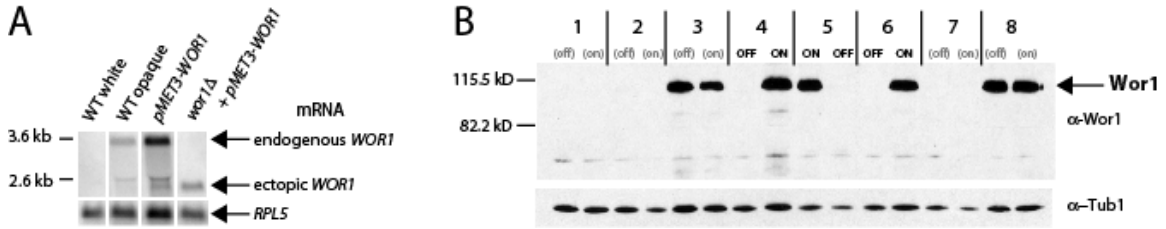


Figure 3. Northern and Western analysis of *WOR1* expression.

*Panel A: Northern analysis of total RNA isolated from strains grown under conditions that induce the pMET3-WOR1 construct. The relevant genotypes are indicated above each lane (all strains are **a** strains). *RPL5* serves as a loading control. Panel B:*

*Immunoblot analysis of *Wor1* protein levels in white and opaque cells of several different strains. *Wor1* was detected in whole cell extract using an antibody (α -*Wor1*) generated against a peptide portion of *Wor1*. Strain 1 (**a**, *wor1* Δ) controls for non-specific binding of the antibody. Strain 2 (CAF2-1, **a**, white) and strain 3 (CAF2-1, **a**, opaque) show the differential expression of *Wor1* between white and opaque cells. Strain 4 (**a**, *pMET3-WOR1*), strain 5 (**a**, *wor1* Δ + *pMET3-WOR1*), and strain 6 (**a**/ α , *pMET3-WOR1*), show that the *pMET3-WOR1* construct is tightly regulated by media conditions and that the protein is not grossly over-expressed. Strain 7 (SNY87, **a**, white) and strain 8 (SNY87, **a**, opaque) again show the differential expression of *Wor1* in white versus opaque cells.*

*The blot was stripped and re-probed with α -Tub1 as a loading control. “ON” and “OFF” indicate media conditions used to regulate the *pMET3-WOR1* construct, as described in Figure 2.*

Figure 4.

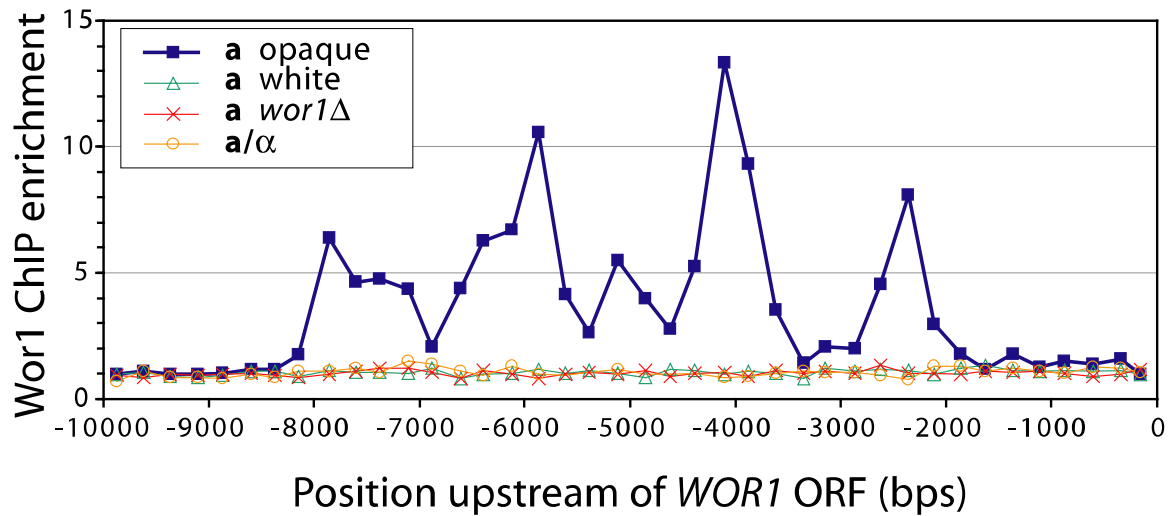


Figure 4. *Wor1* protein is bound to the region upstream of its gene.

Chromatin immunoprecipitation was performed with α -*Wor1* antibodies in wildtype **a** opaque, wildtype **a** white, wildtype **a/α**, and *wor1Δ* **a** strains. *Wor1* ChIP enrichment was detected by quantitative PCR at ~250bp intervals across the 10.3kb intergenic region. Shown are enrichment values at each position upstream of *WOR1* relative to a control gene (*ADE2*) that is not regulated by white-opaque switching.

Table 1.

Strain		Phenotype on inducing media	% "opaque" colonies when replated to repressing media	n
<i>pMET3</i> control	a	white	0.38%	789
<i>pMET3-WOR1</i>	a	opaque	97%	443
<i>wor1</i> Δ + <i>pMET3</i> control	a	white	< 0.44%	228
<i>wor1</i> Δ + <i>pMET3-WOR1</i>	a	opaque-like	< 0.34%	295
<i>pMET3</i> control	a/α	white	<0.13%	770
<i>pMET3-WOR1</i>	a/α	opaque-like	<0.13%	768

Table 1. Transient ectopic expression of *WOR1* forms stable opaque colonies in a strains containing the endogenous *WOR1* genes.

Ectopic expression of *pMET3-WOR1* was induced by growth on appropriate media, and strains formed opaque or opaque-like colonies as described in the text. When replated onto media that represses expression of the *pMET3-WOR1* construct, only the **a** strains that contain the endogenous copies of *WOR1* were able to maintain the opaque state.

Figure 5

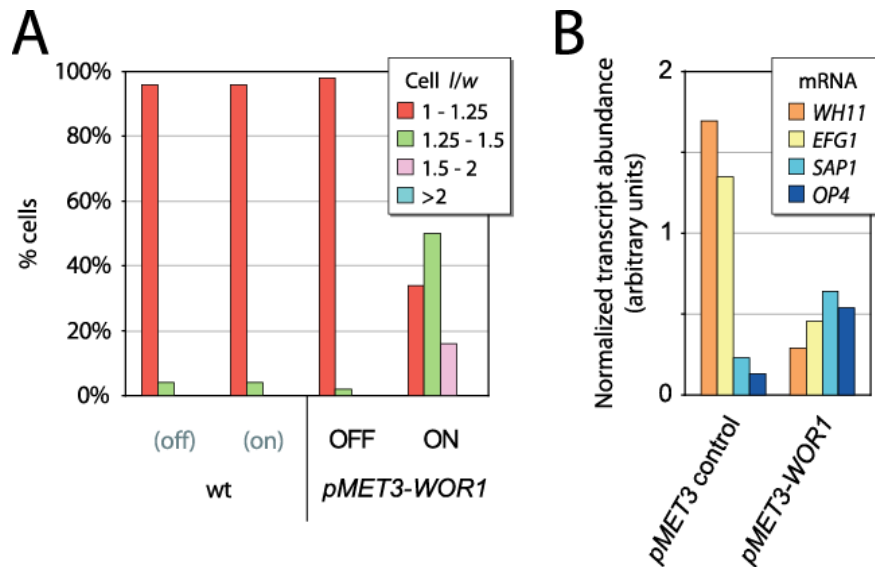


Figure 5. Ectopic expression of *WOR1* in *a/a* cells induces opaque-like characteristics.

Ectopic expression of *WOR1* was regulated using the *pMET3-WOR1* construct in *a/a* strains. *Panel A: Ectopic expression of WOR1 causes white cells to resemble opaque cells in appearance.* Cell dimensions were measured in DIC images, and populations of cells were compared based on the distribution of length/width ratios for 50 cells/strain/condition. “ON” and “OFF” indicate media conditions used to regulate the *pMET3-WOR1* construct, as described in Figure 2. *Panel B: Ectopic expression of WOR1 in white cells causes them to express genes characteristic of opaque cells.* Quantitative RT-PCR was used to monitor transcription of the white-specific genes *WH11* and *EFG1* and the opaque-specific genes *SAP1* and *OP4* under conditions that induce the *pMET3-WOR1* construct. All values were normalized to *PAT1*, a transcript that is not regulated by white-opaque switching.

Figure 6.

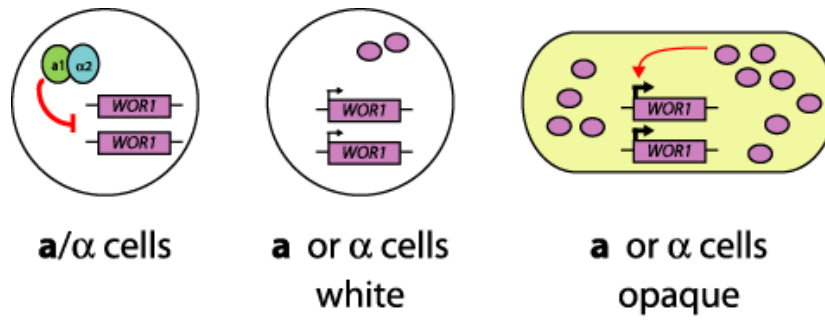


Figure 6. A model for a positive Wor1 feedback loop in regulation of white-opaque switching.

Table 2. Strains used in this study

General Description	Strain	Mating type	Genotype	Reference	Use
CAF2-1		a/α	<i>URA3/ura3::Δimm434</i>	1	Figure 6, parent to RZY12
CAF2-1 a white	RZY12	a	<i>URA3/ura3::Δimm434</i>	this work	Figures 2, 3
CAF2-1 a opaque	RZY491	a	<i>URA3/ura3::Δimm434</i>	this work	Figures 2, 3
CA14		a/α	<i>ura3::Δimm434/ura3::Δimm434</i>	1	Parent to RZY9, 326, 330, 331
CA14 a	RZY9	a	<i>ura3::Δimm434/ura3::Δimm434</i>	this work	Parent to RZY338, 339, 496
	RZY330,				
<i>pMET3-WOR1</i> a/α	RZY331	a/α	<i>ura3::Δimm434/ura3::Δimm434, RP10/rp10::pRZ25</i>	this work	Figures 3, 5, 6
<i>pMET3</i> control a/α	RZY326	a/α	<i>ura3::Δimm434/ura3::Δimm434, RP10/rp10::pCaEXP</i>	this work	Figure 5, 6
	RZY338,				
<i>pMET3-WOR1</i> a	RZY339	a	<i>ura3::Δimm434/ura3::Δimm434, RP10/rp10::pRZ25</i>	this work	Figures 2, 3, 5
<i>pMET3</i> control a	RZY496	a	<i>ura3::Δimm434/ura3::Δimm434, RP10/rp10::pCaEXP</i>	this work	Figure 5
SN87		a/α	<i>URA3/ura3::Δimm434 his1/his1 leu2/leu2</i>	2	Figure 4, parent to RZY47
SN87 a white	RZY47	a	<i>URA3/ura3::Δimm434 his1/his1 leu2/leu2</i>	this work	Figures 3, 4
SN87 a opaque	RZY511	a	<i>URA3/ura3::Δimm434 his1/his1 leu2/leu2</i>	this work	Figures 3, 4
SN78		a/α	<i>ura3::Δimm434/ura3::Δimm434 his1/his1 leu2/leu2</i>	2	Parent to RZY389
<i>wor1</i> Δ + <i>pMET3-</i>	RZY407,				
<i>WOR1</i> a	RZY411	a	<i>ura3::Δimm434/ura3::Δimm434 his1/his1 leu2/leu2</i> <i>wor1::HIS1/wor1::LEU2 RP10/rp10::pRZ25</i>	this work	Figures 3, 5, 6
<i>wor1</i> Δ + <i>pMET3</i>					
control a	RZY389	a	<i>ura3::Δimm434/ura3::Δimm434 his1/his1 leu2/leu2</i> <i>wor1::HIS1/wor1::LEU2 RP10/rp10::pCaEXP</i>	this work	Figure 5
	RZY219,				
<i>wor1</i> Δ	RZY235	a	<i>URA3/ura3::Δimm434 his1/his1 leu2/leu2 wor1::HIS1/wor1::LEU2</i>	this work	Figures 3, 4, WO switching assay
	RZY215,				
<i>cek2</i> Δ	RZY216	a	<i>URA3/ura3::Δimm434 his1/his1 leu2/leu2 cek2::HIS1/cek2::LEU2</i>	this work	WO switching assay
	RZY230,				
<i>fgr23</i> Δ	RZY233	a	<i>URA3/ura3::Δimm434 his1/his1 leu2/leu2 fgr23::HIS1/fgr23::LEU2</i>	this work	WO switching assay
	RZY207,				
<i>far1</i> Δ	RZY229	a	<i>URA3/ura3::Δimm434 his1/his1 leu2/leu2 far1::HIS1/far1::LEU2</i> <i>ura3::Δimm434/ura3::Δimm434 mta1 Δa2 Δ::hisG pMAL2-</i> <i>STE3/MAL2 cagl::HIS1/cagl::URA3</i>	this work	WO switching assay
<i>cagl</i> Δ	MMY198	a		this work	WO switching assay

1. Fonzi, W. A. & Irwin, M. Y. (1993) *Genetics* **134**, 717-28.
2. Noble, S. M. & Johnson, A. D. (2005) *Eukaryot Cell* **4**, 298-309.

Table 3. Primers used in this study

Description	Primer Sequence (5'-3')*
Deletion construction	
<i>WOR1</i> 5' flank (forward)	CCTGTATTGGTATTGGTGAG
<i>WOR1</i> 5' flank (reverse)	cacggcgcgacctagcagcggCAACCCCTTAAATATATATAAGACAG
<i>WOR1</i> 3' flank (forward)	gtcagcggcgcgcatccctgcCGGTGATTCTGTATTATTTGGGGC
<i>WOR1</i> 3' flank (reverse)	CCCTTCATGAATAGTTCC
<i>FAR1</i> 5' flank (forward)	GGCATGTGATTTGAGTTAAGG
<i>FAR1</i> 5' flank (reverse)	cacggcgcgacctagcagcggGTCTAACACTTTAAGTGGTAGAG
<i>FAR1</i> 3' flank (forward)	gtcagcggcgcgcatccctgcGTGCTGGTGCAACCATCATCTGTG
<i>FAR1</i> 3' flank (reverse)	GATTATGAGTTGCTATCACGAATGG
<i>CEK2</i> 5' flank (forward)	GCGTTTCAGTACTTTCCTTATC
<i>CEK2</i> 5' flank (reverse)	cacggcgcgacctagcagcggGTACACAGCTTTGGCTTTATGG
<i>CEK2</i> 3' flank (forward)	gtcagcggcgcgcatccctgcACTTTACTTAAATTAATTACTTTTAC
<i>CEK2</i> 3' flank (reverse)	TCGCTATCAGGAGGGGACAG
<i>FGR23</i> 5' flank (forward)	GCAGAATTAGAGTCTAGAAGATTGG
<i>FGR23</i> 5' flank (reverse)	cacggcgcgacctagcagcggCTCAGCAAGTGTGGGTATTC
<i>FGR23</i> 3' flank (forward)	gtcagcggcgcgcatccctgcCTACTTTCCTTTATTATTAATAC
<i>FGR23</i> 3' flank (reverse)	ATTCCGTTACAACCCGACCC
<i>CAG1</i> -5DR	TCTTAATGTACATTAATAAATCTGTCITTTAGTTTACCITTTTTTAAATACCAGTATTCAATCgtttccagtcacgacgtt
<i>CAG1</i> -3DR	AAAAAATTTAAACTGAACATTAATGTGAAAGTAAAAAAGATATCGCCTACTTCTTGCAAtgtggaattgtgagcggafa
pRZ25 construction	
<i>WOR1</i> ORF (forward)	ccaagatctATGTCTAATTCAAGTATAGTCCCTAC
<i>WOR1</i> ORF (reverse)	cccccgggCTAAGTACCGGTGTAATACGACCC
Quantitative RT-PCR	
<i>WH11</i> (forward)	CAGAACAATTCAAGGATAAGGTTACTG
<i>WH11</i> (reverse)	TTGGAGTCACAAAAATAGCATCAG
<i>EFG1</i> (forward)	CATCACAACCAGGTTCTACAACCAAT
<i>EFG1</i> (reverse)	CTACTATTAGCAGCACCCACCC
<i>SAP1</i> (forward)	TTCAACAAGATGTTGCTCAAG
<i>SAP1</i> (reverse)	GTTGACCGTTAGCGTAGCTC
<i>OP4</i> (forward)	CCTCAAAAGCTGCTACCTC
<i>OP4</i> (reverse)	GTATCAACAGTTGGAGTAGAAGTAG
<i>PAT1</i> (forward)	TTATCGGAATGGTCCTCGTG
<i>PAT1</i> (reverse)	CCAGAAGAACCATCATCAAC
Northern probes	
<i>WOR1</i> (forward)	TGGGTATATTCATAACACAAGAGATGCATTA
<i>WOR1</i> (reverse)	GACCATGAAATACCATCTGTCCATCTTTG
<i>RPL5</i> (forward)	TCCC GTTCCAAACTCCTT
<i>RPL5</i> (reverse)	GGTAATTCGTGAGCATAAGCAGC

*lower case sequence represents exogenous sequence used for fusion PCR or UAU gene disruption (in deletion oligos) or to introduce restriction sites (*WOR1* ORF oligos)

Chapter 3

Interlocking Transcriptional Feedback Loops Control

White-Opaque Switching in *Candida albicans*

Interlocking Transcriptional Feedback Loops Control White-Opaque Switching in *Candida albicans*

Rebecca E. Zordan^{1†}, Mathew G. Miller^{1†}, David J. Galgoczy¹, Brian B. Tuch¹, and Alexander D. Johnson^{1,2},

[†]These authors contributed equally to this work.

¹Department of Biochemistry and Biophysics and ²Department of Microbiology and Immunology, University of California, San Francisco, California, USA

Abstract

The human pathogen *Candida albicans* can assume either of two distinctive cell types, designated “white” and “opaque”. Each cell type is maintained for many generations; switching between them is rare and stochastic and occurs without any known changes in the nucleotide sequence of the genome. The two cell types differ dramatically in cell shape, colony appearance, mating competence, and virulence properties. In this work, we investigate the transcriptional circuitry that specifies the two cell types and controls the switching between them. First, we identify two new transcriptional regulators of white-opaque switching, *CZF1* and *WOR2*. Analysis of a large set of double mutants and ectopic expression strains revealed genetic relationships between *CZF1*, *WOR2*, and two previously identified regulators of white-opaque switching, *WOR1* and *EFG1*. Using chromatin immunoprecipitation, we show that Wor1 binds the intergenic regions upstream of the three additional transcriptional regulators of white-opaque switching (*CZF1*, *EFG1*, and *WOR2*), and also occupies the promoters of numerous white and

opaque-enriched genes. Based on these interactions, we have placed these four genes in a circuit controlling white-opaque switching whose topology is a network of positive feedback loops, with the master regulator *WOR1* occupying a central position. Our observations indicate that a key role of the interlocking feedback loop network is to stably maintain each epigenetic state through many cell divisions.

INTRODUCTION

Transcriptional circuits are central to the regulation of many biological processes. Often the logic of the circuit, rather than the nature of its components, makes up its most critical feature. In this paper we describe an interlocking network of positive feedback loops that underlies white-opaque switching in the human fungal pathogen *Candida albicans*. White-opaque switching is an epigenetic phenomenon, where genetically identical cells can exist in two distinctive cell types, white and opaque [1]. Each cell type is stably inherited for many generations, and switching between the two types of cells occurs stochastically and rarely, roughly one switch in 10^4 cell divisions [2]. The white form is the default cell type, and we propose that the main purpose of the network of interlocking feedback loops is, once excited, to stably maintain the opaque cell type through many cell divisions. Thus, we propose the feedback loop network driving opaque formation is activated infrequently, but once activated, it is stably propagated through many cell generations.

Despite possessing the same genome, white and opaque cells have many phenotypic differences. Approximately 400 genes are differentially expressed between the two cell types, and the cells differ in their appearance under the microscope and in the

color and shape of the colonies they produce on solid media [1,3,4]. They also differ in their behavior towards other *C. albicans* cells: opaque cells, but not white cells, are highly competent for mating; they respond to mating pheromone with polarized growth, and they can subsequently undergo cell and nuclear fusion with opaque cells of the opposite mating type [5,6,7,8]. Finally, the two types of cells appear to interact differently with their mammalian host, with opaque cells appearing more suited for skin infections, and white cells appearing to fare better in blood stream infections [9,10].

Several transcriptional regulators have been identified that play key roles in maintaining the white and opaque cell types, and in controlling the switching between them. Cells of mating type **a**/ α are blocked for white-opaque switching, with all cells remaining locked in the white phase [5]. This block occurs through the action of two homeodomain proteins ($\alpha 1$ and $\alpha 2$), encoded at the *MTL α* and *MTL α* locus, respectively. The $\alpha 1$ and $\alpha 2$ proteins likely act together as a heterodimer to repress transcription of *WOR1*, a positive regulator of the opaque state [11,12,13]. *Wor1* is required for establishment and maintenance of the opaque state, and ectopically expressed *WOR1* drives cells into the opaque form. In **a** and α cells (both of which are permissive for switching), *WOR1* is expressed at low levels in white cells, but in opaque cells *Wor1* activates its own synthesis, and *WOR1* expression levels rise dramatically. High levels of *Wor1*, produced by this positive feedback loop, are necessary to maintain the opaque state. Finally *Efg1*, which has been studied extensively for its role as regulator of the filamentous growth and pathogenesis in **a**/ α (i.e., non-switching) strains of *C. albicans*, also plays a part in white-opaque switching: in **a** and α cells (but not **a**/ α cells) cells

deleted for *EFG1* exist almost exclusively in the opaque state [14,15] (this work). Thus *EFG1* is needed to stably maintain the white state.

In this paper we identify two additional transcription regulators of white-opaque switching, *CZF1* and *WOR2*. The former has been previously studied as an important regulator of filamentous growth in \mathbf{a}/α (non-switching) cells [16], but a role in white-opaque switching has not been previously described. *WOR2* has not been previously described in any context, and we named the gene *White-Opaque Regulator 2* based on its key role white-opaque switching, as described in this paper. In order to understand the genetic relationships of *WOR1*, *EFG1*, *CZF1* and *WOR2*, we constructed a large set of single and double mutants and analyzed them for white-opaque switching. We also ectopically expressed these regulators in mutant strains in various combinations and monitored their effects on switching and maintenance of the white and opaque states. Finally, we carried out chromatin immunoprecipitation experiments to establish direct regulatory connections between the central regulator, *Wor1*, and the other targets. We found that *Wor1* binds upstream of: (1) all four transcriptional regulators investigated in this paper (*WOR1*, *CZF1*, *WOR2*, *EFG1*); (2) genes whose transcription is regulated by the white-opaque switch; and (3) a large number of genes that are not differentially transcribed during the white-opaque switch, suggesting an additional, previously unrecognized component of white-opaque switching, one that may require additional environmental inputs to fully reveal. Based on the combined results of these experiments, we have placed *MTLa1*, and *MTLa2*, *WOR1*, *CZF1*, *WOR2*, and *EFG1* into a single genetic circuit regulating the white-opaque switch. This circuit is formed from a

network of interlocking positive feedback loops, and we believe that this network can account for the stability of the white and opaque states through many cell generations.

RESULTS

Identification of new regulators of white-opaque switching

One of the most striking characteristics of the white-opaque switch is the large number of genes that are differentially regulated between the two types of cells.

Approximately 400 genes have altered transcription; roughly half are up-regulated in the white phase, with the remaining half up-regulated in the opaque phase [3,4]. Several of these regulated genes encode transcriptional regulators, as predicted by the presence of a sequence-specific DNA-binding motif encoded in the gene. We tested a set of opaque-enriched transcription factors for possible roles in regulating the white-opaque switch.

Opaque-enriched genes were previously identified through microarray analyses that compared the gene expression profiles of isogenic white and opaque cells [3,4].

Genes up-regulated in opaque cells were searched for homology to transcriptional regulatory proteins using BLAST searches (<http://www.ncbi.nlm.nih.gov/BLAST/>) and Pfam motif searches (<http://www.sanger.ac.uk/Software/Pfam/>). From a set of 237 opaque-enriched genes, we chose to study six genes encoding putative transcriptional regulators: *CZF1* (orf19.3127), *WOR2* (orf19.5992), *HAP3* (orf19.4647), orf19.4972, *CSRI* (orf19.3794) and *PHO23* (orf19.1759). Both *CZF1* and *WOR2* are predicted to contain a zinc cluster (Zn(2)-Cys(6)) motif, a known DNA-binding domain in fungal transcriptional regulators [17]; indeed *WOR2* had been provisionally named *ZCF33* to

indicate it was the 33rd protein annotated with this zinc cluster motif. *HAP3* is predicted to contain a motif similar to the CCAAT-binding factor. The genes *CSRI* and orf19.4972 are predicted to each contain multiple C₂H₂ zinc fingers, a well-characterized DNA binding domain. Because chromatin structure has been proposed to play a role in regulating the white-opaque switch [18], we also chose to investigate the opaque-enriched transcript *PHO23*, which encodes a protein containing a PHD domain and is predicted to be a part of the *RPD3* histone deacetylase complex.

For each of these candidate genes, we attempted to make homozygous deletion mutants in a white strain that is mating type **a**, and is thus permissive for switching to the opaque cell type (*C. albicans* is diploid, and it is therefore necessary to knock out two copies of each gene). Multiple independent deletion mutants of each target gene were made from independent heterozygous mutants. Despite numerous attempts, we were unable to create a homozygous knockout mutant of the *CSRI* gene and did not study *CSRI* further. White-opaque switching can occur in strains that are mating type **a** or α but not **a**/ α . Most of the work presented in this paper was performed in **a** strains, but we know that Wor1 is also required for opaque formation in α strains (not shown) [15], suggesting that white-opaque switching is controlled the same way in **a** and α strains. Consistent with this idea, a large set of microarray data indicates that the set of genes regulated by white-opaque switching is virtually identical in **a** and α cells [3].

For the five remaining candidates, we performed quantitative white-to-opaque switching assays as described previously [5] on at least two independent deletion mutants for each candidate gene, and multiple experiments were performed for each mutant (Table 1). As shown in Table 1, two mutants, the *czf1* Δ /*czf1* Δ and *wor2* Δ /*wor2* Δ

knockouts, had a dramatic effect on white-opaque switching, forming opaque colonies much less frequently than did otherwise isogenic wild type (WT) **a** strains. The *CZF1* deletion strain formed opaque sectors and colonies ~50-fold less frequently than WT **a** strains. The *wor2Δ/wor2Δ* mutant was never observed to form opaque colonies, representing a switching frequency at least 180-fold below that of the parent strain. Due to the key role this gene has in white-opaque switching, as described in this paper, we named the gene *WOR2* (*White-Opaque Regulator 2*). These results implicate both *CZF1* and *WOR2* in the white-opaque switch; formally, they function as activators of the opaque state.

To verify the defects in white-opaque switching were attributable to the disrupted genes, we complemented the *czf1Δ/czf1Δ* and *wor2Δ/wor2Δ* deletion mutants. Ectopic expression constructs, controlled by the *MET3* promoter were introduced into the *RP10* locus, as described previously [19]. Both the *czf1Δ/czf1Δ pMET3-CZF1* and *wor2Δ/wor2Δ pMET3-WOR2* strains were able to form opaque colonies when the *MET3* promoter was induced. However, when an empty vector was introduced, or the strains were grown on media that repressed the *MET3* promoter (and thus the only copy of *CZF1* or *WOR2*, respectively), the strains remained white. These results confirm that the loss of *CZF1* or *WOR2* drastically reduces the ability for the strains to grow as opaque cells.

The deletion mutants lacking either *orf19.4972* or *HAP3* formed opaque colonies at frequencies comparable to WT **a** strains and were not studied further. The *pho23Δ/pho23Δ* mutant switched to the opaque phase approximately six times as frequently as the WT control. If Pho23 works with Rpd3 in *C. albicans*, as is predicted based on homology in *S. cerevisiae*, this result is consistent with a previous finding that

rpd3Δ/rpd3Δ mutants have an increased frequency of inter-conversion between the white and opaque phases [18]. We did not study Pho23 further because of its relatively small affect on switching frequencies, and because these effects could well be indirect: in *S. cerevisiae*, deletion of *RPD3* affects transcription levels of approximately 13% of the genome [20].

Ectopic expression of *CZF1*, but not *WOR2*, results in opaque formation in a cells

We next expressed *CZF1* and *WOR2* ectopically in white cells to test whether either could drive white cells to the opaque form. All ectopic expression constructs described in this study were controlled by the *MET3* promoter integrated at the *RPI0* locus, as previously described [19]. To test if ectopic expression of a given gene causes white-opaque switching, white strains were streaked from frozen stock onto repressing media and grown at room temperature for one week. The strains were then plated for single colonies onto inducing media or repressing media, as a control, and grown for one week at room temperature. The control **a** strain, with an empty vector (pCaEXP) inserted into the *RPI0* locus, switched to the opaque phase at the typical low frequency, producing opaque sectors in approximately 0.5% of the colonies on both media conditions (Table 2), indicating that the media conditions used to control the *MET3* promoter do not significantly influence the frequency of white-opaque switching.

We found that ectopic expression of *CZF1* in WT **a** cells led to a mass conversion to the opaque phase (Table 2), but only when the *MET3* promoter was induced. In contrast, expression of a *pMET3-WOR2* construct did not drive the white-to-opaque switching; the cells remained white, based on colony appearance (Table 2) and cell shape

(not shown). We know that the *pMET3-WOR2* construct is functional from the complementation studies described earlier, thus this result indicates that the ectopic expression of *WOR2*, at least at the level driven by the *MET3* promoter, is not sufficient to drive opaque formation in an otherwise WT **a** strain.

Genetic epistasis shows that *WOR1* is downstream of *CZF1* and *WOR2* in the regulation of the white-opaque switch

Previous work on the regulation of white-opaque switching identified *WOR1* as a master regulator of the white-opaque switch [11,12,13]. In the next set of experiments, we tested the genetic interactions between *WOR1*, *CZF1* and *WOR2* in order to understand how they work together to regulate the switch. As is the case for *CZF1* and *WOR2*, deletion of *WOR1* drastically reduces the frequency of opaque formation. Like *CZF1*, ectopic expression of *WOR1* causes mass conversion to the opaque phase in otherwise wild-type **a** cells.

We first expressed *WOR1* ectopically in a *czf1Δ/czf1Δ* or *wor2Δ/wor2Δ* **a**-cell strain and observed the effects on white-opaque switching. We found that when *WOR1* was ectopically expressed in white *czf1Δ/czf1Δ* mutants, most of the colonies grew in the opaque phase or had opaque sectors (Table 2), although the colonies had a slightly rougher texture than did conventional opaque colonies on inducing media (not shown). Inspection of the cells from the opaque colonies revealed elongated cells, typical of opaque cells (Figure 1). In a control experiment, a *czf1Δ/czf1Δ* mutant with pCaEXP, an expression vector lacking *WOR1*, was not converted into opaque cells (Table 2).

When we expressed *WOR1* ectopically in a white *wor2Δ/wor2Δ a* strain, we observed that all of the colonies contained cells that had switched to the opaque phase (Figure 1), usually in the form of opaque sectors, though the opaque sectors were slightly lighter in color than those of normal opaques (Table 2). This strain was never observed to form opaque cells when grown on media that repressed expression of the ectopic *WOR1*. The *wor2Δ/wor2Δ* strain with pCaEXP, an empty expression vector, also appeared locked in the white phase, whether it was grown on the repressing or inducing media (Table 2).

Next, we tested the effects of ectopic expression of *CZF1* in a *wor1Δ/wor1Δ a* strain. We found that these strains remained locked in the white phase (Table 2); they were indistinguishable from a *wor1Δ/wor1Δ* mutant. Finally, we tested the ectopic expression of *WOR2* in a *wor1Δ/wor1Δ a* strain, and we found no change in the switching frequency, as compared to a *wor1Δ/wor1Δ* mutant (Table 2). This result was expected, given that induction of the *WOR2* ectopic construct had no effect in a wild-type background.

Taken together, these results indicate that *CZF1* and *WOR2* function upstream of *WOR1*; thus ectopic expression of *WOR1* suffices for opaque cell formation whether or not *WOR2* and *CZF1* are present. However, the converse is not true: deletion of *WOR1* cannot be overcome by ectopic expression of *CZF1*.

***CZF1* contributes to formation of the opaque state, but is not necessary for heritability of the opaque state.**

Unlike *wor1Δ/wor1Δ* and *wor2Δ/wor2Δ* mutants, *czf1Δ/czf1Δ* mutants do form opaque colonies, albeit infrequently. As described above, ectopic *CZF1* expression can induce a switch to the opaque state. To clarify *CZF1*'s role in white-opaque switching, we examined switching in the reverse direction, where opaque cells switch to white cells. When opaque isolates of wild type **a** strains are replated on repressing media, about 16% of the colonies switch back to the white form (Table 1). The rare opaque isolates of *czf1Δ/czf1Δ* **a** strains were nearly as stable as WT opaques; upon replating, 23% of the colonies contained white cells.

Because opaque isolates in *czf1Δ/czf1Δ* strains are rare, we sought to create more opaque *czf1Δ/czf1Δ* isolates in order to test the stability of the opaque cells lacking Czf1. To do this, we used the *pMET3-WOR1* ectopic expression construct to drive *czf1Δ/czf1Δ* strains to the opaque state, as described above. When the *pMET3-WOR1* construct was subsequently repressed in the *czf1Δ/czf1Δ* opaque **a** strains, at least 92% of the colonies remained opaque (Table 3). Similarly, a pulse of *pMET3-WOR1* in wild type white **a** cells is sufficient to generate stable opaque populations; the ectopic Wor1 expression can be repressed and the strains will largely continue to grow in the opaque phase (Table 3) [11]. These data indicate that, although its presence is important to form opaque cells, Czf1 contributes minimally to the stability (that is, the heritability) of the opaque state, once it has been established.

***WOR2* is necessary for the stability of the opaque state**

In parallel with the studies described above, we examined *WOR2*'s role in maintaining the heritability of the opaque state. As described, when *WOR1* was

ectopically expressed in *wor2Δ/wor2Δ* mutants, opaque cells are formed. When the *pMET3-WOR1* construct was then repressed in these cells (Table 3), the majority of the cells reverted to the white form (Table 3). In contrast, *WOR2/WOR2* control strains remained in the opaque form for many generations after the pulse of *WOR1* expression. These results indicate that *Wor2* contributes greatly to the stability of the opaque state, once it has been formed.

Deletion of *EFG1* causes opaque formation in *a*, but not *a/a* strains.

Thus far, we have only considered the role of the opaque-enriched transcription factors *WOR1*, *CZF1*, and *WOR2* in the regulation of the white-opaque switch. However, a fourth regulator, *EFG1*, which is up-regulated in white cells, is known to participate in white-opaque switching [14,15]. Experiments reported by Sonneborn, *et al* [14], suggested that depletion of *Efg1* induced the formation of opaque cells in some *a/a* strain backgrounds, but not in others. To clarify these results, we constructed new isogenic homozygous *efg1Δ/efg1Δ* mutants in *a* or *a/a* strains. In the mating type *a* strain, we found the *efg1Δ/efg1Δ* mutation caused a majority of the population to switch to the opaque phase; over 98% of the colonies contained opaque sectors (Table 4), with many colonies showing multiple sectors. We also observed a small number of entirely white colonies, indicating that *EFG1* is not strictly necessary for growth in the white phase. We also examined the opaque-to-white switching frequency in *efg1Δ/efg1Δ* mutants; we found that they switched to the white phase ~80 times less frequently than WT *a* strains (Table 4). Thus, deletion of *EFG1* dramatically increased the likelihood the cells will grow in the opaque phase, confirming previous studies in WO-1, an *α* strain [15].

In contrast to the previous reports, we never observed opaque colonies or sectors in the *efg1Δ/efg1Δ* mutant in an **a**/ α strain, despite observing over 3200 colonies (data not shown). We obtained the previously published *efg1Δ/PCK_{pr}-EFG1* **a**/ α mutant that showed opaque cell formation when remaining allele of *EFG1* was repressed [14]. Using PCR to amplify the *MTLa1* and *MTLa2* genes, we determined that this mutant was an **a** strain, likely due to spontaneous loss of one copy of chromosome 5, which carries the mating type-like (*MTL*) locus (Figure 2). Additionally, each of the *efg1Δ/efg1Δ* mutants that were locked in the white phase was confirmed to be an **a**/ α strains (Figure 2). These results indicate that the loss of Efg1 from **a** cells causes massive conversion to the opaque state, but this conversion is blocked in **a**/ α cells. Thus Efg1 functions upstream of the α 1- α 2 block of white-opaque switching.

Epistasis among *EFG1*, *CZF1*, and *WOR2*

To understand the genetic interplay between *EFG1*, *CZF1*, and *WOR2*, we created strains that lacked the white-enriched regulator (*EFG1*) and each of the opaque-enriched regulators (*CZF1* or *WOR2*). These double homozygous knockouts were then tested in quantitative switching assays and monitored for the frequency of forming white, opaque, and sectorial colonies. Nearly all colonies of the *efg1Δ/efg1Δ czf1Δ/czf1Δ* mutant were in the opaque phase or contained opaque sectors (Table 4), reflecting the phenotype of the *efg1Δ/efg1Δ* mutant. When the opaque colonies isolated from *efg1Δ/efg1Δ czf1Δ/czf1Δ* were replated to test the heritability of the state, only 0.08% of the colonies returned to the white state, in comparison with the normal opaque-to-white switching frequency, where ~16% of the colonies are white or have white sectors. Thus, the

efg1Δ/efg1Δ czf1Δ/czf1Δ opaque cells are approximately 200-fold more stable than WT opaque cells, a stability similar to that of *efg1Δ/efg1Δ* mutants (Table 4). Thus, in both forward and reverse switching frequency, the *efg1Δ/efg1Δ czf1Δ/czf1Δ* double mutants closely resembled the *efg1Δ/efg1Δ* single mutant.

We also examined the switching behavior of an *efg1Δ/efg1Δ wor2Δ/wor2Δ* mutant. In this strain, white colonies accounted for ~99% of the total colonies seen, reflecting the phenotype of the *wor2Δ/wor2Δ* mutant. We also tested the stability of these rare opaque colonies that were formed by the *efg1Δ/efg1Δ wor2Δ/wor2Δ* mutant. When replated, these opaque cells proved to be highly unstable; over 98% of the colonies were white or contained white sectors. Thus, in both forward and reverse switching, the *efg1Δ/efg1Δ wor2Δ/wor2Δ* double mutant resembled the *wor2Δ/wor2Δ* mutant.

Wor1 is bound to DNA upstream of *CZF1*, *WOR2*, and *EFG1*

The genetic epistasis data presented above places *WOR1* at the center of white-opaque regulation; formally, it is the most “downstream” regulator of opaque formation, as its deletion blocks white-opaque switching in all contexts tested. Moreover, ectopic *WOR1* expression suffices to switch white cells to opaque cells when any of the other opaque-enriched transcription factors are deleted. Previous work indicated that Wor1 expression is maintained through an auto-stimulatory positive feedback loop, mediated by Wor1 binding at its own promoter [11]. Expression of *Czf1*, *Wor2*, and *Efg1* are all regulated by white-opaque switching; in the opaque form, *CZF1* and *WOR2* are up-regulated, and *EFG1* is down-regulated relative to the white form. Thus, in a formal sense all three are regulated by Wor1.

To test whether Wor1 directly regulates *CZF1*, *WOR2*, and *EFG1*, we performed chromatin-immunoprecipitation (ChIP) using an affinity purified antibody (α -Wor1_{Nterm}), raised against a peptide near the N-terminus of Wor1. Precipitated DNA was amplified, fluorescently labeled, and competitively hybridized against genomic DNA (input DNA) on custom DNA tiling microarrays containing 60-mer oligonucleotides tiled at 80 base pair (bp) intervals across the entire *C. albicans* genome (ChIP-chip). Two microarrays were hybridized with DNA from two separate IPs of an opaque wild type **a** strain; a single ChIP was performed in a *wor1* Δ /*wor1* Δ (white) **a** strain as a control.

We examined the Wor1 ChIP data using previously published software that implements a statistical model and integrates data from several neighboring spots along chromosomes to identify IP enrichment peaks [21]. Using standard parameters, this procedure identified 206 peaks of Wor1 enrichment across the genome in opaque cells. These peaks of Wor1 enrichment were confirmed by visual inspection of ChIP-chip data plotted along chromosomes. Twenty-five of these peaks also appeared in the ChIP-chip of a *wor1* Δ /*wor1* Δ strain, and likely represent cross reactivity or particularly “sticky” proteins; they were removed from further analysis, leaving a set of 181 peaks of Wor1 enrichment. In parallel, we performed a series of ChIP-chip experiments using a different antibody against Wor1 (raised against a peptide at the C-terminus of the Wor1 protein, α -Wor1_{Cterm}) and identified 122 peaks of Wor1 enrichment in opaque strains that were not detected in the *wor1* Δ /*wor1* Δ control strain. By comparing the sets of peaks of Wor1 enrichment identified using both antibodies, we found that 112 peaks are enriched for Wor1 in opaque cells (but not *wor1* Δ /*wor1* Δ strains) using both antibodies. Thus, 112/122 (92%) of the peaks identified using the α -Wor1_{Cterm} were also found using the N-

terminal antibody, indicating the set of peaks identified with α -Wor1_{Cterm} is almost entirely a subset α -Wor1_{Nterm} CHIP-chip data. We found that 112/181 (62%) of the targets identified in using the α -Wor1_{Nterm} antibody were also detected using the α -Wor1_{Cterm} in opaque cells. Because the experiments using α -Wor1_{Nterm} exhibited very little cross-reactivity in *wor1* Δ /*wor1* Δ strains and virtually encompassed the set found using α -Wor1_{Cterm}, we chose the targets identified in the α -Wor1_{Nterm} CHIP-chip as our set of high-confidence Wor1 targets for further analysis.

With 181 peaks identified as high confidence Wor1 targets using the α -Wor1_{Nterm} antibody, we turned to the question of identifying the genes potentially regulated by Wor1. We chose to limit the set to the 170 peaks positioned in intergenic regions upstream of at least one open reading frame (ORF); this eliminated three peaks positioned within ORFs and eight peaks positioned between convergent ORFs. Because some of the 170 peaks of Wor1 enrichment lay in the intergenic region of divergently transcribed genes, there are 221 genes potentially regulated by Wor1 (Supplemental Table S1).

We found clear Wor1 enrichment at the intergenic regions immediately upstream of the *CZF1*, *WOR2* and *EFG1* coding sequences (Figure 3). In the ~7.6 kb of intergenic sequence upstream of *CZF1*, we found segments that were enriched up to 20-fold for Wor1, as compared to a *wor1* Δ /*wor1* Δ control strain. Upstream of the *WOR2* coding sequence, we found segments enriched up to 11-fold. Wor1 was enriched up to ~12-fold in the 10.1 kb upstream of *EFG1*. We also verified that Wor1 was found upstream of the *WOR1* gene using the tiling arrays, showing enrichment up to ~80-fold in the opaque cells, as compared to the control *wor1* Δ /*wor1* Δ strain (Figure 3) [11]. These results

confirm that Wor1 is present at its own promoter in opaque cells, and reveal that Wor1 is also present at the promoters of *CZF1*, *WOR2*, and *EFG1* in opaque **a** cells.

We also compared the set of 221 genes potentially regulated directly by Wor1 to the set of genes differentially transcribed between white and opaque cells [3]. We found Wor1 enrichment at the intergenic regions upstream of 38 opaque-enriched genes and 20 white-enriched genes (Supplemental Table S1), suggesting that Wor1 directly controls expression of approximately 15% of the genes regulated by white-opaque switching. These results also suggest that Wor1 may function in opaque cells as both a transcriptional repressor and as an activator. Though there is some ambiguity in ascribing Wor1 regulation at divergently transcribed genes, we estimate that Wor1 also binds more than 100 genes that have not been previously identified as white- or opaque-enriched by transcriptional profiling.

As described above, Wor1 protein is bound at the intergenic DNA upstream of the genes *WOR1*, *EFG1*, *CZF1*, and *WOR2*. Each of these genes has a remarkably long upstream region of DNA (at least 7kb in each case), and Wor1 appears to be bound at multiple positions along these regions. From the ChIP-chip experiments, we found that occupancy of large intergenic regions is a general characteristic of Wor1. Analysis of the intergenic regions at all 6077 gene promoters in the *C. albicans* genome (excluding those at telomeres) revealed a median promoter length of 623bp, whereas the median promoter length of the 181 gene promoters bound by Wor1 was 3390bp (data not shown). This preference is especially pronounced when considering the intergenic regions over 10kb; Wor1 enrichment was seen at 12 of 19 of these intergenic regions. Intriguingly, over half (7 of 12) of these intergenic regions lie upstream of sequence-specific DNA binding

proteins — *WOR1*, *RFG1*, *TCC1*, *WOR2*, *ZCF37*, *EFG1*, and *RME1* — suggesting *Wor1* may exert much of its control over the white-opaque switch indirectly through other transcriptional regulators.

DISCUSSION

In this paper, we have dissected the genetic circuitry controlling white-opaque switching in the fungal pathogen *C. albicans*. White-opaque switching is an epigenetic change between two distinctive types of cells, both containing the same genome. The white-opaque switch is crucial for many aspects of *C. albicans* biology, including interactions with other *C. albicans* cells (pheromone sensing and mating) and interactions with the host (opportunistic pathogenesis). Our results are summarized in Figures 4 and 5, where the circuitry controlling this switch is diagrammed. This network of positive feedback loops is responsible for the heritability of each state, as well as the frequency of switching between them, and we propose that the structure of this network makes an important contribution to the biology of white-opaque switching.

The default state can be considered the white cell type: most clinical isolates of *C. albicans* are **a**/ α cells, and they are locked in the white state through $a1$ - $\alpha2$ repression of *WOR1* (Figure 5A). However, even in **a** and α cells, which are permissive for white-opaque switching, the white cell type still seems to be the default, in that white cells are generally more stable than opaque cells (Figure 5B). For example, opaque cells at 24°C are stable for many generations, but above 30°C they become unstable and rapidly switch back *en masse* to the white form, which is stable under these conditions [1,2]. There are no known environmental conditions which comparably destabilize the white form. In our

model, the opaque form is generated when the series of positive feedback loops shown in Figure 4 become excited (Figure 5C). Thus, in opaque cells, *WOR1* likely directly induces *CZF1* and *WOR2* expression, and in turn, *CZF1* and *WOR2* both activate *WOR1*. *CZF1* does this by repressing a repressor of the opaque state (*EFG1*), the net effect being a positive feedback loop.

The multiple feedback loops observed in the opaque state are reminiscent of those seen in differentiated animal cells, such as those of the *Drosophila* eye ([22], reviewed in [23]) and the mammalian myoblast ([24], reviewed in [25]). A series of such feedback loops (as opposed to a single loop) buffers the circuit against transient fluctuations in any single regulatory protein and therefore provides additional stability to the excited form of the circuit. In addition, the nature of the circuit probably defines the switching frequency. For example, deletion of *CZF1* decreases the white-to-opaque switching frequency by approximately 10-fold, but has little effect on the backwards switching rate. Thus, the primary role of *CZF1* seems to be in modulating the switching frequency; in contrast, *WOR1* and *WOR2* are both required to maintain the opaque state; thus their roles are more integral to the switch itself.

Although the overall logic of the circuit shown in Figure 4 can explain many features of white-opaque switching, there appear to be several unusual features of the circuit components themselves that likely also play important roles in white-opaque switching. For example, our ChIP-chip experiments revealed that *Wor1* binding shows a bias towards genes with unusually long upstream intergenic regions – as defined by the distance from the 5' end of the open reading frame to the next annotated coding region. This observation suggests that these genes bound by *Wor1*, which include the four

transcriptional regulators that form the interlocking feedback loops (*WOR1*, *EFG1*, *CZF1*, and *WOR2*) are also controlled by a number of other transcriptional regulators. It is known that the frequency of white-opaque switching can be influenced by environmental cues (e.g. temperature and oxidative stress) [1,26], and it seems plausible that different rates of switching could be “set” by individually adjusting the levels of the regulatory proteins that make up the circuit. For example, since deletion of *CZF1* reduces the frequency of white-to-opaque switching 10-fold, regulation of the level of Czf1 by environmental signals could directly control the “forward” switching rate. Another unusual feature of the circuit concerns the wide distribution of Wor1 over much of the upstream regions of *WOR1*, *EFG1*, *CZF1*, and *WOR2* (Figure 3), suggesting a highly cooperative transcriptional response to the intracellular levels of *WOR1*. This, combined with the interlocking positive feedback loops, could be responsible for the switch-like behavior of the system, specifically the failure to readily observe a cell type intermediate between white and opaque in wild-type switching strains.

The switch from the white to the opaque form growth alters transcription of approximately 400 genes. We know that the master regulator Wor1 ultimately controls all of these genes, since deletion of *WOR1* locks cells in the white form, and ectopic expression of *WOR1* converts white cells *en masse* to opaque cells. Our ChIP-chip analysis revealed that Wor1 directly regulates approximately 15% of this gene set (20 white-enriched genes and 38 opaque-enriched genes). Since Wor1 is also bound upstream of *CZF1*, *EFG1*, *WOR2*, and 20 additional transcriptional regulators (see Supplemental Table S1), it seems likely that much of white-opaque switching program is regulated indirectly by Wor1 through its effects on other transcriptional regulators.

An unexpected outcome of the Wor1 ChIP-chip experiments was the presence of Wor1 at a large number of genes that were not identified as white- or opaque-enriched in previous microarray analyses [3]. There are several explanations for this observation. First, Wor1 could control these genes in both white and opaque cells, with their transcription being unaffected by the white-to-opaque transition. We think this explanation is unlikely because Wor1 is up-regulated 45-fold in opaque cells [3], and it seems unlikely that this change could have no impact on expression of target genes. To test this idea directly, we performed a Wor1 ChIP-chip experiment in white cells, and found that Wor1 is not bound at any of these target genes (data not shown). A second possibility, one that we favor, is that Wor1 may occupy the promoters of these 100 genes in opaque cells, preparing their expression to respond to unknown environmental signals, perhaps those generated by the host. According to this idea, the standard laboratory conditions used for transcriptional profiling would not have included the necessary environmental stimuli, and thus these genes would not have been identified as regulated by the white-opaque switch. This idea suggests there are additional aspects to white-opaque switching which have not been previously recognized.

Finally we note that white-opaque switching does not appear to be a general feature of fungi, even those that are closely related to *C. albicans*. Indeed it may have arisen during *C. albicans*' long association with its warm-blooded hosts. The evolution of a complex circuit composed of interlocking feedback loops is relatively simple to imagine, as it could occur stepwise simply through the acquisitions of cis-acting sequences in genes for transcriptional regulators used for other purposes in the cell. We note that *CZF1* also represses *EFG1* in the regulation of hyphal growth under embedded

conditions [27], and this genetic relationship has been maintained in the regulation of the white-opaque switch. Thus *EFG1* and *CZF1* have other key functions in the cell—even in cells that are genetically blocked for white-opaque switching—and their involvement in white-opaque switching could well be a recent adaptation, functioning to modulate the stability of the two states and the frequency of switching between them. The independent evolution of interlocking transcriptional feedback loops in a variety of distinct biological contexts (white-opaque switching in *C. albicans*, eye development in flies, and muscle development in mammals, for example) suggests they are particularly effective ways of providing, from the same genome, distinctive cell types that can be stably propagated for many generations.

METHODS

All strains and primers used in this study are listed in Supplemental Tables S2 and S3, respectively. DNA sequences of *C. albicans* genes were obtained from the *Candida* Genome Database (www.candidagenome.org)

Media

Standard laboratory media have been described previously [28]. Synthetic complete media, supplemented with 2% glucose and 100µg/ml uridine (SCD+Urd) was used to maintain strains in the white and opaque phases at room temperature. For ectopic expression experiments, cells were grown on inducing media (SCD-Met-Cys+Urd) or repressing media (SCD+Met+Cys+Urd) to control expression of the *MET3* promoter, as described previously [11,19].

Plasmids

The plasmid containing the *pMET3-WOR1* construct (pRZ25) has been described before [11]. To make the *pMET3-WOR2* and *pMET3-CZF1* constructs, the *WOR2* or *CZF1* ORFs was PCR-amplified from SC5314 genomic DNA using primers containing BamHI and SphI restriction sites, and cloned into a BamHI/SphI-digested pCaEXP, to create the plasmids pAJ2230 and pAJ2231, respectively.

Strain construction

All strains were derived from SC5314. *EFG1*, *CZF1* or *WOR2* was deleted using a modified Ura-blaster protocol [29]. In short, the recyclable *URA3-dpl200* marker was PCR-amplified from pDDB57 using long oligonucleotides identical to the sequence immediately flanking each ORF targeted for deletion. The deletion construct was transformed into CHY439 ($\alpha1\Delta\alpha2\Delta$, Ura-) or CAI4 (\mathbf{a}/α , Ura-) and transformants were selected on SD-Ura media. 5- fluoroorotic acid was used to counter-select against *URA3* marker, and the resulting Ura- isolates were used for subsequent rounds of gene deletion or to create the ectopic expression strains. For each knockout target, at least two homozygous deletion mutants were created from independent heterozygous mutants. When creating double mutants, *CZF1* and *WOR2* were each deleted in an *efg1Δ/efg1Δ* ($\alpha1\Delta\alpha2\Delta$, Ura-) mutant. In the case of the *efg1Δ/efg1Δ wor2Δ/wor2Δ* mutant, two independent double mutants were created from two independent *efg1Δ/efg1Δ* homozygous deletion mutants. Each *WOR1* allele was deleted from the strain SNY78 (\mathbf{a}/α , His-, Leu-, Ura-) using fusion knockout constructs described previously [11]. The

resulting strain was grown on sorbose-containing media to generate **a/a** strains (see [6] and references therein), creating the *wor1Δ/wor1Δ* (**a/a**, Ura-) strain.

Ectopic expression constructs pAJ2230, pAJ2231, pRZ25 (described above), or pCaEXP (empty control vector [19]) were linearized to direct integration to the *RP10* locus and transformed into Ura- isolates of WT, *wor2Δ/wor2Δ*, *czf1Δ/czf1Δ*, or *wor1Δ/wor1Δ* strains. To create the duplicate ectopic expression strains listed in Table S2, ectopic expression constructs were introduced into independent *wor1Δ/wor1Δ* or *wor2Δ/wor2Δ* strains. The *czf1Δ/czf1Δ* (Ura-) strains used to create the *czf1Δ/czf1Δ* + *pMET3-WOR1* ectopic expression strains are different Ura- loopout isolates generated by 5-fluoroorotic acid counter-selection of the same *czf1Δ/czf1Δ* (Ura+) strain. The *czf1Δ/czf1Δ* + *pMET3-CZF1* complementation strains were made from the same *czf1Δ/czf1Δ* knockout strain.

Basic white-opaque switching assays

Switching frequencies between the white and opaque phases were determined in plate-based assays, as described previously, with modifications [5]. Strains were streaked from frozen stock onto SCD+Urd and grown at RT for 5-7 day. For each strain, at least 5 entirely white colonies were resuspended into dH₂O, diluted, and plated for single colonies on SCD+Urd. After growth at RT for one week, we examined the colonies and counted the number of switch events (as evidenced by the presence of opaque sectors, or entirely opaque colonies). The same process was used to assess opaque-to-white switching, but the original frozen stocks contained opaque isolates of each strain, and we monitored switching by the presence of white sectors or entirely white colonies. The data

shown in Tables 1 and 4 were taken from the same representative experiment and only tested one strain of each genotype. In repetitions of the switching assays (not shown), multiple independent deletion mutants of each genotype were tested and yielded results similar to those shown in Tables 1 and 4.

White-opaque switching using ectopic expression constructs and cell images

Switching assays in strains containing the *pMET3* ectopic expression constructs were performed as described in [11], with modifications. In short, to test if ectopic expression can drive opaque formation, white strains were streaked from frozen stock onto repressing media at RT for five days. At least five fully white colonies were replated for single colonies on inducing media (or repressing, as control). After growth at RT for one week, colony phenotypes were recorded. Colonies were resuspended in sterile water and cells were examined by using differential interference contrast microscopy on an Axiovert 200M microscope (Carl Zeiss, Oberkochen, Germany). All experimental strains, excepting the *wor1* Δ /*wor1* Δ + *pMET3-WOR2* strains, were tested in at least two repetitions of the switching assay. Data shown in Table 2 are from a single representative experiment, and each strain listed is an independent ectopic expression mutant.

To test if the resulting colony phenotypes were stable after the ectopic expression was repressed, opaque strains (formed by induction of the ectopic expression constructs) were streaked from frozen stock onto inducing media at room temperature. At least five opaque colonies were resuspended in sterile dH₂O and replated onto repressing media (or inducing, as control) and grown at RT for one week. Colony phenotypes were recorded.

Two independently-derived strains were tested for each ectopic expression scenario, and experiments were performed at least twice. Data shown in Table 3 are from a single representative experiment, and each strain listed is an independent ectopic expression mutant.

Determination of mating type in *C. albicans*

To determine the mating type of *C. albicans* strains, we PCR amplified the “a” and “α” alleles of each gene located within the *MTL* locus (*PAP*, *OBP*, *PIK*, *MTLa1*, *MTLa2*, *MTLa1*, *MTLa2*) [30]. PCR products for every “a” allele were seen in all strains tested; products for each “α” allele were seen in all strains except SS4, provided courtesy of Sonneborn *et al.* (not shown) [14]. PCR products for the *MTLa1* and *MTLa2* genes are shown in Figure 2.

ChIP experiments

Overnight cultures (200ml) were grown in SCD+Urd for ≈16h at 25°C to an OD₆₀₀ of 0.4. Cells were formaldehyde cross-linked by adding formaldehyde (37%) to a 1% final concentration. Treated cultures were mixed by shaking and incubated for 15 minutes at room temperature. 2.5M glycine was added to a final concentration of 125mM, and treated cultures were mixed and incubated 5 minutes at room temperature. Cells were pelleted at 3,000 × g for 5 minutes at 4°C and washed twice with 100ml 4°C TBS (20mM TrisHCl, pH7.6/150mM NaCl).

Spheroplasting and ChIP were carried out as previously described, with modifications [11,31]. Cell pellets were resuspended in 39 ml Buffer Z (1 M sorbitol, 50

mM Tris-Cl [pH 7.4]), 28 μ l of β -ME was added (14.3 M, final concentration 10 mM), and cells were vortexed. 20 μ l of lyticase (Sigma, MO, United States) solution (2 mg/ml in Buffer Z) was added, and cell suspensions were incubated 15 minutes at 30°C. Spheroplasted cells were then spun at 3,000 \times g, 10 min, at 4 °C and resuspended in 500 μ l 4°C lysis buffer (50 mM HEPES-KOH, pH 7.5, 140 mM NaCl, 1 mM EDTA, 1% Triton X-100, 0.1% sodium deoxycholate) with protease inhibitors. All subsequent ChIP and wash steps were done at 4°C. DNA was sheared by sonication 10 times for 10 sec at power setting 2 on a Branson 450 sonicator (Danbury, CT), incubating on ice for 2 min between sonication pulses. Extracts were clarified by centrifugation. 50 μ l of extract were set aside as ChIP input material

For the immunoprecipitation (IP), 450 μ l of lysis buffer was added to 50 μ l extract, and 5 μ l of α -Wor1_{Nterm} antibody was added. α -Wor1_{Nterm} is an affinity-purified antibody generated against a peptide QVLDKQLEPVSRPHERER, located near the N-terminus of Wor1 (Bethyl Laboratories, Montgomery, TX). The IP was incubated 2 hrs at 4°C, with agitation. Then, 50 μ l of a 50% suspension of protein A-Sepharose Fast-Flow beads (Sigma, St. Louis, MO, United States) in lysis buffer was added to the IP and incubated 1.5hr at 4°C, with agitation. The beads were pelleted 1 min at 3,000 \times g. After removal of the supernatant, the beads were washed with a series of buffers for five min for each wash: twice in lysis buffer, twice in high salt lysis buffer (50 mM HEPES-KOH, pH 7.5, 500 mM NaCl, 1 mM EDTA, 1% Triton X-100, 0.1% sodium deoxycholate), twice in wash buffer (10 mM Tris-HCl [pH 8.0], 250 mM LiCl, 0.5% NP-40, 0.5% sodium deoxycholate, 1mM EDTA), and once in TE (10 mM Tris, 1 mM EDTA [pH 8.0]). After the last wash, 100 μ l of elution buffer (50 mM Tris-HCl [pH 8.0], 10 mM

EDTA, 1% SDS)) was added to each sample, and the beads were incubated at 65 °C for 15 min. The beads were spun for 1 min at 10,000 × g, and the supernatant was removed and retained. A second elution was carried out with 150 µl elution buffer 2 (TE, 0.67% SDS) and eluates from the two elution steps were combined. For the ChIP input material set aside, SDS (1% final concentration) and 200µl TE were added. ChIP and input samples were incubated overnight at 65°C to reverse the formaldehyde crosslinks. 250µl proteinase K solution (TE, 20 µg/ml glycogen, 400 µg/ml Proteinase K) were added to each sample, and samples were incubated at 37°C for 2h. Samples were extracted once with 450 µl Tris buffer-saturated phenol/chloroform/isoamyl alcohol solution (25:24:1). 55µl 4M LiCl and 1ml 100% ethanol (4°C) were added and the DNA was precipitated 1hr at 4°C. The DNA was pelleted by centrifugation at 14,000 × g for 15 min at 4 °C, washed once with cold 75% ethanol, and allowed to air dry. The samples were resuspended in 25µl TE containing 100µg/ml RNaseA and incubated 1hr at 37°C.

ChIPs were also carried out in experiments not shown using affinity-purified antibody generated against a peptide DDAVGNSSGSYYTGT, located at the C terminus of Wor1 (α -Wor1_{Cterm}) (Bethyl Laboratories, Montgomery, TX) [11]. ChIP was performed in WT opaque strains twice using α -Wor1_{Nterm} and three times using the α -Wor1_{Cterm} antibodies. Control ChIPs were performed in the *wor1* Δ /*wor1* Δ mutants using α -Wor1_{Nterm} once, and the α -Wor1_{Cterm} was used twice.

DNA amplification and labeling

ChIP-enriched DNA was amplified and fluorescence labeled as described [32]. Labeled DNA for each channel was combined and hybridized to arrays in Agilent hybridization chambers for 40 hours at 65°C, according to protocols supplied by Agilent

(Agilent Technologies, Santa Clara, CA). Arrays were then washed and scanned, using an Axon Instruments Genepix 4000A scanner.

Tiling Array Design

Approximately 185,000 60-mer oligo probes were designed across the entire *Candida* genome (contig20 haploid genome assembly) at approximately 80 bp intervals, excluding non-unique regions of the genome (see Supplemental Protocol S1 for further information). Custom microarrays were manufactured by Agilent Technologies (Agilent Technologies, Santa Clara, CA). Array design and ChIP-chip data are available on GEO.

Data Analysis

Arrays were blank subtraction normalized, inter-array median normalized, and intra-array median normalized using Agilent ChIP Analytics 1.3 software (Agilent Technologies, Santa Clara, CA). After normalization, average ratios across replicate arrays (where relevant) were used for further analysis. After normalization, the single array error model was applied across replicate arrays (where relevant), to derive a p-value statistic to represent the probabilities that data at each spot occurred within experimental noise. A segment is a region of adjacent probes containing peaks of Wor1-enrichment, where the enrichment above input is considered to be statistically significant, based on the parameters set in the software. Using the ChIP Analytics software, the Whitehead Neighborhood Model was applied using default parameters as described [21] to map the segments according to their chromosomal positions. When comparing ChIP-chip experiments in WT opaque strains against *wor1Δ/wor1Δ* strains, or between α -Wor1

ChIP-chip experiments performed in WT opaque strains using the two different Wor1 antibodies, any overlapping segments were eliminated from further analysis.

Within each segment, we used ChIP Analytics software to identify the location of highest Wor1 enrichment (corresponding to the probe with the lowest $P[\bar{x}]$ -value). The positions of peaks were then assessed in relationship to ORFs throughout the *C. albicans* genome; an ORF was identified as being potentially regulated by Wor1 if there was a segment of Wor1-enrichment within the intergenic region immediately upstream of the given coding sequence.

ACKNOWLEDGEMENTS

We thank Joachim Ernst (Institut für Mikrobiologie, Germany) for providing the *EFGI* mutant strains SS4 and HLC52. We also thank Hana El-Samad, David Pincus, and members of the Johnson Lab for many helpful discussions and reagents. R.E.Z. was supported by an Achievement Rewards for College Scientists (ARCS) Foundation scholarship. M.G.M. was supported by a Howard Hughes Medical Institute Fellowship. D.J.G. and B.B.T. were supported by fellowships from the National Science Foundation. Research was supported by grants from the Ellison Foundation and the National Institutes of Health (RO1 AI49187) to A.D.J.

REFERENCES

1. Slutsky B, Staebell M, Anderson J, Risen L, Pfaller M, et al. (1987) "White-opaque transition": a second high-frequency switching system in *Candida albicans*. *J Bacteriol* 169: 189-197.
2. Rikkerink EH, Magee BB, Magee PT (1988) Opaque-white phenotype transition: a programmed morphological transition in *Candida albicans*. *J Bacteriol* 170: 895-899.
3. Tsong AE, Miller MG, Raisner RM, Johnson AD (2003) Evolution of a combinatorial transcriptional circuit: a case study in yeasts. *Cell* 115: 389-399.
4. Lan CY, Newport G, Murillo LA, Jones T, Scherer S, et al. (2002) Metabolic specialization associated with phenotypic switching in *Candida albicans*. *Proc Natl Acad Sci U S A* 99: 14907-14912.
5. Miller MG, Johnson AD (2002) White-opaque switching in *Candida albicans* is controlled by mating-type locus homeodomain proteins and allows efficient mating. *Cell* 110: 293-302.
6. Bennett RJ, Uhl MA, Miller MG, Johnson AD (2003) Identification and characterization of a *Candida albicans* mating pheromone. *Mol Cell Biol* 23: 8189-8201.
7. Lockhart SR, Zhao R, Daniels KJ, Soll DR (2003) Alpha-pheromone-induced "shmooing" and gene regulation require white-opaque switching during *Candida albicans* mating. *Eukaryot Cell* 2: 847-855.
8. Bennett RJ, Miller MG, Chua PR, Maxon ME, Johnson AD (2005) Nuclear fusion occurs during mating in *Candida albicans* and is dependent on the *KAR3* gene. *Mol Microbiol* 55: 1046-1059.

9. Lachke SA, Lockhart SR, Daniels KJ, Soll DR (2003) Skin facilitates *Candida albicans* mating. *Infect Immun* 71: 4970-4976.
10. Kvaal CA, Srikantha T, Soll DR (1997) Misexpression of the white-phase-specific gene WH11 in the opaque phase of *Candida albicans* affects switching and virulence. *Infect Immun* 65: 4468-4475.
11. Zordan RE, Galgoczy DJ, Johnson AD (2006) Epigenetic properties of white-opaque switching in *Candida albicans* are based on a self-sustaining transcriptional feedback loop. *Proc Natl Acad Sci U S A* 103: 12807-12812.
12. Huang G, Wang H, Chou S, Nie X, Chen J, et al. (2006) Bistable expression of WOR1, a master regulator of white-opaque switching in *Candida albicans*. *Proc Natl Acad Sci U S A* 103: 12813-12818.
13. Srikantha T, Borneman AR, Daniels KJ, Pujol C, Wu W, et al. (2006) TOS9 regulates white-opaque switching in *Candida albicans*. *Eukaryot Cell* 5: 1674-1687.
14. Sonneborn A, Tebarth B, Ernst JF (1999) Control of white-opaque phenotypic switching in *Candida albicans* by the Efg1p morphogenetic regulator. *Infect Immun* 67: 4655-4660.
15. Srikantha T, Tsai LK, Daniels K, Soll DR (2000) EFG1 null mutants of *Candida albicans* switch but cannot express the complete phenotype of white-phase budding cells. *J Bacteriol* 182: 1580-1591.
16. Brown DH, Jr., Giusani AD, Chen X, Kumamoto CA (1999) Filamentous growth of *Candida albicans* in response to physical environmental cues and its regulation by the unique CZF1 gene. *Mol Microbiol* 34: 651-662.

17. MacPherson S, Laroche M, Turcotte B (2006) A fungal family of transcriptional regulators: the zinc cluster proteins. *Microbiol Mol Biol Rev* 70: 583-604.
18. Srikantha T, Tsai L, Daniels K, Klar AJ, Soll DR (2001) The histone deacetylase genes HDA1 and RPD3 play distinct roles in regulation of high-frequency phenotypic switching in *Candida albicans*. *J Bacteriol* 183: 4614-4625.
19. Care RS, Trevethick J, Binley KM, Sudbery PE (1999) The MET3 promoter: a new tool for *Candida albicans* molecular genetics. *Mol Microbiol* 34: 792-798.
20. Hughes TR, Marton MJ, Jones AR, Roberts CJ, Stoughton R, et al. (2000) Functional discovery via a compendium of expression profiles. *Cell* 102: 109-126.
21. Pokholok DK, Harbison CT, Levine S, Cole M, Hannett NM, et al. (2005) Genome-wide map of nucleosome acetylation and methylation in yeast. *Cell* 122: 517-527.
22. Czerny T, Halder G, Kloter U, Souabni A, Gehring WJ, et al. (1999) twin of eyeless, a second Pax-6 gene of *Drosophila*, acts upstream of eyeless in the control of eye development. *Mol Cell* 3: 297-307.
23. Silver SJ, Rebay I (2005) Signaling circuitries in development: insights from the retinal determination gene network. *Development* 132: 3-13.
24. Molkenin JD, Olson EN (1996) Combinatorial control of muscle development by basic helix-loop-helix and MADS-box transcription factors. *Proc Natl Acad Sci U S A* 93: 9366-9373.
25. Tapscott SJ (2005) The circuitry of a master switch: MyoD and the regulation of skeletal muscle gene transcription. *Development* 132: 2685-2695.

26. Kolotila MP, Diamond RD (1990) Effects of neutrophils and in vitro oxidants on survival and phenotypic switching of *Candida albicans* WO-1. *Infect Immun* 58: 1174-1179.
27. Vences MD, Haas C, Kumamoto CA (2006) Expression of the *Candida albicans* morphogenesis regulator gene *CZF1* and its regulation by *Efg1p* and *Czf1p*. *Eukaryot Cell* 5: 825-835.
28. Guthrie C, and G. R. Fink (1991) *Guide to yeast genetics and molecular biology*. San Diego, CA: Academic Press.
29. Wilson RB, Davis D, Enloe BM, Mitchell AP (2000) A recyclable *Candida albicans* *URA3* cassette for PCR product-directed gene disruptions. *Yeast* 16: 65-70.
30. Hull CM, Johnson AD (1999) Identification of a mating type-like locus in the asexual pathogenic yeast *Candida albicans*. *Science* 285: 1271-1275.
31. Liu CL, Kaplan T, Kim M, Buratowski S, Schreiber SL, et al. (2005) Single-nucleosome mapping of histone modifications in *S. cerevisiae*. *PLoS Biol* 3: e328.
32. Iyer VR, Horak CE, Scafe CS, Botstein D, Snyder M, et al. (2001) Genomic binding sites of the yeast cell-cycle transcription factors *SBF* and *MBF*. *Nature* 409: 533-538.

Table 1.

Strain	White → Opaque		Opaque → White	
	Switching frequency	n	Switching frequency	n
WT	5.4%	1263	16.48%	2761
<i>czf1</i> Δ / <i>czf1</i> Δ	0.1%	2400	23.58%	725
<i>wor2</i> Δ / <i>wor2</i> Δ	<0.03%	3000	--N/A--	
<i>hap3</i> Δ / <i>hap3</i> Δ	5.2%	1410	--not tested--	
<i>orf19.4972</i> Δ / <i>orf19.4972</i> Δ	4.0%	1360	--not tested--	
<i>pho23</i> Δ / <i>pho23</i> Δ	30.3%	597	--not tested--	

Table 1. White-opaque switching frequency in mutants lacking putative opaque-enriched transcriptional regulators.

White-opaque switching assays were performed to determine the white-to-opaque switch frequency (left columns) and opaque-to-white switch frequency (right columns) for each homozygous mutant. Values shown represent the percentage of total colonies which displayed colony phenotypes different from the original state, either as sectors or entire colonies. All strains are mating-type **a** strains. As described in the Materials and Methods, all white-opaque switching assays described in this paper were performed multiple times using multiple independent mutant strains, giving qualitatively similar results. The results shown are for a single mutant from a representative experiment.

Table 2.

Strain	Ectopic expression construct	OFF → OFF		OFF → ON	
		Switching frequency	n	Switching frequency	n
WT	control	0.48%	210	0.53%	561
WT	<i>CZF1</i>	1.04%	193	100%	615
WT	<i>WOR2</i>	1.38%	145	1.19%	589
WT	<i>WOR1</i>	1.38%	145	100%	598
<i>czf1</i> Δ/ <i>czf1</i> Δ	control	<0.64%	156	<0.15%	676
<i>czf1</i> Δ/ <i>czf1</i> Δ	<i>WOR1</i>	13.71%	124	100%	417
<i>wor2</i> Δ/ <i>wor2</i> Δ	control	<0.61%	163	<0.15%	682
<i>wor2</i> Δ/ <i>wor2</i> Δ	<i>WOR1</i>	<0.65%	153	100%	519
<i>wor2</i> Δ/ <i>wor2</i> Δ	<i>WOR1</i>	<0.60%	168	100%	595
<i>wor1</i> Δ/ <i>wor1</i> Δ	control	<0.57%	174	<0.13%	752
<i>wor1</i> Δ/ <i>wor1</i> Δ	<i>CZF1</i>	<0.45%	223	<0.17%	573
<i>wor1</i> Δ/ <i>wor1</i> Δ	<i>CZF1</i>	<0.58%	172	<0.16%	609
<i>wor1</i> Δ/ <i>wor1</i> Δ	<i>WOR2</i>	<0.48%	209	<0.14%	709
<i>wor1</i> Δ/ <i>wor1</i> Δ	<i>WOR2</i>	<0.60%	166	<0.19%	525
<i>wor1</i> Δ/ <i>wor1</i> Δ	<i>WOR1</i>	<0.99%	101	100%	416

Table 2. White-to-opaque switching frequencies in strains ectopically expressing *CZF1*, *WOR1*, or *WOR2*.

White isolates grown on media that represses the ectopic expression construct were replated onto repressing media as a control (OFF → OFF), or onto inducing media (OFF → ON). Switching frequency was calculated as the percentage of total colonies that contained opaque sectors or were entirely opaque. As explained in the text, the opaque colonies vary in appearance when *WOR1* is ectopically expressed in each mutant strain. All strains are **a** strains. As described in the Materials and Methods, all white-opaque switching assays described in this paper were performed multiple times using multiple independent mutant strains, giving qualitatively similar results. The results shown are from a single representative experiment; each row represents an independently derived strain tested in this representative experiment.

Figure 1.

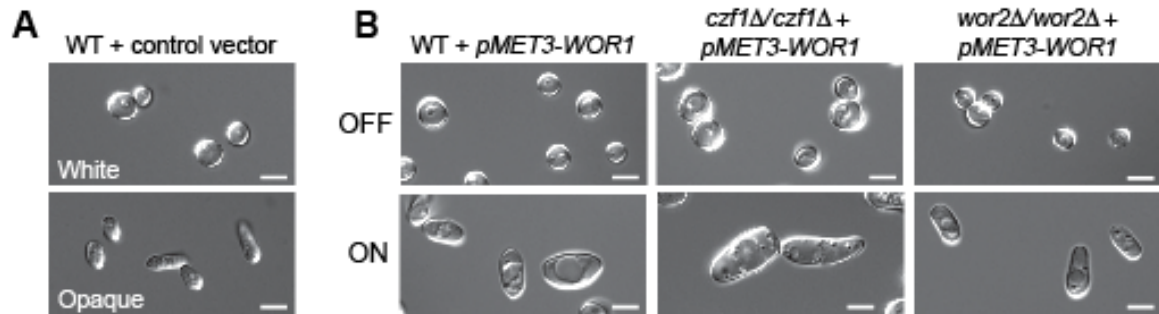


Figure 1. Ectopic expression of *WOR1* drives opaque formation in *czf1Δ/czf1Δ* or *wor2Δ/wor2Δ* strains.

Panels are DIC images of cells resuspended from colonies. *Panel A*: White and opaque isolates of WT strains with an empty control vector, grown on media that induces the *MET3* promoter (on). *Panel B*: Ectopic expression of *WOR1* in WT, *czf1Δ/czf1Δ*, or *wor2Δ/wor2Δ* strains; cells were grown on media to repress (OFF) or induce (ON) the *pMET3-WOR1* construct. All strains are **a** strains. Scale bar = 5μm.

Table 3.

Strain	Ectopic expression construct	ON → ON		ON → OFF	
		Switching frequency	n	Switching frequency	n
WT	control	<0.37%	272	1.2%	1046
WT	<i>WOR1</i>	<0.97%	103	2.1%	908
<i>czf1</i> Δ/ <i>czf1</i> Δ	<i>WOR1</i>	7.5%	93	6.7%	475
<i>czf1</i> Δ/ <i>czf1</i> Δ	<i>WOR1</i>	2.6%	195	<0.25%	407
<i>wor2</i> Δ/ <i>wor2</i> Δ	<i>WOR1</i>	27%	202	79%	876
<i>wor2</i> Δ/ <i>wor2</i> Δ	<i>WOR1</i>	31%	141	91%	1114

Table 3. Stability of the opaque state when ectopic expression of *WOR1* is repressed.

Opaque cells grown on media that induces ectopic *WOR1* expression were replated onto inducing media (ON → ON) as a control, or onto repressing media (ON → OFF), to turn off ectopic *WOR1* expression. Switching frequency was calculated as the percentage of total colonies that contained white sectors or were entirely white. As explained in the text, the opaque colonies vary in appearance when *WOR1* is ectopically expressed in each mutant strain. All strains are **a** strains. As described in the Materials and Methods, all white-opaque switching assays described in this paper were performed multiple times using multiple independent mutant strains, giving qualitatively similar results. The results shown are from a single representative experiment; each row represents an independently derived strain tested in this representative experiment.

Table 4.

Strain	White → Opaque		Opaque → White	
	Switching frequency	n	Switching frequency	n
WT	5.4%	1263	16.48%	2761
<i>efg1</i> Δ/ <i>efg1</i> Δ	98.3%	904	0.21%	1428
<i>efg1</i> Δ/ <i>efg1</i> Δ; <i>czf1</i> Δ/ <i>czf1</i> Δ	98.4%	1172	0.08%	1209
<i>efg1</i> Δ/ <i>efg1</i> Δ; <i>wor2</i> Δ/ <i>wor2</i> Δ	0.09%	2120	98.77%	810

Table 4. Epistasis among *EFG1*, *CZF1*, and *WOR2* in the regulation of white-opaque switching.

White-opaque switching assays were performed to determine the white-to-opaque switch frequency (left columns) and opaque-to-white switch frequency (right columns) for each homozygous mutant. Values shown represent the percentage of total colonies which displayed colony phenotypes different from the original state, either as sectors or entire colonies. All strains are mating-type **a** strains. As described in the Materials and Methods, all white-opaque switching assays described in this paper were performed multiple times using multiple independent mutant strains, giving qualitatively similar results. The results shown are for a single mutant from a representative experiment, which was the same experiment shown in Table 1; thus the switching frequency in the WT strain is identical.

Figure 2.

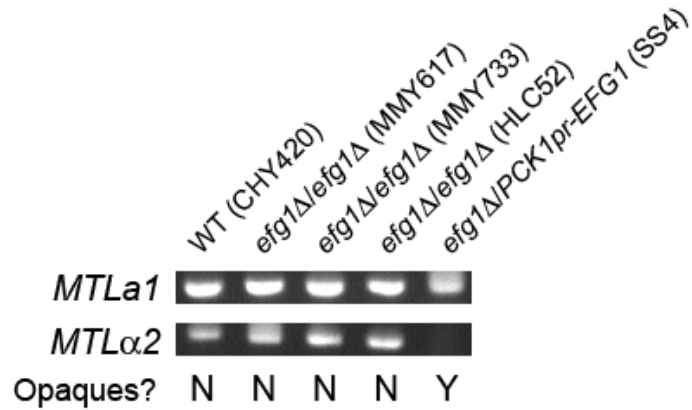


Figure 2. Verification of mating type in *efg1Δ/efg1Δ* strains.

Whole cell PCR was performed to verify the presence of the *MTLα1* and *MTLα2* genes in a series of *efg1Δ/efg1Δ* mutants. As described in Materials and Methods, PCR amplification of the **a** and **α** alleles of each of the five genes present at the mating type locus confirm these results. The ability of each mutant to form opaque colonies, as described in the Results, is indicated with Y (yes) or N (no).

Figure 3.

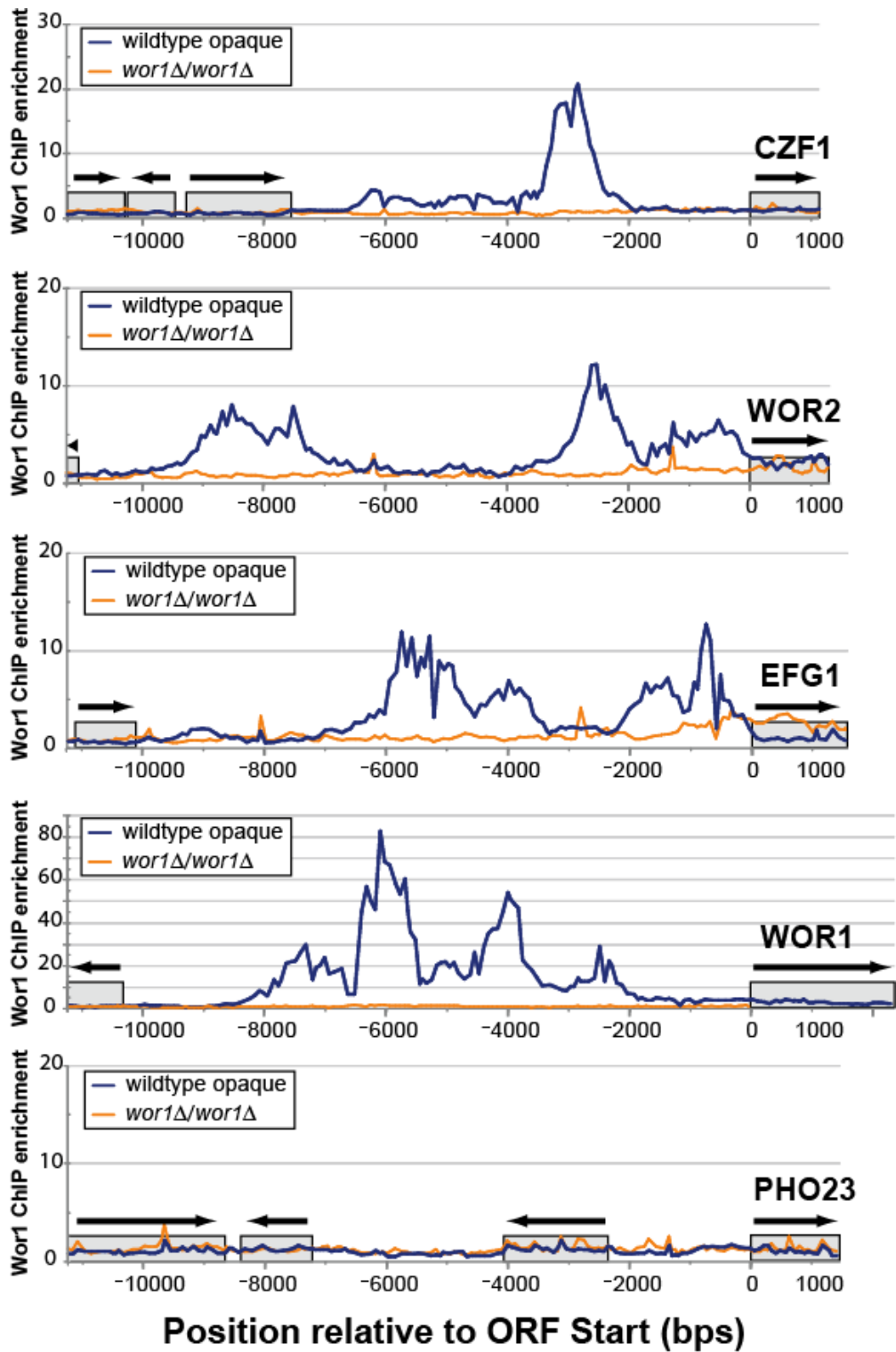


Figure 3. Wor1 binds upstream of the *CZF1*, *WOR2*, *EFG1*, and *WOR1* genes.

ChIP was performed with α -Wor1_{Nterm} antibodies in a wild type opaque **a** strain or a *wor1* Δ /*wor1* Δ (white) **a** strain. The ChIP enrichment was detected by hybridization to a *C. albicans* tiling microarray with probes every ~80bp across the genome. The top three panels show Wor1 enrichment upstream of the *CZF1*, *WOR2*, and *EFG1* ORFs. The fourth panel serves as a positive control of Wor1 enrichment, seen at the *WOR1* promoter [11]. The bottom panel, showing the DNA upstream of *PHO23*, serves as an example of the low levels of Wor1-enrichment seen throughout the majority of the genome. Grey boxes indicate ORFs and arrows indicate the orientation of each coding sequence along the chromosome.

Figure 4.

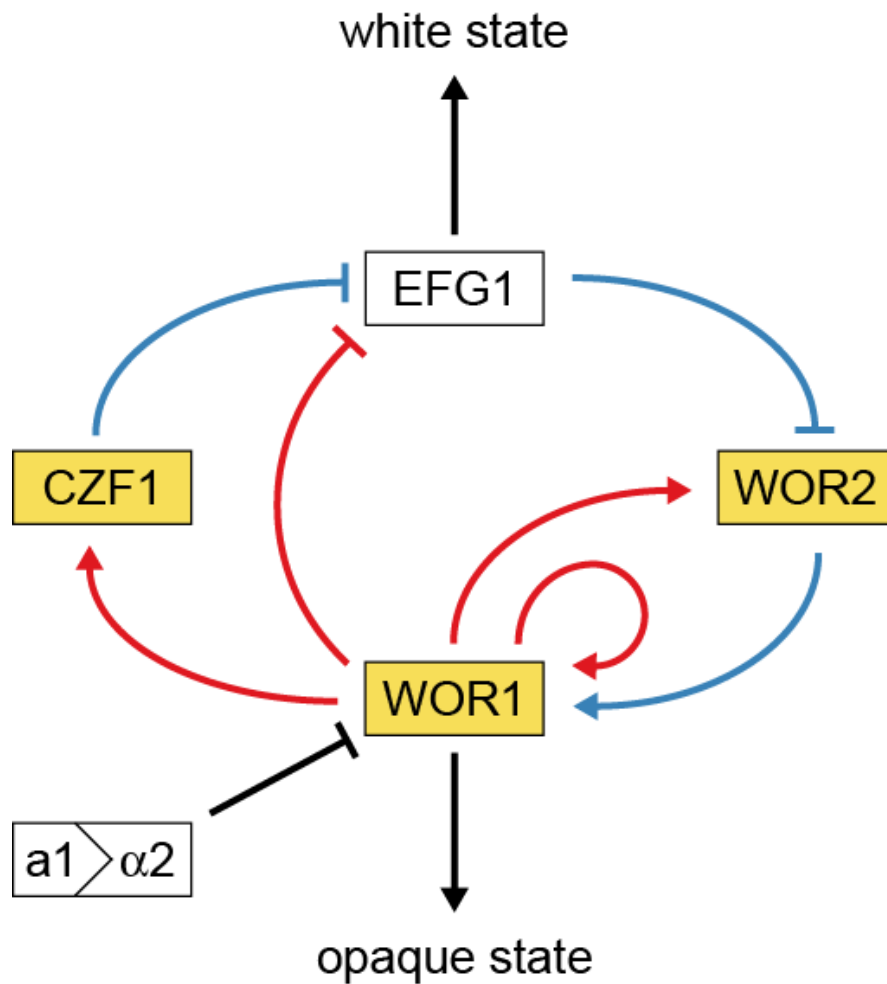


Figure 4. Model of the genetic network regulating the white-opaque switch.

White and gold boxes represent genes enriched in the white and opaque states, respectively. Blue lines represent relationships based on genetic epistasis. Red lines represent Wor1 control of each gene, based on Wor1 enrichment in chromatin immunoprecipitation experiments. Activation (arrowhead) and repression (bar) are inferred based on white- and opaque-state expression of each gene.

Figure 5.

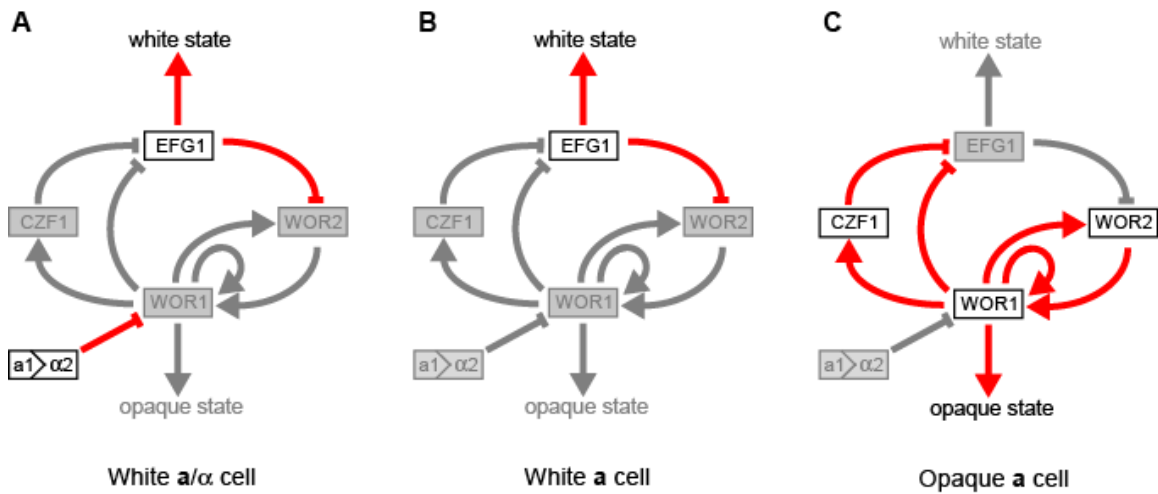


Figure 5. Activity of the white-opaque genetic regulatory network in different cell types.

In each scenario, genes indicated by white boxes are up-regulated and genes in gray boxes are down-regulated. Red lines represent active regulatory relationships; gray lines represent relationships that are inactive, due to the down-regulation of the effector gene.

Panel A: In white a/α cells, the a1-α2 heterodimer represses *WOR1*, keeping the Wor1-mediated feedback loops inactive. This allows Efg1 expression and formation of white cells.

Panel B: In white a cells, Efg1 expression contributes to the formation of white cells and down-regulates *WOR2*. This helps keep Wor1 expression low in white cells, even though the a1-α2 repression of *WOR1* has been lifted.

Panel C: In opaque a cells, Wor1 expression levels are up-regulated, which in turn activates the represented positive feedback loops; the net effect being increased Czf1, Wor2 and Wor1 expression, and decreased Efg1 expression.

Table S1. (page 1 of 6)

Classification	ID	Min P [x]	OpWh expression ratios (log ₂)	Gene name	<i>S. cerevisiae</i> orthologs	Description
TRANSCRIPTIONAL REGULATORS	orf19.4884	8.45E-07	4.11	WOR1	YEL007W	switching
	orf19.2823	8.93E-07	0.43	RFG1		hyphal genes
	orf19.6734	1.10E-06	0.09	TCC1		hyphal genes
	orf19.4056	4.37E-06	0.68	GAT2		Putative DNA-binding transcription factor
	orf19.4972	6.02E-06	2.37			Putative transcription factor (Zn finger)
	orf19.3127	7.85E-06	1.83	CZF1		Predicted transcription factor involved in hyphal growth
	orf19.7436	1.06E-05	-0.77	AAF1		Possible transcriptional regulatory protein
	orf19.5026	2.59E-05	0.26		YML081W	Putative transcription factor (Zn finger)
	orf19.5992	2.65E-05	1.77	WOR2		Putative transcription factor (Zn cluster)
	orf19.2654	4.49E-05	-0.03	RMS1	SET7	Possible transcriptional regulatory protein (SET domain)
	orf19.7381	4.90E-05	-0.17	ZCF37		Putative transcription factor (Zn finger)
	orf19.610	5.17E-05	-2.40	EFG1	SOK2	Transcriptional repressor (bHLH) involved in hyphal growth and white-opaque switching
	orf19.2356	1.12E-04	0.67	CRZ2	CRZ1	Putative transcription factor (Zn finger)
	orf19.4000	1.23E-04	-0.06		PHO2	Predicted ORF; putative transcription factor (homeobox)
	orf19.173	1.43E-04	-0.25			Putative transcription factor (Zn finger)
	orf19.6514	1.79E-04	0.15	CUP9	TOS8	homeostasis
	orf19.5729	3.14E-04	-0.44	FGR17		Putative transcription factor (Zn cluster)
	orf19.1543	3.47E-04	-0.68	OPI1	OPI1	Transcriptional factor (leucine zipper) involved in inositol biosynthesis
	orf19.5210	3.94E-04	0.81		XBP1	Predicted ORF; putative transcriptional regulator
	orf19.7046	4.04E-04	0.27	MET28		Putative transcription factor (bzip)
	orf19.4342	4.69E-04	0.53		SUT1	Putative transcription factor (Zn cluster)
	orf19.723	4.97E-04	0.32	BCR1	YPL230W	Transcription factor (Zn finger) involved in biofilm formation
	orf19.2432	5.11E-04	0.71	HAC1		Putative transcription factor (bZIP)
orf19.5001	5.47E-04	0.32	CUP2	HAA1	Similar to <i>S. cerevisiae</i> Cup2p, a copper-binding transcription factor	
TRANSLATION/ mRNA processing	orf19.7382	2.18E-06	-0.35	CAM1	CAM1	Putative translation elongation factor eEF1 gamma
	orf19.2639	9.09E-06	-0.38			Predicted ORF; putative structural protein of ribosome
	orf19.5991	2.65E-05	-0.24		DBP10	Predicted ORF; putative RNA helicase
	orf19.5495	9.31E-05	-0.53			Similar to <i>S. cerevisiae</i> NAB6, a putative RNA-binding protein
	orf19.6002	9.70E-05	-0.65	RPL8B	RPL8B	Predicted ribosomal protein
	orf19.2652	3.83E-04	0.22	TEF4		Putative translation elongation factor
	orf19.7041	4.78E-04	0.42		PTA1	Predicted ORF; putative role in mRNA processing

Table S1. (page 2 of 6)

Classification	ID	Min P[\bar{x}]	Op/Wh expression ratios (\log_2)	Gene name	<i>S. cerevisiae</i> orthologs	Description
MANNOsyl-TRANSFERASES	orf19.4900	2.45E-06	0.36		INT4 MNT	Predicted ORF; putative alpha(1,3) mannosyltransferase
	orf19.4279	4.00E-06	2.29	MNN1	MNN1	Putative alpha-1,3-mannosyltransferase
	orf19.849	7.82E-06	0.25		MNN4	Predicted ORF; possible role in protein glycosylation
	orf19.4394	5.84E-05	0.17			Predicted ORF, putative alpha(1,3) mannosyltransferase
	orf19.2881	1.02E-04	0.28	MNN4		Protein required for normal mannosylphosphorylation of oligosaccharides linked to cell wall proteins
	orf19.6996	4.48E-04	2.20			Predicted ORF; putative alpha(1,3) mannosyltransferase
	orf19.5171	6.04E-04	-0.35	PMT1	PMT1	Protein mannosyltransferase
	orf19.7549	6.52E-04	-0.47	PMT5		Protein mannosyltransferase
CELL WALL	orf19.4072	4.01E-06	0.67	IFF6		Putative GPI-anchored protein of unknown function
	orf19.4975	6.02E-06	0.20	HYR1		Predicted cell wall protein
	orf19.4651	1.58E-05	1.28	PGA53		Putative GPI-anchored protein of unknown function
	orf19.5124	3.52E-05	-0.51	RBR3		Cell wall protein
	orf19.3618	3.75E-05	-1.27	YWP1	FLO1	Cell wall protein in yeast cells; putative GPI-anchor
	orf19.3642	4.32E-05	-1.14	SUN41	SUN4	Putative cell wall protein
	orf19.220	4.75E-05	-1.18	PIR1	PIR1	Structural protein of cell wall
	orf19.2833	5.58E-05	4.74	PGA34		Putative GPI-anchored protein
	orf19.7586	6.56E-05	-0.32	CHT3	CTS1	Chitinase
	orf19.5144	1.46E-04	3.89	PGA28		Putative GPI-anchored protein
	orf19.7218	2.00E-04	-0.22	RBE1	PRY1	Putative cell wall protein
	orf19.2332	4.40E-04	0.02			Predicted ORF; putative role in cell wall biogenesis
	orf19.5267	4.41E-04	0.79			Putative cell wall protein
	orf19.570	5.42E-04	-0.33	IFF8		Putative GPI-anchored protein of unknown function
orf19.3895	6.09E-04	1.06	CHT2		Chitinase	
CELL CYCLE	orf19.1960	8.97E-06	0.26	CLN3	CLN3	G1 cyclin
	orf19.6028	1.45E-05	0.16	HGC1	CLN2	Hypha-specific G1 cyclin-related protein
	orf19.5032	5.47E-05	-1.26	SIM1	UTH1	Regulator of DNA replication
	orf19.5493	9.31E-05	-0.41	GSP1	GSP1	Small RAN G-protein
	orf19.1907	1.36E-04	-0.13	EMC9		Similar to <i>S.cerevisiae</i> NNF2, which has a putative role in chromosome segregation
	orf19.5999	2.52E-04	-0.13	DYN1		Dynein heavy chain
	orf19.4438	3.35E-04	-0.39	RME1		Protein similar to <i>S. cerevisiae</i> meiotic regulator Rme1p
	orf19.4927	3.71E-04	0.16	BNI1	BNI1	Formin
	orf19.1189	4.48E-04	-3.37			Predicted ORF; putative role in mitosis
	orf19.7564	4.92E-04	-0.32	DPB2	DPB2	Probable subunit of DNA polymerase II
	orf19.5118	7.45E-04	-0.14	SDS24	SDS24	Similar to <i>S. cerevisiae</i> SDS24, which has a predicted role in meiosis

Table S1. (page 3 of 6)

Classification	ID	Min P[\bar{x}]	Op/Wh expression ratios (\log_2)	Gene name	<i>S. cerevisiae</i> orthologs	Description
ASSORTED METABOLIC PROCESSES	orf19.4769	1.65E-06	-2.51	IPT1	IPT1	Inositol phosphoryl transferase
	orf19.7551	3.54E-06	-0.02	ALO1	ALO1	D-arabinono-1,4-lactone oxidase
	orf19.933	5.66E-06	0.45		UBC13	Predicted ORF; putative ubiquitin conjugating enzyme
	orf19.7522	5.77E-06	-1.45			Predicted ORF; possible role in NAD biosynthesis
	orf19.1409	7.54E-06	-0.13	VAC7	VAC7	Predicted role in vacuolar inheritance
	orf19.4699	1.52E-05	0.93		TGL3	Putative phospholipase of patatin family
	orf19.3707	2.30E-05	-1.25	YHB1	YHB1	Nitric oxide dioxygenase
	orf19.3708	2.30E-05	0.93	SAP2		Secreted aspartyl proteinase
	orf19.3664	2.51E-05	0.10	HSP31	HSP30	Putative chaperone
	orf19.4505	3.88E-05	4.71	ADH3		Predicted alcohol dehydrogenase
	orf19.7585	6.56E-05	-1.10	INO1	INO1	Inositol-1-phosphate synthase
	orf19.656	6.95E-05	0.05	DPP1		Putative diacylglycerol pyrophosphate phosphatase
	orf19.850	1.22E-04	0.61		NTA1	Predicted ORF; putative N-terminal asparagine amidohydrolase activity
	orf19.3674	1.38E-04	1.32		GAL10	Predicted ORF; putative UDP-glucose 4-epimerase activity
	orf19.3675	1.38E-04	0.30	GAL7	GAL7	Predicted ORF, putative UTP:galactose-1-phosphate uridylyltransferase
	orf19.2945	1.61E-04	0.35	PUT4		Putative proline permease
	orf19.4476	1.90E-04	1.73			Predicted ORF; putative aryl-alcohol dehydrogenase
	orf19.4322	2.29E-04	0.05	DAP2	DAP2	Predicted dipeptidyl aminopeptidase
	orf19.272	2.40E-04	-0.19	FAA21	FAA2	Predicted acyl CoA synthetase
	orf19.646	3.77E-04	-0.29	GLN1	GLN1	Predicted glutamate synthase
	orf19.1847	4.09E-04	0.06	ARO10	ARO10	Predicted pyruvate decarboxylase
	orf19.7610	4.40E-04	0.92	PTP3	PTP3	Predicted protein tyrosine phosphatase
	orf19.568	5.42E-04	-0.56	SPE2	SPE2	Predicted ORF, putative adenosylmethionine decarboxylase
	orf19.767	6.93E-04	0.06	ERG3	ERG3	C-5 sterol desaturase involved in ergosterol biosynthesis
orf19.7592	7.41E-04	-0.21	FAA4	FAA4	Predicted acyl CoA synthase	
orf19.5117	7.45E-04	-0.69	OLE1	OLE1	Fatty acid desaturase (stearoyl-CoA desaturase), involved in oleic acid synthesis	
TRANSPORT	orf19.5994	1.53E-06	0.80	RHB1	RHB1	arginine/lysine transport
	orf19.3669	5.17E-06	-0.36	SHA3	SKS1	Putative serine/threonine kinase involved in glucose transport
	orf19.1232	8.48E-06	0.13	VRG4	VRG4	GDP-mannose transporter
	orf19.4885	9.48E-06	-0.32	MIR1	MIR1	Putative mitochondrial phosphate transporter
	orf19.4456	1.59E-05		GAP4		Putative amino acid permease
	orf19.24	1.67E-05	-2.39	RTA2	RSB1	Putative role in fatty acid transport
	orf19.2602	1.88E-05		OPT1	OPT1	Oligopeptide transporter
	orf19.3663	2.51E-05	0.79	PHO91	PHO91	Putative low-affinity phosphate transporter
	orf19.5604	3.70E-05	-0.12	MDR1	FLR1	Multidrug efflux pump of plasma membrane
	orf19.1727	4.83E-05	0.61	PMC1	PMC1	Vacuolar calcium P-type ATPase
	orf19.2209	4.87E-05	0.62	YVC1	YVC1	Similar to <i>S. cerevisiae</i> Yvc1p, a vacuolar cation channel
	orf19.5383	5.77E-05	-0.14	PMA1	PMA1	Plasma membrane H(+)-ATPase
	orf19.5307	6.28E-05	3.64		JEN1	Predicted ORF; putative lactate transporter

Table S1. (page 4 of 6)

Classification	ID	Min P[\bar{x}]	Op/Wh expression ratios (\log_2)	Gene name	<i>S. cerevisiae</i> orthologs	Description
TRANSPORT (continued)	orf19.655	6.95E-05		PHO84	PHO84	Putative high-affinity phosphate transporter
	orf19.3668	7.40E-05	2.96	HGT2		Putative glucose transporter
	orf19.2882	1.02E-04	-1.28	XUT1		Putative xanthine-uric acid/H ⁺ symporter
	orf19.3415	1.36E-04	0.75	PTK2	PTK2	Putative protein kinase of polyamine import
	orf19.2946	1.61E-04	-0.29	HNM4		Putative choline permease
	orf19.7219	2.00E-04	-0.01	FTR1	FTR1	High-affinity iron permease
	orf19.6000	2.52E-04	0.42	CDR1	PDR5	Multidrug transporter of ABC superfamily
	orf19.4980	2.53E-04	-2.16	HSP70	SSA4	Putative chaperone of Hsp70 family
	orf19.6496	2.90E-04	0.72	TRS33	TRS33	Predicted ORF; putative role in ER-to-Golgi transport
	orf19.4346	3.08E-04	-0.02		SEC16	Predicted ORF; putative role in vesicle-mediated transport
	orf19.1932	3.15E-04	0.78	CFL4		Similar to ferric reductase
	orf19.1585	3.53E-04	1.64	ZRT2	ZRT2	Predicted zinc transporter
	orf19.1978	3.74E-04	2.41	GIT2		Putative glycerophosphoinositol permease
	orf19.6770	4.16E-04	-1.86			Predicted ORF; putative cytoskeletal adaptor
	orf19.7565	4.92E-04	-0.88	GNP3		Putative high-affinity glutamine permease
	orf19.3122	5.04E-04	0.94	ARR3	ARR3	Putative arsenite transporter
	orf19.2942	5.70E-04	0.12	DIP5	DIP5	Putative permease for dicarboxylic amino acids
	orf19.4304	5.74E-04	-0.80	GAP1		General amino acid permease
	orf19.5170	6.04E-04	0.67	ENA21		Predicted ORF, putative sodium transporter
	orf19.111	6.78E-04	-1.79	CAN2	CAN1	Putative amino acid permease
orf19.2003	6.78E-04	-0.62	HNM1		Predicted ORF; putative role in choline transport	
orf19.2002	6.78E-04	-0.30		NIC96	Predicted ORF; putative component of nuclear pore	
OTHER PROCESSES	orf19.7152	2.60E-06	0.66			Putative role in cysteine synthesis
	orf19.3239	3.62E-06	0.31		CTF18	Predicted ORF; putative role in sister chromatid cohesion
	orf19.935	5.66E-06	1.88	AGA1		Protein similar to agglutinin subunit
	orf19.696	6.56E-06	0.08	STE2	STE2	Receptor for alpha factor mating pheromone
	orf19.218	4.75E-05	-0.24	BUD20		Role in filamentous growth; similar to <i>S. cerevisiae</i> Bud20p, which affects bud site selection
	orf19.177	1.04E-04	-1.16		BEM1	Predicted ORF; putative role in establishing cell polarity
	orf19.3218	1.31E-04	1.41		YJR124C	Putative multidrug resistance protein
	orf19.6494	2.90E-04	0.48	WHI3	WHI3	Predicted ORF; putative role in regulating cell size
	orf19.4347	3.08E-04	-0.22		PRR1	Predicted ORF; putative protein kinase
	orf19.7513	3.13E-04	1.94		DIT2	Predicted ORF; putative oxidase involved in spore formation
	orf19.7042	3.40E-04	1.40			Unknown function; induced by nitric oxide
	orf19.7414	4.07E-04	-0.87	ALS6		ALS family protein
	orf19.721	4.97E-04	-0.03		GRC3	Predicted ORF; putative role in RNA processing
	orf19.1120	5.57E-04	0.09	FAV2		Unknown function; expression changes in response to mating pheromone
	orf19.768	5.93E-04	0.95	SYG1	SYG1	Predicted role in signal transduction

Table S1. (page 5 of 6)

Classification	ID	Min P[\bar{x}]	Op/Wh expression ratios (\log_2)	Gene name	S. cerevisiae orthologs	Description
UNKNOWN & PREDICTED ORFS	orf19.6805	5.37E-07	4.31			
	orf19.4883	8.45E-07	0.43			
	orf19.2822	8.93E-07	0.03			
	orf19.6736	1.10E-06	-0.10		YOR205C	
	orf19.467	1.90E-06	2.72			
	orf19.7151	2.60E-06	-0.63			
	orf19.2962	3.32E-06	0.14			
	orf19.7550	3.54E-06	-0.22	IFA14		
	orf19.3238	3.62E-06	0.09			
	orf19.4280	4.00E-06	0.45			
	orf19.1958	5.41E-06	0.28			
	orf19.7521	5.77E-06	-0.23			
	orf19.6715	6.04E-06	0.24			
	orf19.6713	6.04E-06	-0.11			
	orf19.695	6.56E-06		RGS2		
	orf19.868	7.33E-06	-3.71	ADAEC		
	orf19.867	7.33E-06	0.25			
	orf19.1959	8.97E-06	-0.11		OTU2	
	orf19.2638	9.09E-06	1.85			
	orf19.6027	1.45E-05	0.43			
	orf19.4698	1.52E-05	-0.26			
	orf19.450	1.85E-05	-0.01			
	orf19.3336	2.14E-05	-0.05			
	orf19.413	2.22E-05	2.98			
	orf19.413.1	2.22E-05	-2.21			
	orf19.2247	2.99E-05	1.54			
	orf19.7055	3.30E-05	-0.07			
	orf19.7054	3.30E-05	0.24			
	orf19.4349	3.44E-05	1.23			
	orf19.3643	4.32E-05	-0.10			
	orf19.4231	4.78E-05	-0.52	PTH2		
	orf19.206	4.79E-05	0.47			
	orf19.1728	4.83E-05	0.58			
	orf19.2210	4.87E-05	1.14			
	orf19.7380	4.90E-05				
	orf19.5302	5.03E-05		PGA31		
	orf19.5843	5.08E-05	-0.31			
	orf19.2459	5.57E-05	1.45			
	orf19.6968	5.71E-05	-0.41			
	orf19.5308	6.28E-05	0.30			

Table S1. (page 6 of 6)

Classification	ID	Min P[\bar{x}]	Op/Wh expression ratios (\log_2)	Gene name	<i>S. cerevisiae</i> orthologs	Description
UNKNOWN & PREDICTED ORFs (continued)	orf19.3282	6.59E-05	1.32			
	orf19.4820	6.67E-05	-0.53			
	orf19.4688	6.82E-05	0.06	DAG7		
	orf19.1301	7.06E-05	0.97			
	orf19.6556	7.82E-05	1.97			
	orf19.6555	7.82E-05	-0.12		HOT13	
	orf19.2725	9.11E-05	-0.02			
	orf19.2724	9.11E-05	2.03			
	orf19.4818	9.48E-05	0.62			
	orf19.1821	1.04E-04	-0.05			
	orf19.851	1.22E-04	-1.61			
	orf19.3216	1.31E-04	-0.03			
	orf19.4792	1.33E-04	0.33			
	orf19.4793	1.33E-04	-0.09		TMA16	
	orf19.1906	1.36E-04	-0.94			
	orf19.5145	1.46E-04	0.06	SSP96		
	orf19.3713	1.57E-04	-0.45			
	orf19.3714	1.57E-04	0.07			
	orf19.6311	1.72E-04	1.29			
	orf19.4321	2.29E-04	-0.38			
	orf19.258	2.45E-04	0.05			
	orf19.7502	3.06E-04	1.01			
	orf19.5728	3.14E-04	1.52		YJR111c	
	orf19.6874	3.26E-04	-1.14			
	orf19.7043	3.40E-04	1.59		YLR050C	
	orf19.1544	3.47E-04	-0.05		BUG1	
	orf19.3694	3.53E-04	-0.18			
	orf19.2653	3.83E-04	-0.15			
	orf19.6769	4.16E-04	0.38		YHL029C	
	orf19.2333	4.40E-04	0.64		YHR009C	
	orf19.3122.2	5.04E-04				
	orf19.2943.5	5.70E-04	#N/A			
	orf19.5933	5.75E-04	0.65			
	orf19.4906	5.81E-04	-0.09			
	orf19.3897	6.09E-04	1.59			
	orf19.1486	6.21E-04	-0.46			
	orf19.5069	6.21E-04	2.54		SAE3	
	orf19.4646	7.74E-04	-0.08			
	orf19.1286	9.21E-04	0.12			
	orf19.1285	9.21E-04	-0.34		YPR091C	

Table S1. ORFs with Wor1 bound at the intergenic DNA upstream of their coding sequences.

ORFs potentially directly regulated by Wor1, identified in ChIP-chip experiments performed by David Galgoczy. *ID*: orf19# of each ORF with Wor1-enrichment in the intergenic region immediately upstream of its coding sequence. *MinP[\bar{x}]*: the lowest P[\bar{x}] value for a probe within each segment of Wor1 enrichment. As calculated by Chip Analytics, the P[\bar{x}] statistic estimates the probability that a set of neighboring probes, within a window surrounding a given probe, are not enriched. *Op/Wh expression ratios (log₂)*: log₂ ratios for each ORF, compiled from expression microarrays performed by Annie Tsong comparing white and opaque isogenic strains [3]. For each MTL mutant capable of white-opaque switching, opaque/white expression ratios were calculated for each ORF. These expression ratios were then averaged between all MTL genotypes examined. Values greater than 1 indicate the gene is up-regulated at least 2-fold in the opaque state; values less than -1 indicate the gene is up-regulated at least 2-fold in the white state. *Gene name, S. cerevisiae orthologs, and Description* of each ORF were taken from the Candida Genome Database on 4/22/07 (www.candidagenome.org). Information was edited and supplemented by hand, based on current work, Pfam searches (<http://www.sanger.ac.uk/Software/Pfam/>), and GO annotations.

Table S2. Strains used in this study (page 1 of 2)

Description	Strain	Mating type	Genotype	Source	Figure/Table
Basic white-opaque switching assays					
WT	CHY420	$\alpha 1 \Delta a 2 \Delta$	<i>ura3::limm434/ura3::limm434 MTLa/mla1::HisG-URA3-HisG mtl2::HisG</i>	1	Table 1, Table 4, Figure 2
WT (opaque)	MMY288	$\alpha 1 \Delta a 2 \Delta$	<i>ura3::limm434/ura3::limm434 MTLa/mla1::HisG-URA3-HisG mtl2::HisG</i>	this study	Table 1
	MMY633	$\alpha 1 \Delta a 2 \Delta$	<i>ura3::limm434/ura3::limm434 MTLa/mla1::HisG mtl2::HisG czf1::dpi200/czf1::URA3-dpi200</i>	this study	Table 1
<i>czf1</i> Δ <i>czf1</i> Δ	MMY737	$\alpha 1 \Delta a 2 \Delta$	<i>ura3::limm434/ura3::limm434 MTLa/mla1::HisG mtl2::HisG czf1::dpi200/czf1::URA3-dpi200</i>	this study	Table 1
<i>czf1</i> Δ <i>czf1</i> Δ (opaque)	MMY834	$\alpha 1 \Delta a 2 \Delta$	<i>ura3::limm434/ura3::limm434 MTLa/mla1::HisG mtl2::HisG wor2::dpi200/wor2::URA3-dpi200</i>	this study	Table 1
<i>wor2</i> Δ <i>wor2</i> Δ	MMY627	$\alpha 1 \Delta a 2 \Delta$	<i>ura3::limm434/ura3::limm434 MTLa/mla1::HisG mtl2::HisG hap3::dpi200/hap3::URA3-dpi200</i>	this study	Table 1
<i>hap3</i> Δ <i>hap3</i> Δ	MMY637, MMY638*	$\alpha 1 \Delta a 2 \Delta$	<i>ura3::limm434/ura3::limm434 MTLa/mla1::HisG mtl2::HisG</i>	this study	Table 1
<i>orf19</i> Δ <i>orf19</i> Δ <i>orf19</i> Δ 4972 Δ	MMY656, MMY657*	$\alpha 1 \Delta a 2 \Delta$	<i>ura3::limm434/ura3::limm434 MTLa/mla1::HisG mtl2::HisG orf19</i> 4972:: <i>dpi200/orf19</i> 4972:: <i>URA3-dpi200</i>	this study	Table 1
<i>pho23</i> Δ <i>pho23</i> Δ	MMY641, MMY643*	$\alpha 1 \Delta a 2 \Delta$	<i>ura3::limm434/ura3::limm434 MTLa/mla1::HisG mtl2::HisG pho23::dpi200/pho23::URA3-dpi200</i>	this study	Table 1
<i>efg1</i> Δ <i>efg1</i> Δ	MMY620, MMY622	$\alpha 1 \Delta a 2 \Delta$	<i>ura3::limm434/ura3::limm434 MTLa/mla1::HisG mtl2::HisG efg1::dpi200/efg1::URA3-dpi200</i>	this study	Table 4
<i>efg1</i> Δ <i>efg1</i> Δ <i>czf1</i> Δ <i>czf1</i> Δ	MMY753	$\alpha 1 \Delta a 2 \Delta$	<i>ura3::limm434/ura3::limm434 MTLa/mla1::HisG mtl2::HisG efg1::dpi200/efg1::dpi200 czf1::URA3-dpi200</i>	this study	Table 4
<i>efg1</i> Δ <i>efg1</i> Δ <i>wor2</i> Δ <i>wor2</i> Δ	MMY756, MMY759	$\alpha 1 \Delta a 2 \Delta$	<i>ura3::limm434/ura3::limm434 MTLa/mla1::HisG mtl2::HisG efg1::dpi200/wor2::URA3-dpi200</i>	this study	Table 4
WT (α/α)	MLY323	<i>alpha</i>	<i>ura3::limm434/ura3::limm434 his1/his1 leu2/leu2::LEU2</i>	this study	Results
<i>wor1</i> Δ <i>wor1</i> Δ (α/α)	RZY425, RZY429	<i>alpha</i>	<i>ura3::limm434/ura3::limm434 his1/his1 leu2/leu2 wor1::HIS1/wor1::LEU2</i>	this study	Results
Determining the mating type of <i>efg1</i> Δ <i>efg1</i> Δ strains					
<i>efg1</i> Δ <i>efg1</i> Δ (α/α)	MMY617, MMY733	<i>alpha</i>	<i>ura3::limm434/ura3::limm434 efg1::dpi200/efg1::URA3-dpi200</i>	this study	Figure 2
<i>efg1</i> Δ <i>PCK_r</i> - <i>EEG1</i>	SS4	<i>a</i>	<i>ura3::immm434/ura3::immm434 ade2::hisG/ade2::hisG efg1 Δ::ADE2 [URA3-PCK1p]::EEG1</i>	3	Figure 2
<i>efg1</i> Δ <i>efg1</i> Δ (α/α)	HLC52	<i>alpha</i>	<i>ura3::immm434/ura3::immm434 efg1::hisG/efg1::hisG-URA3-hisG</i>	4	Figure 2
ChIP-chip					
<i>wor1</i> Δ <i>wor1</i> Δ	RZY219	<i>alpha</i>	<i>URA3/ura3::limm434 his1/his1 leu2/leu2 wor1::HIS1/wor1::LEU2</i>	2	Figure 3
WT (opaque)	RZY511	<i>alpha</i>	<i>URA3/ura3::limm434 his1/his1 leu2/leu2</i>	2	Figure 3

* Denotes independent homozygous knockout strains tested in replicates of the white-opaque switching assay shown in Table 1. In all cases, this independent deletion mutant had the same phenotype as the mutant documented in this paper.

1. Miller MG, Johnson AD (2002) White-opaque switching in *Candida albicans* is controlled by mating-type locus homeodomain proteins and allows efficient mating. Cell 110: 293-302.
3. Somebarn A, Tebarth B, Ernst JF (1999) Control of white-opaque phenotypic switching in *Candida albicans* by the *Efg1p* morphogenetic regulator. Infect Immun 67: 4655-4660.
4. 1. Lo HJ, Kohler JR, DiDomenico B, Loeberberg D, Cacciapuoti A, et al. (1997) Nonfilamentous *C. albicans* mutants are avirulent. Cell 90: 939-949.

Table S2. Strains used in this study (page 2 of 2)

Description	Strain	Mating type	Genotype	Source	Figure/Table
Ectopic expression strains					
WT empty vector	MMY768	$\alpha 1\Delta$ ura2 Δ	ura3::limm434/ura3::limm434 MTLA/mtla1::HisG mtl2::HisG RP10/rp10::pCaEXP	this study	Table 2, Figure 1
WT empty vector (opaque)	MMY888	$\alpha 1\Delta$ ura2 Δ	ura3::limm434/ura3::limm434 MTLA/mtla1::HisG mtl2::HisG RP10/rp10::pCaEXP	this study	Table 3, Figure 1
WT pMET3-CZF1	MMY797	$\alpha 1\Delta$ ura2 Δ	ura3::limm434/ura3::limm434 MTLA/mtla1::HisG mtl2::HisG RP10/rp10::pAJ2231	this study	Table 2
WT pMET3-WOR2	MMY786	$\alpha 1\Delta$ ura2 Δ	ura3::limm434/ura3::limm434 MTLA/mtla1::HisG mtl2::HisG RP10/rp10::pAJ2230	this study	Table 2
WT pMET3-WOR1	RZY338	afa	ura3::limm434/ura3::limm434 RP10/rp10::pRZ25	2	Table 2, Figure 1
WT pMET3-WOR1 (opaque)	RZY617	afa	ura3::limm434/ura3::limm434 RP10/rp10::pRZ25	this study	Table 3
czf1 Δ /czf1 Δ empty vector	MMY776	$\alpha 1\Delta$ ura2 Δ	ura3::limm434/ura3::limm434 MTLA/mtla1::HisG mtl2::HisG czf1::dpl200 RP10/rp10::pCaEXP	this study	Table 2
MMY803,					
MMY804		$\alpha 1\Delta$ ura2 Δ	ura3::limm434/ura3::limm434 MTLA/mtla1::HisG mtl2::HisG czf1::dpl200 RP10/rp10::pAJ2231	this study	Results
czf1 Δ /czf1 Δ + pMET3-WOR1	RZY462	$\alpha 1\Delta$ ura2 Δ	ura3::limm434/ura3::limm434 MTLA/mtla1::HisG mtl2::HisG czf1::dpl200 RP10/rp10::pRZ25	this study	Table 2, Figure 1
czf1 Δ /czf1 Δ + pMET3-WOR1 (opaque)	RZY572, RZY620	$\alpha 1\Delta$ ura2 Δ	ura3::limm434/ura3::limm434 MTLA/mtla1::HisG mtl2::HisG czf1::dpl200 RP10/rp10::pRZ25	this study	Table 3
wor2 Δ /wor2 Δ empty vector	MMY772	$\alpha 1\Delta$ ura2 Δ	ura3::limm434/ura3::limm434 MTLA/mtla1::HisG mtl2::HisG wor2::dpl200 RP10/rp10::pCaEXP	this study	Table 2
MMY787,					
MMY789		$\alpha 1\Delta$ ura2 Δ	ura3::limm434/ura3::limm434 MTLA/mtla1::HisG mtl2::HisG wor2::dpl200 RP10/rp10::pAJ2230	this study	Results
RZY463,					
RZY466		$\alpha 1\Delta$ ura2 Δ	ura3::limm434/ura3::limm434 MTLA/mtla1::HisG mtl2::HisG wor2::dpl200 RP10/rp10::pRZ25	this study	Table 2, Figure 1
RZY589,					
RZY590		$\alpha 1\Delta$ ura2 Δ	ura3::limm434/ura3::limm434 MTLA/mtla1::HisG mtl2::HisG wor2::dpl200 RP10/rp10::pRZ25	this study	Table 3
wor1 Δ /wor1 Δ + empty vector	RZY449	afa	ura3::limm434/ura3::limm434 his1/his1 leu2/leu2 wor1::HIS1/wor1::LEU2 RP10/rp10::pCaEXP	2	Table 2
RZY451,					
RZY454		afa	ura3::limm434/ura3::limm434 his1/his1 leu2/leu2 wor1::HIS1/wor1::LEU2 RP10/rp10::pAJ2231	this study	Table 2
RZY563,					
RZY569		afa	ura3::limm434/ura3::limm434 his1/his1 leu2/leu2 wor1::HIS1/wor1::LEU2 RP10/rp10::pAJ2230	this study	Table 2
wor1 Δ /wor1 Δ + pMET3-WOR2	RZY407	afa	ura3::limm434/ura3::limm434 his1/his1 leu2/leu2 wor1::HIS1/wor1::LEU2 RP10/rp10::pRZ25	2	Table 2

* Denotes independent homozygous knockout strains tested in replicates of the white-opaque switching assay shown in Table 1. In all cases, this independent deletion mutant had the same phenotype as the mutant documented in this paper.

1. Miller MG, Johnson AD (2002) White-opaque switching in *Candida albicans* is controlled by mating-type locus homeodomain proteins and allows efficient mating. *Cell* 110: 293-302.
3. Someborn A, Tebarth B, Ernst JF (1999) Control of white-opaque phenotypic switching in *Candida albicans* by the Efg1p morphogenetic regulator. *Infect Immun* 67: 4655-4660.
4. 1. Lo HJ, Kohler JR, DiDomenico B, Loeberberg D, Cacciapuoti A, et al. (1997) Nonfilamentous *C. albicans* mutants are avirulent. *Cell* 90: 939-949.

Table S3. Primers used in this study

Name	Sequence (5' to 3')*
Ectopic Expression Constructs	
WOR2 forward	cgcgatccATGACACAAATTACCTTCGTGTTTC
WOR2 reverse	cgccgcgcatgctTATATTAAGTAAATCAGCCAC
CZF1 forward	cgcgatccATGAGTTCAATACCCCAATATC
CZF1 reverse	cgccgcgcatgctTATTTACTTCTGTATTC AAC
Gene Deletion	
EFG1 forward	GTGTTTTATAAATCCCTTTTTTAATTAGCCCTTTTTGCCTCCACATTAGTTGCTCAGGTCACGTTATTTAAATATATTgitttccagtcacgacggt
EFG1 reverse	TGGGAGAAGATTATGATCTATACGTATTTCTTTTTTATTTTCTCTAAATTTGAATGAAGAAACCTTTCCAATCATtgiggaattgagcgggata
WOR2 forward	GAAGCTAATACAAAACAATAAATAATTTTGCAGTTATCCCAAATACATATACACATAAATGACTAACATCAGCgtttcccagtcacgacggt
WOR2 reverse	TCCTAGTATCATTAACATCAAAAGTATGAATATATTGGATTATTTACTATATACACATTTTGTCTACTACTACTCtgggaattgagcgggata
CZF1 forward	TTTCGATTAACAACATTCAAAACGAAACTATCTGGTATTTAAATTTCCATTTTCAACATCAAGTGTTTAAATATCAACAgitttcccagtcacgacggt
CZF1 reverse	ACACTAACATATAACAAGAGTGGTGAATTTACCTTTTTTATGAGTTTTTTTAAACGATATCCCTCCAACACACAGAGAAAGCtgggaattgagcgggata
HAP3 forward	GTTTTATTTTTATTTTTTAACTAATCTTCTCTCTTTTACATGTGAGGAGATCGTATAGTTGGAAAGATAgitttcccagtcacgacggt
HAP3 reverse	TATAACATAAATACACAGAATTTCTCTACTTTAACAATAATCACCAAGTTGGCAAAA-AAAAAACCCACAtgiggaattgagcgggata
orf19_4972 forward	GTTATAATTTCTAACCGATTAGAGCTGGAGACTTCTTGTTAATTAAGTCAGAGGCATTGCAATCCCATCTATTATTGAgitttcccagtcacgacggt
orf19_4972 reverse	TTCTAATTTTAAAAGTTCTAATAATGGCAATCTCAAACTATGTCCTTCCCTGGTTAACCAACATCTTTAGTTTtgggaattgagcgggata
PHO23 forward	TTCAATTCGATATACCTTTGAACATATTCATATCCAAAACCCAGTAAATTAACCGACCCGACACACAGGTAATTCCTTAAACAgitttcccagtcacgacggt
PHO23 reverse	TATTACTATTAATTAATTTGTTTATTACACATATGATGTATGTTGATACGACTCTTGGTTTTTATTTGGTGtgggaattgagcgggata
Mating Type Verification	
MTLa1 ORF forward	CCTGCATGAAGAAACAGAAACC
MTLa1 ORF reverse	CTATAGGCTGTTGTTCTTCTCG
MTLa2 ORF forward	GGTCATTTCCCAATGATATCC
MTLa2 ORF reverse	TTACCCTGTACAGATCTTGG
MTLa1 ORF forward	CATTCTGGTCGGATGCTCC
MTLa1 ORF reverse	GTACCCGATAGTAACTGATTG
MTLa2 ORF forward	CACATCTGGAGGCACCTTTTG
MTLa2 ORF reverse	GGTCTTTTTGCAGATACGGA
PIKa ORF forward	CCTCCTTTACATTAGAGGAC
PIKa ORF reverse	GGCAGCCTCGGATACGAAAC
PIKa ORF forward	CTAGTAGAGTTGGCAGGCC
PIKa ORF reverse	CGGCAGCACTGAAACTTTTCG
PAPa ORF forward	GGAATTGAATTGATGAATGAC
PAPa ORF reverse	CAGCCCTCTTCCCTTTTCGCA
PAP α ORF forward	CATGCCGATTCAATGGCCCC
PAP α ORF reverse	CTGGCATTCGATGAAGTCTA
OBPa ORF forward	GTGGTCAATGGAGCTGATAC
OBPa ORF reverse	ACATGGTGGTCCCAACTCC
OBP α ORF forward	CCTTCAATTGCATCGTAAAGTACC
OBP α ORF reverse	GAAGTAGACTCAGGTCATGC

*Lower case sequence represents exogenous sequence used for URA3-dpi200 gene disruption (in gene deletion oligos), or to introduce restriction sites (ectopic expression constructs).

Protocol S1. *C. albicans* Tiling Array Design

We designed custom ChIP-Chip arrays for *C. albicans* by tiling 182,900 probes of length 60bp across the ~14.3 Mb of sequence included in what, at the time of design, was the most recent build of the genome (Assembly 20 from Andre Nantel in April 2006). Rather than choose probes spaced uniformly, an effort was made to optimize four characteristics of the oligo set (uniqueness, GC content, self-annealing and sequence complexity), while still maintaining probe spacing that is close to uniform. We used a previously developed algorithm, ArrayOligoSelector[1], to score all possible probes for each of these four characteristics. These scores, as well as a penalty for a too-long or too-short distance to the neighboring probe, were integrated into a single score via a weighting scheme. Due to the lack of studies which systematically explore the importance of uniform spacing and each of the four probe characteristics on ChIP-chip quality, we chose weights based largely on intelligent guessing. Stronger weights were given to probe spacing, GC content and uniqueness than to self-annealing and sequence complexity. A Monte Carlo optimization was employed to search for the highest scoring probe set.

The highest scoring probe set found had median probe spacing (measured from oligo start to oligo start) of 80bp with a range of ~30bp to ~130bp (Figure S1).

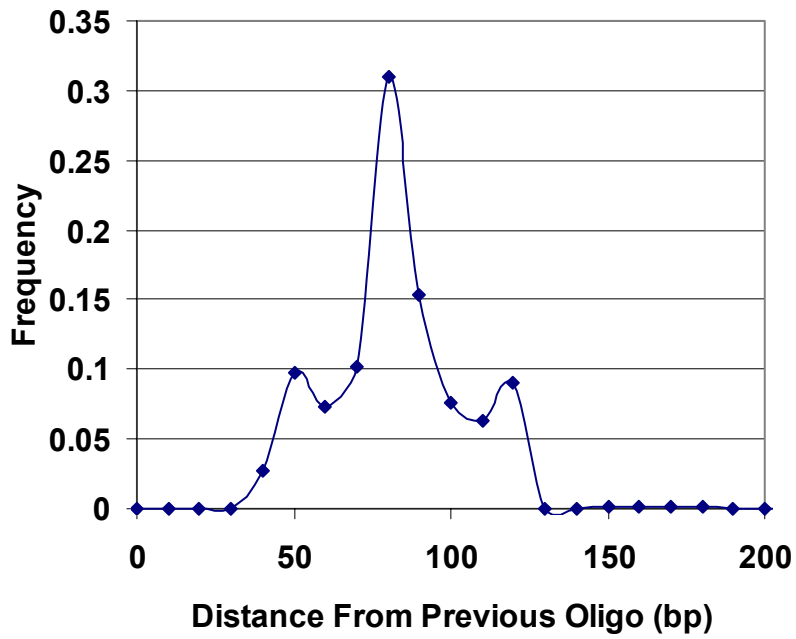


Figure S1. Oligo probe spacing across the *C. albicans* genome

The uniqueness of the probe set (blue curve) was significantly higher than that for the whole genome (red curve) (Figure S2). A higher uniqueness score indicates a more unique probe that is less likely to be affected by cross-hybridization. Whereas only 27% of all possible probes are completely unique (uniqueness score of 0.0), 40% of the probes in our probe set are completely unique. Note that the tail of this distribution (uniqueness score < 35) has been truncated in the graph.

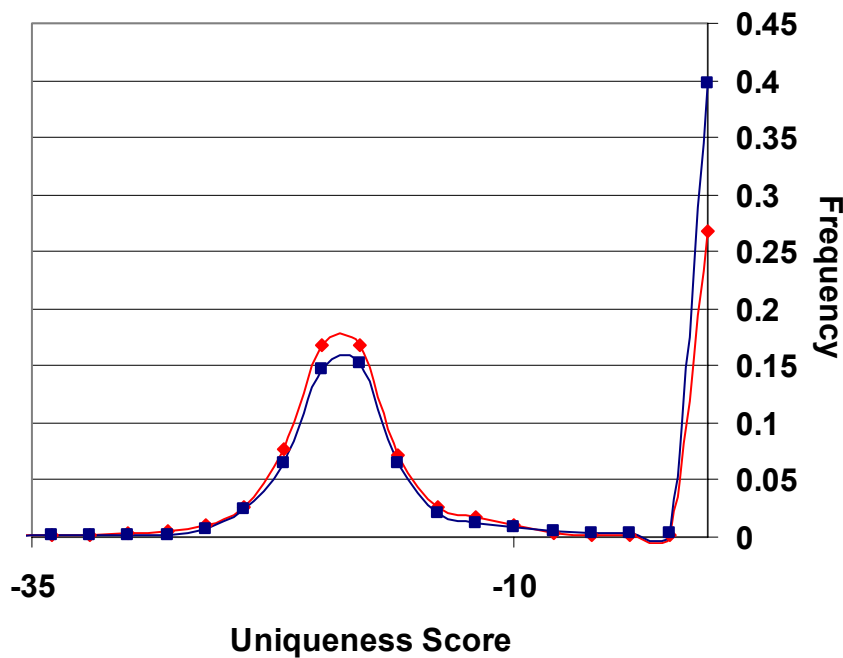


Figure S2. Uniqueness of the probe set

Finally, as shown in Figure S3, the GC content of the chosen oligos (blue curve) was much improved over the genome as a whole (red curve). While the average was kept similar to that of the whole genome (~35%), the variance was considerably reduced.

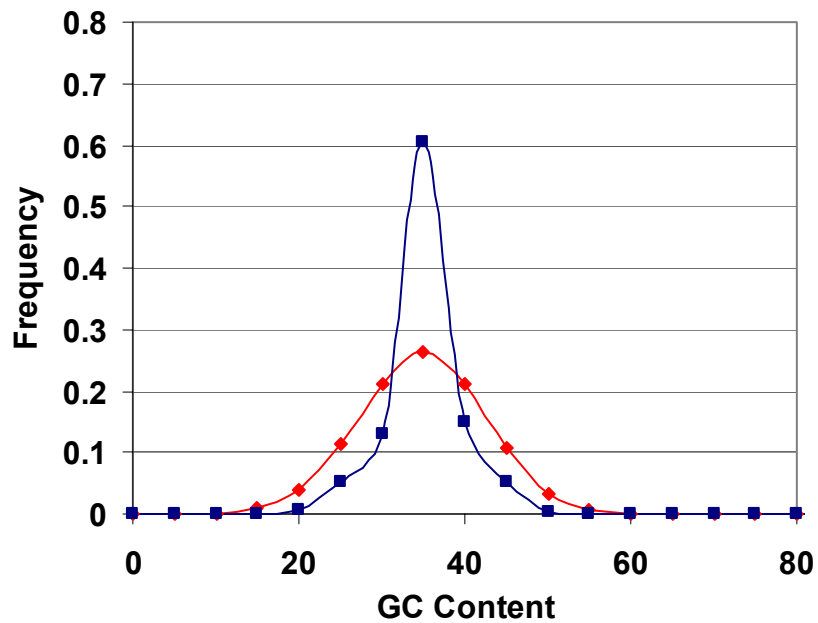


Figure S3. GC content of the probe set

Protocol S1 References

1. Bozdech Z, Zhu J, Joachimiak MP, Cohen FE, Pulliam B, et al. (2003) Expression profiling of the schizont and trophozoite stages of *Plasmodium falciparum* with a long-oligonucleotide microarray. *Genome Biol* 4: R9.

Chapter 4

White-Opaque Switching in Response to Osmolites and Surface Contact

White-Opaque Switching in Response to Osmolites and Surface Contact

INTRODUCTION

The process of white-opaque switching happens stochastically every $10^3 - 10^4$ cell generations in **a** or α cells. This low basal switching rate may allow a population of cells to largely remain in their current state, while committing a few members to the opposite state to “test the waters” of their current environment. However, in certain environments, it may be advantageous for *C. albicans* to be in either the white or the opaque state, and in these situations it would be expected that the yeast has evolved a way to efficiently detect its environment and switch to the desired state *en masse*.

Published reports show that a number of environmental conditions can drive cells into the white or opaque state. High ($\geq 37^\circ\text{C}$) and low temperatures (4°C) drive cells into the white state [1,2]. Conversely, oxidative stress drives *C. albicans* into the opaque state [3]. Initially, this result was somewhat puzzling, as the same publication reported that opaque cells were more susceptible to oxidative killing. However, more recent reports suggest that switching to the opaque state may allow *C. albicans* to evade the host immune system. Polymorphonuclear leukocytes (PMNs) move directionally in response to a chemoattractant released by white, but not opaque cells [4]. Additionally, macrophage cell lines preferentially take up white cells over opaque cells [5]. In this case, macrophage co-incubated white cells will have a higher percentage of the macrophage actively taking up cells, and each macrophage engulfs more white cells per macrophage than in similar experiments performed with opaque cells.

Preliminary data from Matt Miller indicated that certain osmolites might increase the frequency of white-to-opaque switching in *C. albicans* **a/a** or α/α cells. Matt observed that the chemical guanidine HCl caused an increase of white-to-opaque switching. However, it seems that this effect is not due to a prion, because *hsp104* Δ /*hsp104* Δ *C. albicans* strains switched at wild-type rates (unpublished data, Matt Miller). Hsp104 is a chaperone that is necessary to break up aggregated prions and facilitates transmission of prions as cells divide. Nonetheless, guanidine HCl had a dramatic effect on white-opaque switching rates, and led us to consider the possibility that guanidine was altering the switch frequency due to osmotic stress, and not through inhibiting Hsp104 in *C. albicans*. The possibility that osmotic stress could influence switching was intriguing, given that mixed *C. albicans* infections with **a** and α strains in a mouse have yielded **a/a** mating products in the kidneys of the host mice [6].

We used a panel of mutant strains, each with defects in the high osmolarity glycerol (HOG) mitogen activated protein kinase (MAPK) pathway, to examine if osmotic stress could influence white-opaque switching. Based on research of osmosensing in *Candida albicans* at the time of this project, we targeted the genes *SHO1*, *PBS2*, and *HOG1* for deletion. These mutants, as well as wild-type strains, were examined for increase opaque formation in response to the osmolites guanidine HCl, sorbitol, and KCl. Results described in this chapter show that guanidine HCl causes dramatic increases in the frequency of white-to-opaque switching. Sorbitol also induces white-to-opaque switching, and this response to sorbitol is dependent on Sho1.

In the process of examining the HOG pathway, we also considered the possibility that contact sensation was necessary in order to switch to the opaque state, and

thus studied switching on plates with varied amounts of agar or agarose as solidifying agents. We found that the frequency of the white-to-opaque switch, but not the opaque-to-white switch correlated with the concentration of agar or agarose used to solidify the plates. A portion of this response seems to be calcium-dependent, reminiscent of the role of Ca^{2+} -dependent channels in thigmotropism in *C. albicans*. We also found a role for the contact-dependent kinase, Mkc1, in white-opaque switching. Future work in the lab will focus on understanding the mechanism by which *C. albicans* senses contact and hardness of the underlying surface, and how this signal is integrated into the regulation of the white-opaque switch.

RESULTS

Mutations in the HOG MAPK pathway

To test the idea that osmotic stress would induce white-opaque switching, we decided to examine the ability of different osmolites to induce cells to grow in the opaque state. In parallel, we wanted to create a panel of mutants in the high osmolarity glycerol (HOG) pathway and determine if these mutants were able to increase the frequency of white-opaque switching in response to osmolites supplemented to the media.

I constructed *pbs2Δ/pbs2Δ* and *hog1Δ/hog1Δ* mutant strains, in both **a/α** and *a1Δ* strains. These strains appeared healthy when grown on SCD+Uri or YEPD+Ade+Uri at 30°C or 37°C. However, these mutant strains had a cold-sensitive phenotype, appearing to have dead sectors and irregular edges to the colonies when grown on either SCD+Uri or YEPD+Ade+Uri at 25°C. White-opaque switching assays are performed at 25°C, and

the irregular colony morphology seen in *pbs2Δ/pbs2Δ* and *hog1Δ/hog1Δ* strains at this temperature would make it impossible to see any opaque sectors that might form during a switching assay. Thus, these mutants were not tested for their ability to undergo white-opaque switching in response to osmolites.

A *sho1Δ/sho1Δ* (**a/a**) mutant already existed in lab (ATY362); this strain was sorbose-selected to create **a/a** isolates for use in white-opaque switching assays (RZY4). Both CHY420 (*α1Δα2Δ*) and WO-1 (*α/α*) were used as wild-type control strains.

Guanidine HCl and sorbitol increase the frequency of white-to-opaque switching

We assessed the effect of osmotic stimuli on the ability of two wild-type *C. albicans* strains and a *sho1Δ/sho1Δ* strain. These strains were grown in SCD+Uri media to mid-log phase and plated onto SCD+Uri supplemented with three different osmolites, each at three different concentrations. We used 250mM, 500mM or 1M concentration of guanidine HCl, sorbitol, or KCl. Plates were grown at RT for one week and white-opaque switching was monitored by the presence of opaque sectors or fully opaque colonies.

Repeating previous results from Matt Miller, we observed that guanidine HCl triggered a white-to-opaque switch in all strains (WT and *sho1Δ/sho1Δ*) at 250mM or 500mM concentrations (Figure 1, Table 1). Guanidine HCl was toxic to all strains at 1M concentrations. In strains that exhibited switching, colonies often appeared to be fully opaque colonies, though white colonies with opaque sectors were often seen. The high incidence of fully opaque colonies indicates that cells sense guanidine HCl and initiate the switch to the opaque state virtually immediately after the cells contact the plate.

Sorbitol is a non-ionic osmolite that is used routinely in *Saccharomyces cerevisiae* studies of osmosensing. From this study, we observed that wild type **a/a** or α/α *C. albicans* switch to the opaque state in response to sorbitol in the media (Figure 1, Table 1). The strain WO-1, a wild type α/α strain, increased its white-to-opaque switching frequency in a dose-dependent manner correlating with the concentration of sorbitol supplemented to the media. At 1M sorbitol supplemented, 100% of the WO-1 colonies observed were fully opaque. The other wild type strain tested, CHY420, exhibited increased switching to the opaque state in response to sorbitol, but it was not as robust as the response seen in WO-1; only a maximum of 50% of the colonies appeared to be opaque with a 1M sorbitol supplement. Additionally, CHY420 strains grown on sorbitol displayed interesting filamentation behaviors not seen with the other strains tested. In contrast, the *sho1Δ/sho1Δ* strain did not exhibit increased opaque formation in response to sorbitol in the media. In fact, it appeared the *sho1Δ/sho1Δ* mutant switched slightly less frequently than normal when the media was supplemented with sorbitol, though this is within the normal variation we see in white-opaque switching assays. Importantly, this *sho1Δ/sho1Δ* strain switches at the normal basal rate on SCD+Uri plates, and it was able to form opaque colonies in response to guanidine HCL, indicating that the white-opaque switch is intact in this strain. Together, this indicates that sorbitol can increase the frequency of white-to-opaque switching in *C. albicans*, but this response is dependent on Sho1.

Potassium chloride (KCl) did not induce white-to-opaque switching at any concentration in any of the strains tested. All strains switched to the opaque state at the basal rate (less than 1% of colonies were opaque or contained opaque sectors) (Figure 1,

Table 1). Colonies grown on KCl appeared darker than typical white colonies on SCD+Uri plates. These cells were confirmed to be white cells using a number of tests. When examined by DIC microscopy, cells appeared round budding yeast, which is the typical morphology of white cells. These darker cells grew into white colonies when restreaked onto SCD+Uri at 25°C. *C. albicans* grown on plates supplemented with KCl and phloxine B did not stain a dark pink, further indication that the cells in these colonies were composed of white cells.

White-opaque switching does not increase in response to osmolites in liquid media

The switching assays described above demonstrate wild type *C. albicans* (of an appropriate mating type) form opaques more frequently when cells are plated on media supplemented with either guanidine HCl or sorbitol. In that experimental design, *C. albicans* cells are exposed to the osmolite continually once they are plated onto the solid media. We can differentiate between switching events that occur immediately when the cell contacts the plate and those that happen later during the growth of the colony, as the latter situation results in the growth sectoring colonies, rather than fully opaque colonies. To limit the length of the osmotic stimulus used to trigger the white-to-opaque switch, I designed an experimental setup in which *C. albicans* cells are grown to mid-log phase in liquid SCD+Uri supplemented with the desired osmolite. After 13 hours of growth in the osmotically active media (or normal SCD+Uri as a control), cells were plated onto SCD+Uri plates. I reasoned that any switch events stimulated by osmolites in liquid media would be a stable (heritable) switch, and the resulting colonies would grow up as fully opaque colonies on SCD+Uri even after the osmotic stimulus has been removed.

Three strains were tested for their response to osmolites in liquid media: two wild type strains (CHY420 and WO-1) and a *sho1Δ/sho1Δ* mutant. Each of these strains was grown in SCD+Uri supplemented with various concentrations of guanidine HCl, sorbitol, or potassium chloride (KCl) for 13 hours and then plated onto SCD+Uri plates. After incubation at RT for 1 week, colonies were examined to determine the proportion of white, opaque, and sectored colonies (Figure 2). In general, very little white-to-opaque switching was observed; the vast majority of the colonies were fully white. Opaque sectors were observed at the expected basal rate (~1-3%), but no fully opaque colonies were observed in any of the strains, in response to any of the osmotic stimuli (data not shown). This indicates that the *C. albicans* cells are not committed to the opaque state during their exposure to guanidine HCl or sorbitol in liquid media. KCl supplemented to the liquid media had no effect, but none was expected given the results on the plate-based switching assays. Additionally, none of the cells in this experiment exhibited any morphological changes at the time of plating (data not shown). There are many possible explanations for these observations: 1) The cells were not in the appropriate growth phase to respond to osmotic stimuli via white-opaque switching, 2) The cells must be exposed to osmotic stimuli for greater than 13 hours to influence white-opaque switching, or 3) the cells need additional input, possibly surface contact, in order to trigger white-opaque switching. Further experiments will address the 2nd and 3rd possibilities listed above.

Long-term exposure to osmolites in liquid does not stimulate white-opaque switching

One possible reason we failed to observe white-opaque switching in response to osmolites in liquid media is related to the length of time the cells are exposed to the osmolites. In the liquid switching assay, the cells were grown in osmolite-supplemented media for ~13 hours before being plated onto standard lab media. In contrast, the plate-based switching assay exposed cells to the osmolites for roughly one week, or the time that it took for a colony to grow at 25°C. To see if the duration of exposure to osmolites could impact the white-opaque switching response, a pilot experiment was conducted where CHY420 was grown in liquid SCD+Uri, with the full panel of osmotic supplements, for 16 or 24 hours (data not shown). We observed a slight increase in the frequency of opaque formation after grown in the supplemented media for 24 hrs, as compared to 16 hrs. Importantly, a few fully opaque colonies were observed after CHY420 was grown in 1M guanidine HCl, which indicated the cells committed to the opaque state while in the presence of guanidine. As a general note, guanidine HCl seems toxic to *C. albicans* – the number of colonies recovered after plating was inversely correlated with the concentration of the guanidine HCl. It may be hard to determine if the switching phenotype observed is a specific response to guanidine HCl as an osmolite, or a more global response to general stress.

Given these preliminary results, we undertook a long-term liquid switching assay with wild type strain CHY420. In this assay, the strain was grown in liquid SCD+Uri, supplemented with 0.5M guanidine HCl, 1M sorbitol, or 0.5M KCl for one week. The cultures were diluted to an $OD_{600}=0.1$ every 12 hours to keep the cultures in log-phase growth. Aliquots of the cultures were plated onto SCD+Uri at the 24 hour, 72 hour, and 120 hour time points and grown at RT. Colonies were observed after one week to assess

the white-opaque switching frequencies in response to the osmolites in the liquid media. Data from this experiment are shown in Figure 3 and Table 2.

After log-phase growth in liquid SCD+Uri media for five days and growth on SCD+Uri plates for one week, CHY420 switched from the white to the opaque phase at the expected basal rate (between 1-3%). When grown in SCD+Uri supplemented with 0.5M guanidine HCl, the frequency of white-to-opaque switching increased with longer exposure to the osmolite (comparing 24hr to the 120hr time point). CHY420 switched to the opaque state at a low rate (0-1%) when exposed to sorbitol in the liquid media, and this rate did not increase with longer exposures to sorbitol. Opaque sectors were more frequently observed the longer CHY420 was exposed to KCl, reaching a maximum of 3.8% switching after 120 hours; this switching frequency was still in the range of basal white-opaque switching seen with wild-type strains.

Osmolites and plate hardness have an additive effect on white-opaque switching

To this point, we have observed robust white-to-opaque switching when plates are supplemented with guanidine HCl or sorbitol, but this effect is not seen when the osmolites are provided in liquid media. This led us to the idea that perhaps additional inputs are needed to commit cells to the opaque state, such as contact with a surface. To address this issue, we developed a plate-based switching assay where we used SCD+Uri plates with 1% agar, 2% agar (the standard amount), or 5% agar. Additionally, we supplemented plates of each hardness with either 0.5M guanidine HCl, 1M sorbitol, 0.5M KCl. We sought to determine whether contact with a surface and hardness of that underlying substrate impacted the white-to-opaque switching frequency of two wild-type

C. albicans strains: CHY420 ($\alpha 1\Delta\alpha 2\Delta$), and WO-1 (α/α). This information would also be studied in concert with the impact of osmolites in the media, to determine if the hardness as well as the salt stimuli is needed to trigger white-opaque switching. During this experiment I found that *C. albicans* grew more slowly on plates containing 5% agar (2 weeks vs. 1 week at RT); all colonies were counted once they were larger enough to detect any sectors formed. Recent work by Lauren Booth, a graduate student in the lab, has shown that this difference in growth rate can be minimized if plates are used within a few days of pouring them.

Switching of both CHY420 and WO-1 to the opaque phase occurred more frequently as the hardness of the plates increased (Table 3). Overall, switching frequencies in this experiment were somewhat low, given that normal basal switching rates on 2% plates is between 1-3%. However, it is clear that CHY420 switching rates correlated with the “hardness” of the plate. This may also be true of WO-1, but it hard to say strictly since no opaque sectors were seen on the 1% or 2% plates. The opaque sectors and colonies on 5% agar plates appeared fuzzy (Figure 4), which aids in detection of opaque sectors. This morphology is reversible and a result of the hard agar – when replated onto SCD+Uri (2% agar) plates, the fuzzy opaque colonies regained their normal smooth, dull appearance.

In general, the switching rates also increase with the agar content of the plates when osmolites were supplemented to the plates. When CHY420 was grown on SCD+Uri + 0.5M guanidine HCl plates, the white-to-opaque switching rate increased (from 1%-100%) with increasing agar concentration in the plates. WO-1 grew entirely in

the opaque phase on plates supplemented with guanidine HCl, regardless of the agar content of the plates.

The switching frequency of CHY420 also increased (from 1.5% to 15.1%) with increasing agar concentration when grown on plates containing 1M sorbitol. This is a greater increase than seen in plain SCD+Uri media with increasing agar, implying that the sorbitol and agar are having additive effects on the white-to-opaque switching rates. No opaque colonies or sectors were observed when WO-1 was grown on SCD+Uri+1M sorbitol, regardless of the agar content of the plates used. This result was unexpected, given that WO-1 formed opaque colonies robustly in response to 1M sorbitol in previous experiments (Table 1).

When KCl was supplemented to SCD+Uri plates of various agar content, CHY420 increased its white-opaque switching frequency from 0%-2.6% of total colonies. This may be a true increase in opaque formation in response to KCl, but it is difficult to reach any solid conclusions, given the fact that so few colonies were counted on the KCl plates, and the switching rates seen lie within the normal range of switching frequencies on SCD+Uri (2% agar) plates. No opaque colonies were observed when WO-1 was grown on SCD+Uri+ 0.5M KCl plates, regardless of the agar concentration in the plates.

White-to-opaque switching increases on agarose plates

Data presented thus far supports the hypothesis that *Candida albicans* initiates white-opaque switching in response to surface contact. The simplest idea is that *Candida* senses the “hardness” of the surface under it, and this environmental signal is transmitted

somehow into the switching regulatory circuit. However, we had concerns that the agar might be contaminated with trace amounts of osmolites, and the observed switching response is due to increased osmotic stimulus and not surface hardness. To differentiate between these possibilities, a rotation student, Bentley Lim, monitored white-opaque switching in the wild type CAF2-1 (**a/a**) on plates made with alternative solidifying agents. RZY13 and RZY492 are white and opaque isolates, respectively, of CAF2-1 (**a/a**). When grown on plates ranging from 0.5% to 5% agarose, white-to-opaque switching increased correspondingly to a maximum of ~18% of colonies showing switch events on SCD+Uri (5% agarose) plates (Figure 5). These data indicate that the increased white-to-opaque switching observed on plates with increased agar is not due to contaminating osmolites. Interestingly, the opaque-to-white switching frequency did not increase on plates with higher amounts of agarose, indicating that the change in switch frequency is specifically influencing the formation of opaque cells, and not a general increase in switching.

Bentley also attempted to use acrylamide and gelatin as hardening agents for plates. The acrylamide plates never solidified, likely due to oxygen inhibition of polymerization. The gelatin plates (containing 4%, 6%, 8%, 12% and 16% gelatin) were used in a white-opaque switching assay; the concentration of gelatin in the plates had no affect on switching rates (data not shown).

Switching is not affected by nutrient availability

In addition to causing white-to-opaque switching, we also observed that *Candida albicans* grows more slowly on the plates containing higher amounts of agar or agarose.

This could indicate that slowing the growth rate, and not the hardness of the substrate itself, caused the increased white-to-opaque switching. To test this, Bentley performed white-opaque switching assays using the wild-type strain RZY13 on media that contained 0.5x, 1x, or 2x SD to the plates. For each of these concentrations of SD, he also varied the agarose concentration in the plates (0.5%, 1%, 2% or 5%) and performed white-to-opaque switching assays. At the standard concentration of SD (1x), he observed white-to-opaque switching in the colonies increasing from 1%-14% as the agarose concentration increased from 0.5% to 5% (Figure 6). The results were very similar when white to opaque switching was observed on media containing 0.5x SD: opaque colonies or sectors were observed in 0.5% of the colonies on plates containing 0.5% agarose. This switching frequency increased as the agarose concentration in the plates increased, reaching a maximum of 11% colonies exhibiting opaque morphologies on plates that contained 5% agarose. Similarly, when 2.0x SD media was used as a nutrient source, the switching frequency ranged from ~1%-11% as the agarose concentration in the plates increased. Together, this indicates that growth rate, as regulated by nutrient availability, does not affect the frequency of white-opaque switching.

Contact dependent kinases and calcium affect white-opaque switching

Thigmotropism is the process by which *Candida albicans* reorients the direction of hyphal cell growth in response to the topology of the underlying surface. The thigmotropism response is dependent on a Ca^{2+} influx from the environment, and eliminating Ca^{2+} from the media will abrogate any responses to the growth surface.

Bentley tested the possibility that Ca^{2+} played a role in sensing surface hardness in the white-opaque switch.

When 10mM EGTA was added to SCD+Uri plates containing 5% agarose, he found the wild-type strains RZY13 and RZY47 formed opaques less frequently than on SCD+Uri plates (with either 2% or 5% agarose). Conversely, when 10mM CaCl_2 was added to SCD+Uri plates with 5% agar, roughly 10% of the RZY13 colonies were in the opaque state, compared to only a ~6% switch frequency on SCD+Uri+5% agar plates. The wild-type strain RZY47 did not appreciably increase its white-to-opaque switching frequency when CaCl_2 was added to the media. While both of these strains are wild type **a** strains, they have different auxotrophies. RZY13 is an **a/a** isolate of the wild type strain CAF2-1; RZY47 an **a/a** –His-Leu isolate of RM1000, and served as the parental strain in which *mkc1Δ/mkc1Δ* strains were made from (discussed later). The nutritional markers or other genetic differences between these backgrounds may account for the differences between these strains.

Bentley also tested the role of Mkc1 in white opaque switching. Mkc1 is a contact-dependent MAPK (mitogen-activated protein kinase) involved in the fungal cell integrity pathway and is required for invasive hyphal growth and normal biofilm development [7]. Growth on a surface causes *C. albicans* to accumulate the activated form of Mkc1, likely through the ability of the cell integrity pathway to detect physical contact. Mutants lacking Mkc1 are unable to grow in biofilms or as invasive filaments, two processes that involve sensation of contact.

Bentley measured the white-to-opaque switching frequencies for *mkc1Δ/mkc1Δ* mutants on a variety of media (Figure 7). Regardless of the media conditions (2 or 5%

agar, $\pm\text{CaCl}_2$, $\pm\text{EGTA}$), the *mkc1* Δ /*mkc1* Δ strains displayed a 2- to 5-fold increase of white-to-opaque switching over the parental strain RZY47. Because RZY47 and the *mkc1* Δ /*mkc1* Δ mutants are not nutritionally matched, Bentley also tested the wild-type strain RZY13. The *mkc1* Δ /*mkc1* Δ strain also switched to opaque more frequently than RZY13 on all conditions tested.

DISCUSSION

White-opaque switching responds to a number of environmental stimuli, and these preliminary studies show that this process is also regulated by the osmolites guanidine HCl and sorbitol. The ability of *C. albicans* to respond to sorbitol by switching to the opaque state relies on Sho1, a member of the HOG signaling pathway. In the absence of Sho1, cells are still able to switch at the basal stochastic rate, indicating that Sho1 does not play a role in the core mechanism of opaque formation, but instead likely functions to transmit the sorbitol signal to the genetic network controlling white-opaque switching.

These results also suggest that *C. albicans* requires contact with a solid surface in order to initiate opaque formation. The osmolites guanidine HCl and sorbitol, which stimulated robust opaque formation on solid media, did not cause a significant increase in opaque formation when *C. albicans* was grown in liquid media containing these osmolites, even after long exposures in liquid media (Figure 3). Sorbitol may have a slight effect on the white-opaque switch when provided in liquid media, lowering the frequency of opaque formation. This was seen in both the preliminary liquid switching

assay I performed (data not shown) and in the longer-term switching assay. Because these experiments were only performed once, and relatively few colonies were counted to determine switching rates, it is difficult to say if this decreased white-opaque switching frequency is significant. If the experiment is repeated and the ability of sorbitol in liquid media to repress opaque formation is confirmed, this would be intriguing, given the dramatic *increase* in opaque formation sorbitol caused when it was supplemented to plates.

Notably, the strains all grew more slowly and at different rates when osmolites were supplemented to the liquid media, as compared to plain SCD+Uri media. I chose to plate the strains after an equal length of time exposed to the osmotic stimulus, as opposed to waiting for all the strains to reach the same OD before plating. Additionally, we did not see any fully opaque colonies in this experiment, indicating that all switch events occurred after the cells had been plated, not while they were in liquid culture with the osmolites. It is formally possible that the osmolites did have an effect on the white-opaque switch while the cells were in culture, but actual switch to the opaque state did not occur while the cells were in liquid culture.

These results suggested that contact sensation may play a role in white-opaque switching in *C. albicans*. As shown in Table 3, white opaque switching frequencies increased in response to the agar concentration of the plates. This was most clearly seen in the instance where *C. albicans* was grown on SCD+Uri plates that contained 1%, 2%, or 5% agar. One hypothesis is that *C. albicans* prefers possible that the *C. albicans* is sensing the hardness of the surface, and with the increased agar content in the 5% plates, the *C. albicans* is able to sense the harder plates and switch more frequently. An

alternative hypothesis is that the agar used to make the plates is contaminated with trace amounts of osmolites, and by increasing the agar content of the plates we are actually increasing the osmotic stimulus sensed by the *C. albicans*. To address this second issue, a rotation student, Bentley Lim, attempted to grow *C. albicans* on SCD+Uri plates solidified using a variety of substances: agarose, gelatin, and acrylamide. Due to practical considerations, agarose proved to be the most useful in the laboratory setting. Bentley found that wild-type strain RZY13 increased the frequency of opaque formation in a dose dependent manner when plates onto SCD+Uri plates containing 0.5%, 1%, 2%, or 5% agarose. This indicates that the white-opaque switching response to agar and agarose is not due to bulk contaminants found in agar. Additionally, Bentley showed that opaque-to-white switching frequency did not increase in response to increased in the plates, indicating that that overall response is to drive a population of cells to the opaque state, rather than simply increasing switch frequencies in both directions.

Importantly, Bentley also found that RZY13's white-opaque switching response did not increase in response to increasing concentrations of gelatin used to solidify SCD+Uri plates. This presents a disparity between switching responses on agar and agarose, compared to gelatin. One interpretation is that opaque formation does not respond to the hardness of the underlying substrate, but rather to a chemical found in agar and agarose, but not in gelatin. Alternatively, the hardness of the plates may stimulate white-to-opaque switching, but there a component in gelatin inhibits this response.

We performed experiments to test white-to-opaque switching on plates with varied agar concentrations in combination with osmotic stimuli. Confirming earlier results we found that the frequency of opaque formation increased when the media was

supplemented with either 0.5M guanidine HCl or 1M sorbitol, at a given agar concentration. This increase in switching could be tuned by altering the amount of agar in the plates; lowering the agar lowered the switching rates, increasing the agar concentration increased the switching frequency. This suggests that the environmental inputs of osmotic stress and hardness have additive effects on the white-to-opaque switching frequencies of CHY420.

When white-opaque switching in response to agar concentration was tested with WO-1, we had more puzzling results. No switching was seen on SCD+Uri plates containing either 1% or 2% agar. However, 5% of the colonies grown on 5% agar had opaque sectors, a fairly notable increase in switching frequency. This may indicate that WO-1 does switch more frequently on harder surfaces. However, we were not able to draw any conclusions about the response of WO-1 to hardness in combination with osmolites in the media. All of the WO-1 colonies grown on SCD+Uri+0.5M guanidine HCl grew in the opaque phase; and all of the WO-1 colonies grown on SCD+Uri+1M sorbitol or SCD+Uri+ 0.5M KCl grew in the white phase. This is surprising, given that previous experiments had shown that 100% of WO-1 colonies grew as opaques on media supplemented with 0.5M sorbitol (Figure 1). This discrepancy may be due to day-to-day variation in the experiments; I noted earlier that all of the switching rates seem depressed in the varied agar experiments. These experiments could be repeated again to determine the true behavior of WO-1 in response to salts and hard surfaces. Additionally, there is some difference in the response of CHY420 and WO-1 to both surfaces and osmolites in the media; these may be due to general differences in the strains. CHY420 is engineered from the standard laboratory strain, whereas WO-1 is a clinical isolate. The mating type

of these two strains also differs – CHY420 is an α strain, due to the fact that the *MTLa1* and *MTLa2* genes have been deleted; WO-1 is an α/α strain due to chromosome loss and reduplication that occurred prior to its collection. It may be worthwhile to test if mating type can affect the white-opaque switching response to osmolites and surfaces, using appropriately matched isogenic strains.

During these studies of white-opaque switching on plates with different agar content, we observed that colonies grown on 5% agar plates grow noticeably slower than colonies grown on the same media, containing 2% agar. This presents the possibility that the opaque formation we observe on 5% agar plates is actually due to slow growth of the cells. *C. albicans* must go through at least one cell cycle in order to switch between the white and opaque phases. Slowing the cell cycle may allow for increased opaque formation by allowing Wor1 protein levels to accumulate, triggering a white-to-opaque switch. However, it seems unlikely that simply slowing the growth rate triggers white-opaque switching, given that adjusting the SD concentration in the media did not alter switching rates (Figure 6). This theory has also been posed by Richard Bennett during his (as yet unpublished) studies of the link between growth rate and white-opaque switching when *C. albicans* is treated with chemicals that disrupt the cell cycle.

Over the course of white-opaque switching experiments comparing responses to osmolites in plates and in liquid, we noticed that switching was not as robust when the osmolite was supplemented to liquid media. This requirement for the cells to contact a surface in order to get maximal frequencies of opaque formation was also noted by another rotation student Kristen Cook. Kristin tried to express *WOR1* in liquid media to monitor the white-to-opaque switch using microarrays. Induction of *WOR1* in liquid

media did not cause any changes in cell morphology as cells growing in liquid media, even if they had committed to the opaque state as evidenced by colony formation when she plated these cells onto repressing media. Additionally, after *WOR1* induction in liquid media and plating on repressing media, only 50-80% of the colonies were in the opaque phase, which is much less than what is observed when this same strain is induced continually on solid media. This sparked the idea that *C. albicans* must have contact with a surface to maximally induce the white-to-opaque switch. Alternatively, there could be another cue, besides surface contact, that differs between planktonic and colony growth, perhaps the agar chemical itself, or some change in growth rate as a result of plating. During his rotation in the Johnson Lab, Bentley Lim did some preliminary experiments to test the possibility that the same contact sensors that function in thigmotaxis also play a role in sensing contact during white-opaque switching.

Bentley observed that adding EGTA decreased the white-to-opaque switching frequency, while supplementing CaCl_2 increase the switching frequency on SCD+Uri plates with 5% agar. This supports the idea that calcium plays a role in modulating the frequency of white-opaque switching, though it does not strictly confirm that calcium's role in switching is related to contact sensation. To test this more directly, future experiments could add CaCl_2 to the liquid media to attempt to increase the switching frequencies found in liquid media.

Bentley also tested the role of Mkc1, a contact-dependent MAPK involved in the cell integrity pathway, in white-opaque switching. Mkc1 functions in sensing contact and activating invasive filamentation in *C. albicans*; *mkc1 Δ /mkc1 Δ* mutants no longer produce invasive filaments into semisolid plates [7]. Thus, we had predicted that

mkc1Δ/mkc1Δ mutants would not sense contact with plates, and thus not trigger white-opaque switching in response to increased agar concentration of the plates. Bentley's results showing that *mkc1Δ/mkc1Δ* mutants have increased frequency of opaque formation are therefore somewhat unexpected (Figure 7). This could imply that the increased switching observed on plates with higher agar concentrations is due to a chemical component of the agar or agarose, and not the hardness itself. While we do not favor this idea, it is somewhat supported by Bentley's observation that white-opaque switching frequencies did not change on plates containing various concentrations of gelatin. It is also formally possible that Mkc1 phosphorylates Czf1 or Efg1, two transcription factors that are known to function in both invasive filamentation and white-opaque switching. This idea is pure speculation at this point in time, but it is worth being mindful of the relationship between Czf1 and Efg1 in both of these processes, and that we know very little about how phosphorylation of either of these factors influence their activity in white-opaque switching.

More recent work in the Kumamoto lab has identified a putative contact sensor, which they have named Dif1, though this result has not yet been published or and the gene has not been systematically named on the *Candida* Genome Database. Once this information is made publically available, it would be worthwhile to test *dif1Δ/dif1Δ* mutants for their ability to undergo white opaque switching. We would predict that *dif1Δ/dif1Δ* mutants would always switch to the opaque state at the same rate, whether grown in liquid or on plates. The gene *CEK1* has also been identified as another contact-dependent kinase; this gene is another good candidate to test for a role in contact-dependent white-opaque switching.

Future experiments looking at the cell integrity pathway and its role in white-opaque switching could be very enlightening. Both osmotic stress and contact sensation have been shown to involve members of the cell integrity signaling pathway. It is possible that these two types of stimuli activate the cell integrity pathway and somehow transmit this signal to the core network regulating white-opaque switching. Understanding how these signals feed into the transcriptional network controlling white-opaque switching will provide insight into how this major morphological transition is regulating in response to important environmental cues.

MATERIALS AND METHODS

Strains:

A number of wild-type strains were used in these studies. CAF2-1 is a prototrophic **a/a** strain, which was sorbose selected to create **a/a** versions for use in white-opaque switching assays; the white isolate is RZY13, and the opaque isolate is RZY492. CHY420 is a prototrophic $\alpha/\Delta\alpha2\Delta$ strain. WO-1 is the clinical strain in which white-opaque switching was first observed; it is an α/α strain.

Deletion mutants of *SHO1* had been made previously in the lab by Annie Tsong in an **a/a** strain (ATY362). These strains were sorbose-selected and **a/a** isolates were used in the white-opaque switching assays described in this chapter (RZY4).

PBS2 and HOG1 were deleted using a fusion-knockout strategy as described by Noble and Johnson [8]. In short, regions of DNA flanking the gene targeted for deletion was amplified from *C. albicans* SC5314. The flanking pieces of DNA were pieced together with a selectable marker using fusion PCR. The *URA3* selectable marker was

amplified from pDDB57 and the *HIS1* marker was amplified from pGEM-HIS. The deletion constructs were transformed into *C. albicans* strains RM1K' (**a/a**) and MMY55 (*a1Δ*) and plated onto –Ura or –His media to select for transformants. Deletion mutants were verified by colony PCR.

Bentley Lim created the *mkc1Δ/mkc1Δ* mutant by fusion knockout strategy in the parental strain RZY47 (**a/a** –His, -Leu).

Sorbose selection:

The strains CAI4, CAF2-1 and RM1 were sorbose-selected as described in [9] (and references therein) to create **a/a** and *a/a* versions of the parental strains. In short, overnight cultures of the original **a/a** strain were streaked onto a sorbose (or sorbose + Uri, for Ura- strains) plates and grown at 30C for 2 days. Colonies were streaked for singles onto YEPD+Ade+Uri, grown at 30C for 2 days, usually resulting in a single isolate growing as a mix of large and small white colonies. Small white colonies were then restreaked onto new YEPD+Ade+Uri plates and grown; large colonies were not restreaked because experience has shown that these isolates have not lost a copy of Chromosome 5 (containing the MTL). Likewise, any isolate that grew into dull yellow-colored, uniformly sized colonies were also abandoned, as these usually proved to be **a/a** strains. After regrowth of the small isolates, large colonies are now chosen and restreaked, as these typically represent isolates that have duplicated their remaining copy of Chromosome 5. Once these restreaks of the large colonies have regrown, the mating type of a single colony is determined using colony PCR against *OBPa* and *OBPa*, as

described in [9]. We note that RM1 would only form α/α strains, likely due to a recessive lethal allele located on the copy of Chromosome 5 containing the MTL α locus.

Switching experiments:

White-opaque switching assays were performed as described in [9].

Media:

Synthetic complete medium plus 2% glucose and 100 $\mu\text{g/ml}$ uridine (SCD+Uri) was used in white-opaque switching assays. Standard plates were solidified using 2% agar, though 1% and 5% agar plates were also used. Agarose (0.5%, 1%, 2%, 5%) and gelatin (4%, 6%, 8%, 12%, 16%) were also used as hardening agents for solid media. Guanidine HCl, sorbitol, or KCl was added to SCD+Uri media at the concentrations indicated in the text.

REFERENCES

1. Slutsky B, Staebell M, Anderson J, Risen L, Pfaller M, et al. (1987) "White-opaque transition": a second high-frequency switching system in *Candida albicans*. *J Bacteriol* 169: 189-197.
2. Rikkerink EH, Magee BB, Magee PT (1988) Opaque-white phenotype transition: a programmed morphological transition in *Candida albicans*. *J Bacteriol* 170: 895-899.

3. Kolotila MP, Diamond RD (1990) Effects of neutrophils and in vitro oxidants on survival and phenotypic switching of *Candida albicans* WO-1. *Infect Immun* 58: 1174-1179.
4. Geiger J, Wessels D, Lockhart SR, Soll DR (2004) Release of a potent polymorphonuclear leukocyte chemoattractant is regulated by white-opaque switching in *Candida albicans*. *Infect Immun* 72: 667-677.
5. Lohse MB, Johnson AD (2008) Differential phagocytosis of white versus opaque *Candida albicans* by *Drosophila* and mouse phagocytes. *PLoS ONE* 3: e1473.
6. Hull CM, Raisner RM, Johnson AD (2000) Evidence for mating of the "asexual" yeast *Candida albicans* in a mammalian host. *Science* 289: 307-310.
7. Kumamoto CA (2005) A contact-activated kinase signals *Candida albicans* invasive growth and biofilm development. *Proc Natl Acad Sci U S A* 102: 5576-5581.
8. Noble SM, Johnson AD (2005) Strains and strategies for large-scale gene deletion studies of the diploid human fungal pathogen *Candida albicans*. *Eukaryot Cell* 4: 298-309.
9. Zordan RE, Galgoczy DJ, Johnson AD (2006) Epigenetic properties of white-opaque switching in *Candida albicans* are based on a self-sustaining transcriptional feedback loop. *Proc Natl Acad Sci U S A* 103: 12807-12812.

Figure 1.

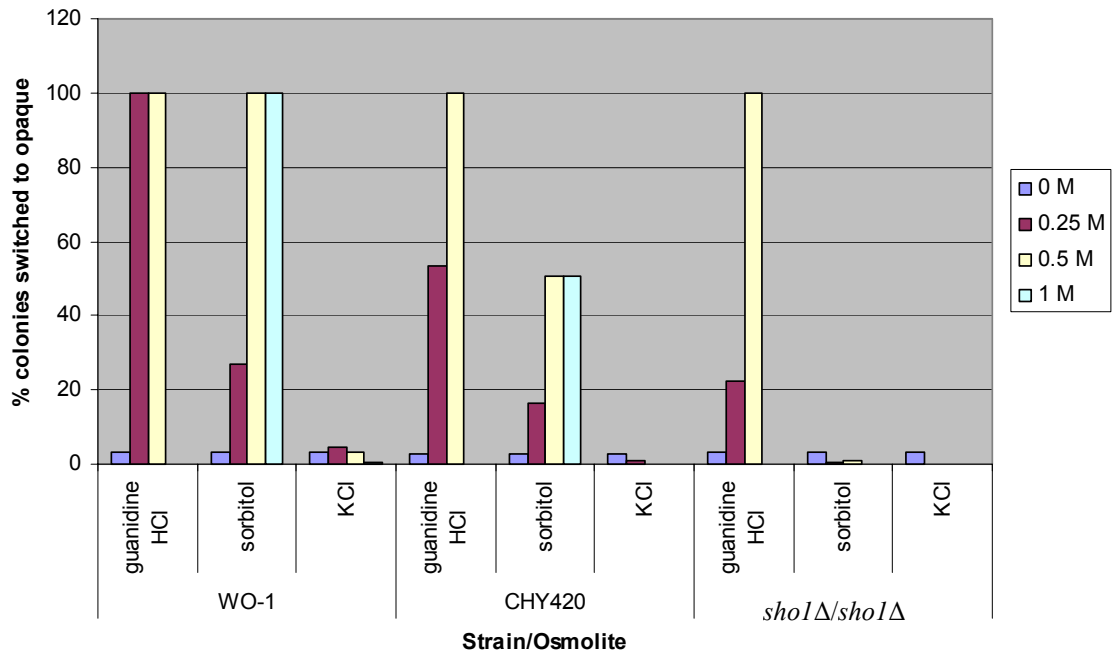


Figure 1. White-to-opaque switching in response to osmolites in solid media

White-opaque switching assays were performed with the wild-type strains WO-1, CHY420, and *sho1Δ/sho1Δ* (**a/a**) mutant. Cells were plated for single colonies on SCD+Uri plates supplemented with various concentrations of guanidine HCl, sorbitol or KCl. Plates were grown at RT for one week and switching frequency was assessed by counting fully opaque colonies or colonies with opaque sectors.

Table 1.

		WO-1				CHY420				<i>sho1 Δ/sho1 Δ</i>			
		white	op sec	opaque	n	white	op sec	opaque	n	white	op sec	opaque	n
control	0M	96.66%	3.34%	0.30%	329	97.12%	2.88%	0.00%	416	96.59%	3.41%	0.00%	352
guanidine HCl	0.25M	0.00%	0.00%	100.00%	301	46.51%	9.74%	43.75%	688	77.43%	21.95%	0.63%	319
	0.5M	0.00%	0.00%	100.00%	375	0.00%	0.79%	99.21%	378	0.00%	100.00%	0.00%	362
sorbitol	0.25M	73.02%	26.98%	0.00%	404	83.55%	16.46%	0.00%	468	99.37%	0.32%	0.32%	315
	0.5M	0.26%	96.62%	3.12%	385	49.53%	49.07%	1.41%	854	98.96%	0.69%	0.35%	289
	1M	0.00%	0.00%	100.00%	359	49.23%	4.86%	45.91%	782	100.00%	0.00%	0.00%	266
KCl	0.25M	95.61%	4.40%	0.00%	296	99.09%	0.91%	0.00%	441	100.00%	0.00%	0.00%	275
	0.5M	96.84%	3.16%	0.00%	285	N/D	N/D	N/D	0	100.00%	0.00%	0.00%	257
	1M	99.42%	0.58%	0.00%	346	100.00%	0.00%	0.00%	472	100.00%	0.00%	0.00%	306

Table 1. White-to-opaque switching in response to osmolites in solid media

White-opaque switching assays were performed with the wild-type strains WO-1, CHY420, and RZY4 (*sho1Δ/sho1Δ*). Cells were plated for single colonies on SCD+Uri plates supplemented with various concentrations of guanidine HCl, sorbitol or KCl. Plates were grown at RT for one week and switching frequency was assessed by calculating the percentage of total colonies that had opaque sectors (op sec) or were fully opaque. These data are represented graphically in Figure 1.

Figure 2.

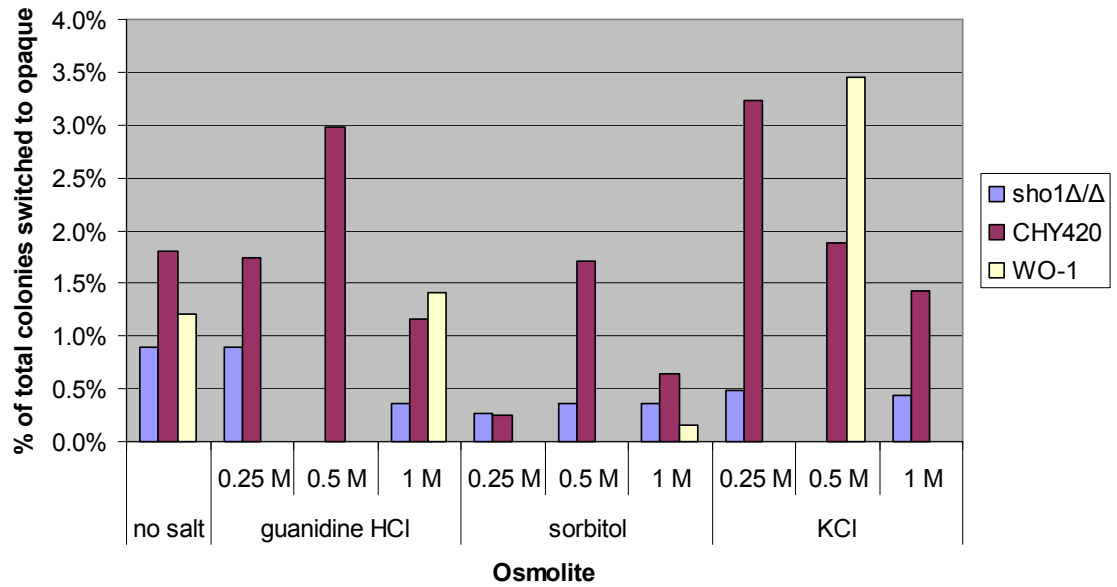


Figure 2. White-to-opaque switching in response to osmolites in liquid media: pilot

The wild-type strains CHY420 and WO-1, and the *sho1Δ/sho1Δ* mutant (**a/a**) were grown in liquid SCD+Uri media supplemented with the indicated osmolites for 13 hours at RT. Cells were then plated onto SCD+Uri (no supplements) and grown at RT for one week, at which time colonies were examined to identify switching events by the presence of opaque sectors or fully opaque colonies.

Figure 3.

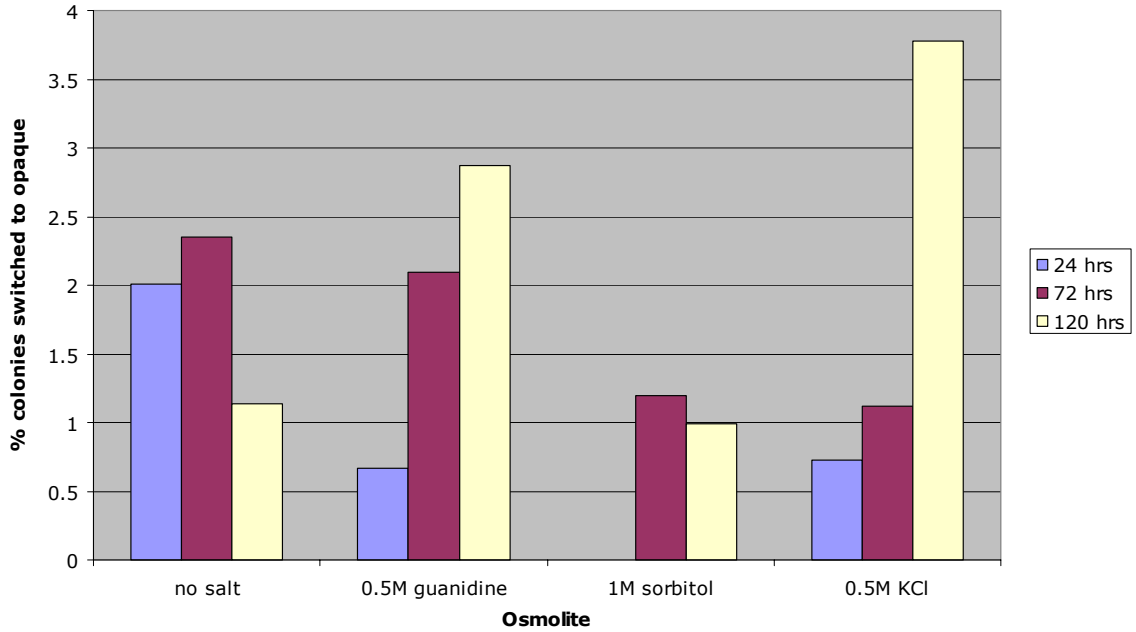


Figure 3. White-to-opaque switching after prolonged exposure to osmolites in liquid media.

The wild-type strain CHY420 was grown in liquid SCD+Uri media, supplemented with the indicated osmolites. Cultures were diluted to $OD_{600}=0.1$ every 12 hours to maintain the cultures in log-phase growth. After 24, 72, or 120 hours growth in the liquid media, cells were plated on SCD+Uri at RT for one week, at which time switching was assessed by observing the percentage of total colonies that contained opaque sectors or were fully opaque.

Table 2.

		% fully white	% op sectors	% fully opaque	n
no salt	24 hrs	98.0%	2.0%	0.0%	399
	72 hrs	97.6%	2.4%	0.0%	468
	120 hrs	98.9%	1.1%	0.0%	352
0.5M guanidine HCl	24 hrs	99.3%	0.7%	0.0%	298
	72 hrs	97.9%	2.1%	0.0%	479
	120 hrs	97.1%	2.9%	0.0%	348
1M sorbitol	24 hrs	100.0%	0.0%	0.0%	628
	72 hrs	98.8%	1.2%	0.0%	498
	120 hrs	99.0%	1.0%	0.0%	403
0.5M KCl	24 hrs	99.3%	0.7%	0.0%	548
	72 hrs	98.9%	1.1%	0.0%	356
	120 hrs	96.2%	3.8%	0.0%	238

Table 2. White-to-opaque switching after prolonged exposure to osmolites in liquid media.

The wild-type strain CHY420 was grown in liquid SCD+Uri media, supplemented with the indicated osmolites. Cultures were diluted to $OD_{600}=0.1$ every 12 hours to maintain the cultures in log-phase growth. After 24, 72, or 120 hours growth in the liquid media, cells were plated on SCD+Uri at RT for one week, at which time switching was assessed by observing the percentage of total colonies that contained opaque sectors or were fully opaque. These data are represented graphically in Figure 3.

Table 3.

Salt	agar	CHY420		WO-1	
		switching frequency	n	switching frequency	n
no salt	1%	0.3%	303	0.0%	450
	2%	0.5%	400	0.0%	437
	5%	2.3%	346	5.1%	450
0.5M guanidine HCl	1%	1.0%	394	100.0%	361
	2%	18.3%	338	100.0%	409
	5%	100.0%	287	100.0%	187
1M sorbitol	1%	1.5%	414	0.0%	394
	2%	5.4%	239	0.0%	407
	5%	15.1%	272	0.0%	366
0.5 M KCl	1%	0.0%	57	0.0%	146
	2%	2.6%	231	0.0%	301
	5%	not tested		not tested	

Table 3. White-to-opaque switching on solid media with different agar concentrations

White isolates of the wild-type strains CHY420 or WO-1 were plated onto SCD+Uri plates made with different amounts of agar. Normal plate recipes use 2% agar. These plates were also supplemented with either 0.5M guanidine HCl, 1M sorbitol, or 0.5M KCl. After one week of growth at RT, switching frequencies were calculated as a percentage of total colonies that had opaque sectors or were full opaque.

Figure 4.

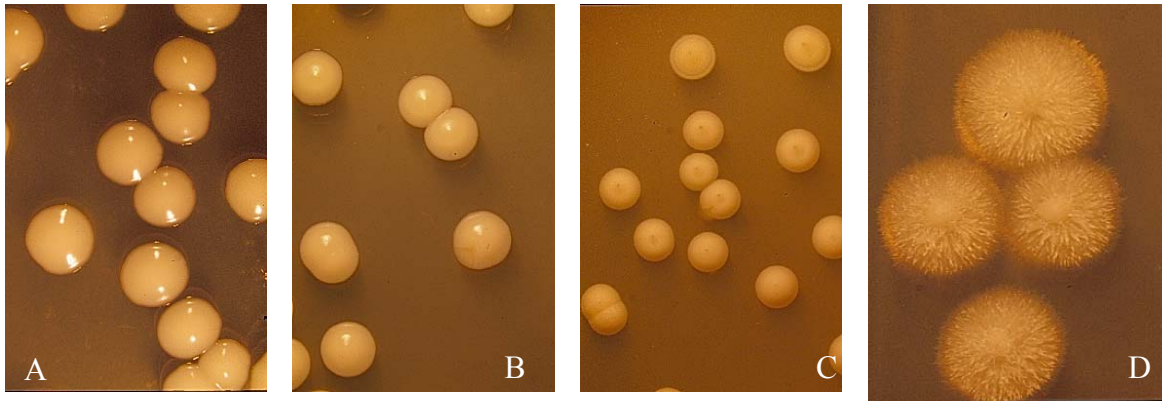


Figure 4. Colony morphology on plates with varied agar and osmolites.

All colonies are CHY420. *Panel A:* SCD+Uri plates, 1% agar. *Panel B:* SCD+Uri plates, 2% agar. *Panel C:* SCD+Uri plates, 5% agar. *Panel D:* SCD+Uri+500mM guanidine HCl.

Figure 5.

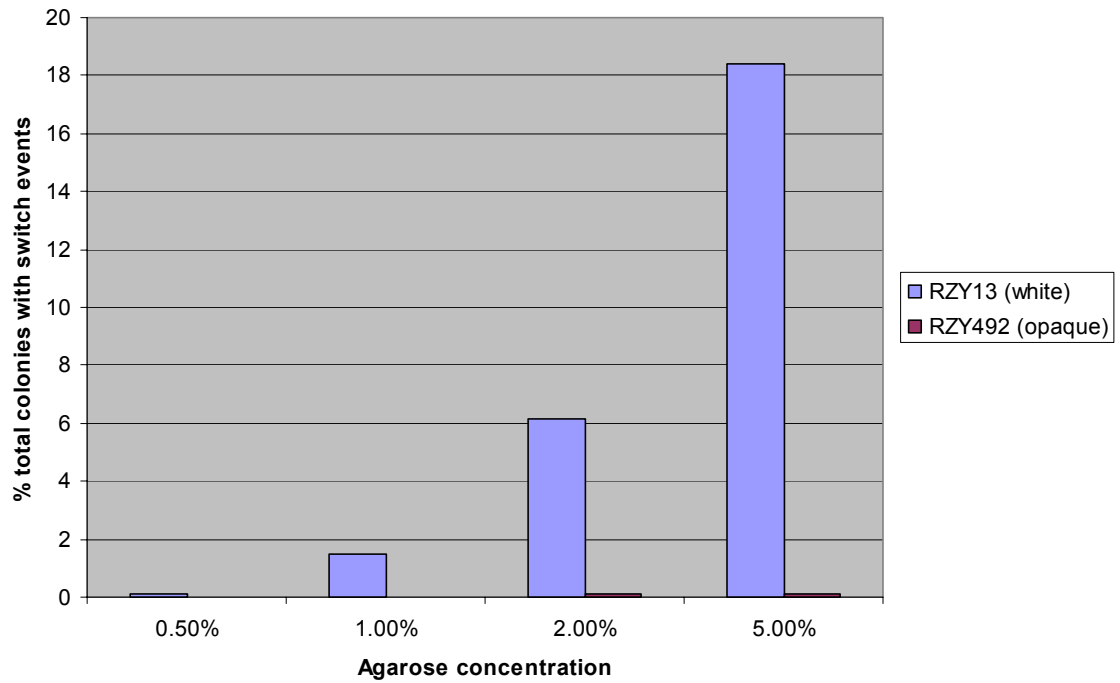


Figure 5. White-opaque switching on agarose plates

White-opaque switching assays were performed on SCD+Uri plates solidified with different concentrations of agarose. RZY13 was used to monitor white-to-opaque switching events; RZY492 was used to monitor opaque-to-white switch events.

Switching frequencies were calculated as the percentage of total colonies that had sectors or full colonies of the opposite state from the original population.

Figure 6.

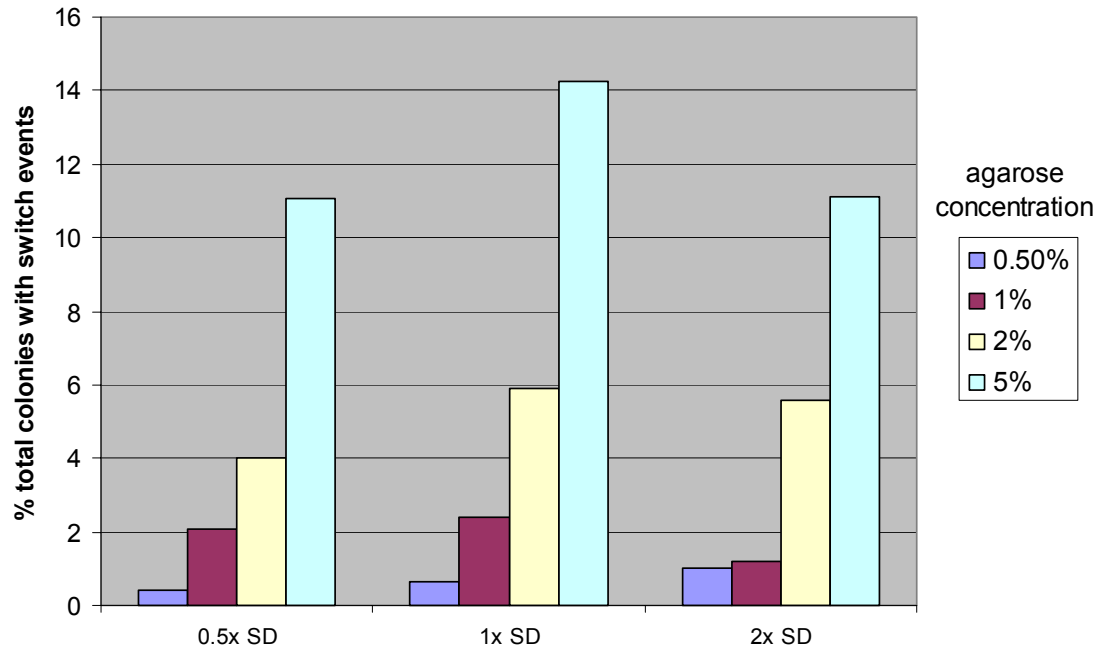


Figure 6. White-to-opaque switching assays in response to agarose and SD concentrations.

White-opaque switching assays were performed using RZY13, a white wild-type strain, plated onto media with different concentrations of SD (to vary nutrient availability) and agarose (to vary the hardness). After growth at RT for one week, colonies were monitored for switch events by counting the percentage of total colonies that had opaque sectors or were fully opaque.

Figure 7.

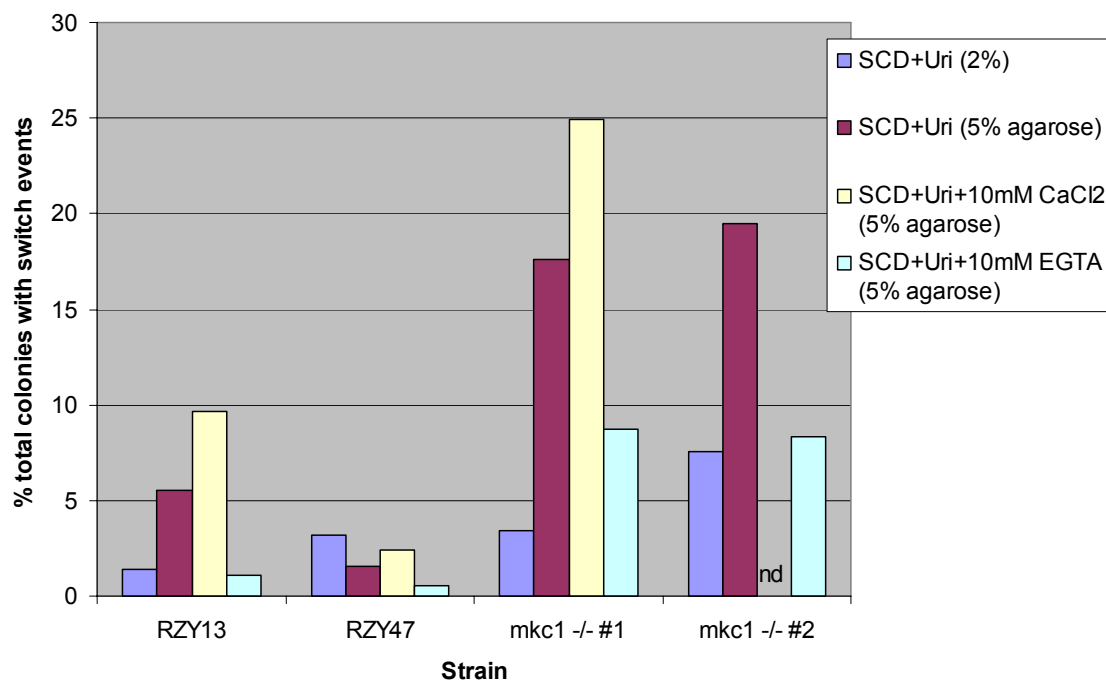


Figure 7. White-to-opaque switching is dependant on calcium availability and signaling in response to contact.

White-to-opaque switching assays were performed with two wild-type strains and two *mkc1* Δ /*mkc1* Δ mutants. Note that RZY13 is an **a/a** isolate derived from CAF2-1 (prototroph) and RZY47 is an **a/a** –His-Leu strain, which was used to generate the *mkc1* Δ /*mkc1* Δ mutants. White isolates of each strain were plated onto SCD+Uri media with varied amounts of agarose. Additionally, 10mM CaCl₂ or 10mM EGTA were supplemented to the media to alter the calcium concentration in the plates. After growth on these plates for one week at RT, switching frequencies were calculated as the percentage of total colonies that had opaque sectors or were fully opaque.

Chapter 5

Conclusions and Future Directions

The work described in this thesis was central in beginning molecular studies of white-opaque switching and the genes responsible for its regulation. The identification of Wor1 as a master regulator of switching has framed all of the other questions that we ask about regulation of switching. To date, Wor1 is the only gene identified that can drive both wild-type **a** and **a/α** cells to the opaque state. Other key regulators, such as Czf1, Efg1, and Wor2, can influence the frequency or the heritability of the switch, but none are absolutely needed for the formation of opaque cells as long as Wor1 is expressed.

Working with other members of the Johnson Lab, we were able to define a transcriptional network composed of interlocking feedback loops. The architecture of this network results in stable Wor1 expression in opaque cells. The nested layers of feedback buffer Wor1 expression against transient fluctuations of Czf1, Efg1, or Wor2 expression. Interestingly, we also found that the $\alpha 1$ - $\alpha 2$ heterodimer blocks white-opaque switching solely through its direct repression of Wor1; aberrant expression of Czf1 or Wor2, or loss of Efg1, will not cause opaque formation in **a/α** cells because Wor1 is effectively shut off. Based on bioinformatic analysis and chromatin immunoprecipitation studies of $\alpha 1$ - $\alpha 2$ binding (Johnson Lab, unpublished, and [1]), it appears that $\alpha 1$ - $\alpha 2$ only represses Wor1 directly and does not regulate Czf1, Efg1, or Wor2. This is important in the context that both Czf1 and Efg1 have roles in regulating filamentation in **a/α** cells. With $\alpha 1$ - $\alpha 2$ repressing Wor1, it allows the cells to alter Czf1 and Efg1 expression during filamentation without inadvertently switching the cells to the opaque state.

Wor1's biochemical role in the cell is an area of great interest. As mentioned in Chapter 2 and Appendix 2, Wor1's amino acid sequence has no identifiable protein

domains, yet Wor1 has clear roles in transcriptional regulation and is associated with chromatin. If Wor1 proves to bind DNA directly, it would be the representative member of a family of fungal proteins with a new DNA-binding fold. Even if Wor1 is not found to bind DNA directly, its role as a transcriptional regulator will be of great interest. Initially, simple confirmations of protein interactions between Wor1, Czf1, Efg1, and Wor2 will be valuable towards interpreting their binding profiles from chromatin immunoprecipitation experiments. Many genes are bound by many of these factors, yet it is unknown whether all of these factors are bound simultaneously. These regulators tend to associate with chromatin across large regions of DNA. It is currently not known whether these binding patterns represent multiple discrete binding sites for each factor, spreading of the proteins along the chromatin (resembling Sir2 spreading across heterochromatin), or whether the binding profile instead represents a higher-order configuration of chromatin which brings together distant regions of DNA. Any of these possibilities are intriguing and will lead to further questions about Wor1's function in the cell.

To date, analysis of Wor1's expression level has focused on transcriptional regulation. However, there are hints that Wor1 expression may be regulated post-transcriptionally. The mRNA transcribed from the *WOR1* locus is considerably larger than the coding sequence of the gene – the 5' untranslated region (UTR) is about 2 kb long, and the 3' UTR is about 175 bp long (personal communication from Aaron Hernday, [1]). The 5' UTR does not contain any ATG codons or splice sites, indicating that the ribosome may scan through the remarkably long 5' UTR before beginning translation. Also, during the analysis of Wor1 expression levels from the *pMET3-WOR1*

ectopic expression construct, we noticed that transcript abundance observed on Northern analysis did not correlate with the Wor1 protein abundance seen in Westerns. In cells transcribing the ectopic Wor1 in addition to the endogenous copies, we saw a 4-fold increase in endogenous transcript levels over wild-type opaque cells, yet both of these cells had the same Wor1 protein abundance (Chapter 2, Figure 3). This implies that translation itself may be regulated. The Wor1 protein is also predicted to be phosphorylated, as evidenced by the presence of consensus phosphorylation sites in its protein sequence. It is not known how phosphorylation affects Wor1 stability, activity, or interactions with other factors.

The transcriptional models of white-opaque switching regulation assume that there is a threshold of Wor1 expression necessary to establish Wor1's feedback loop and maintain the opaque state. As yet, no experiments have been performed to identify the levels of Wor1 needed to maintain an active feedback loop. Insight may be gained through the biochemical studies of Wor1 and analysis of Wor1's promoter, if it is revealed that there is a minimum occupancy of Wor1 needed to activate the positive feedback loop.

The transcriptional network reinforcing Wor1 expression through a series of positive feedback loops is a striking example of a natural bistable network in a eukaryotic system. Bistable systems have been engineered in bacteria in an attempt to understand how cooperativity and combinatorial control can give rise to bistable systems, though it is unclear how well these engineered systems represent real networks, due to the abnormally strong promoters that are used to drive high levels of expression of the regulators being studied. We believe that the white-opaque switch will be a useful,

perhaps more sensitive system in which to study bistability. As members of the Johnson Lab continue to identify regulators, refine the genetic network model, and study the biochemistry of the relevant factors, white-opaque switching will be a more valuable tool for stochastic modeling studies. One critical aspect to examine is how the feedback loops in the current model are destabilized to allow cells to revert to the white phase. It is possible there is an analogous network active in white cells and negative repression between the competing networks causes toggling between the white and opaque states. Another possibility is that the opaque state is destabilized by rapid degradation of the transcriptional regulators, including Wor1. Distinguishing between these options will further our understanding of white-opaque switch and aid in modeling the regulatory network.

Additionally, it will be interesting to learn more about how the white-opaque switch contributes to virulence of *C. albicans*. Our research has shown that contact with solid media and osmolites cause cells to switch to the opaque state – this is intriguing, given the fact that mating products have been recovered from the kidneys of infected mice. Ultimately, we want to learn how these stimuli are fed into the transcriptional network controlling the white-opaque switch on a molecular level. Infection studies examining where opaque cells are formed or shielded within the host would also be useful. From a broader perspective, understanding which environmental conditions influence the switch and knowing which host organs serve as niches for opaque cells will shed light on why *C. albicans* evolved this phenotypic switch.

REFERENCES

1. Srikantha T, Borneman AR, Daniels KJ, Pujol C, Wu W, et al. (2006) TOS9 regulates white-opaque switching in *Candida albicans*. *Eukaryot Cell* 5: 1674-1687.

Appendix 1

Epistasis Between Efg1 and Wor2

INTRODUCTION

Published research described in previous chapters discussed the genetic network underlying the white opaque switch [1]. Our current understanding of the genetic relationship between transcriptional regulators governing the switch places *WOR1* in the central position (Figure 1). The epistatic relationships defined from that work describe a network of interlocking feedback loops that work together to reinforce *WOR1* expression in opaque cells. The model as shown is consistent with all experimental data gathered, but there were a number of puzzling results from the epistasis studies that were not easily represented in the model.

The published version of the model implies that ectopically expressing *WOR2* in **a** strains will drive cells to the opaque state through *WOR1*. However, this was not observed experimentally [1]. Ectopic expression of *WOR2* in $\alpha1\Delta\alpha2\Delta$ cells, controlled using a *pMET3-WOR2* construct, did not cause the cells to switch to the opaque state more frequently than control strains. This was somewhat unexpected, and we originally attributed this result to the possibility that *WOR2* was not being transcribed at sufficient levels from the *MET3* promoter. *Wor2* transcription levels had not been tested in this strain under repressing or inducing conditions, but we had found that expression from *pMET3-WOR2* can at least partially complement the white-opaque switching defect seen in *wor2Δ/wor2Δ* cells (not shown, [1]).

Collaborations with Hana El-Samad and members of her lab at UCSF, working on mathematical modeling of the white-opaque switch, suggested an alternative explanation. If *EFG1* repressed *WOR1* directly, and not solely through *WOR2*, then we would not

predict that ectopically expressing *WOR2* would drive cells to the opaque state. I tested this possibility by inducing expression of *WOR2* in an *efg1Δ/efg1Δ (Δα1Δα2)* mutant. Indeed, we found that ectopically expressing *WOR2* could drive a cells to the opaque state, but only if the strains lacked *EFG1*. This result defines a genetic relationship where *EFG1* blocks white-opaque switching by repressing *WOR1*, separate from of *EFG1*'s repression of *WOR2*.

RESULTS

***WOR2* can drive opaque formation in *efg1Δ/efg1Δ* cells**

In an effort to understand why ectopic expression of *WOR2* would not drive opaque formation in a cells, we introduced the *pMET3-WOR2* ectopic expression construct into *efg1Δ/efg1Δ (α1Δα2Δ)* cells. Though *efgΔ/efg1Δ (α1Δα2Δ)* mutants are known to switch to the opaque state at high frequency, these colonies usually appear mostly white with many opaque sectors. In previous experiments using *WOR1* to drive cells to the opaque state, we observed the entire population of cells switching to the opaque state *en masse*, yielding fully opaque colonies in plate-based switching assays. For this reason, we felt that if *WOR2* could drive cells to the opaque state, we would be able to detect a change in switching behavior despite the high levels of opaque formation observed in *efg1Δ/efg1Δ* mutants.

Results from white-opaque switching assays performed with *efg1Δ/efg1Δ* strains, containing either an empty control vector or the *pMET3-WOR2* are shown in Figure 2. A control strain, and three strains containing the *pMET3-WOR2* construct were generated

from each of two independent *efg1Δ/efg1Δ* mutants. When these cells were kept on repressing media (SD+Met+Cys), all but one of the strains generated mostly white colonies with opaque sectors. When these same cells were plated onto inducing media (SD-Met-Cys), the populations containing the *pMET3-WOR2* construct switched to the opaque state, generating fully opaque colonies. These data were gathered in a single experiment. Previous experiments using different *efg1Δ/efg1Δ pMET3-WOR2* strains (though generated from the same *efg1Δ/efg1Δ* parents used here) gave similar results, but the data is not shown because two of the isolates gave discordant results.

The morphology of the *efg1Δ/efg1Δ* opaque generated by ectopically expressing *WOR2* is consistent with the morphology of fully opaque *efg1Δ/efg1Δ* mutants, though they appear somewhat smaller and fuzzier than wild-type opaque colonies. As shown in Figure 3, the colonies appear to have a fuzzy light-colored center, surrounded by a more darker-colored ring of cells around the periphery of the colony which expands as the colony grows. For the purposes of this assay, these colonies were considered to be fully opaque, since the fuzzy appearance is distinctly different than the shiny, smooth white colonies seen in *efg1Δ/efg1Δ* mutants. However, the white-colored fuzzy center of these colonies should be reexamined to accurately determine the component cells' white- or opaque-status. I planned to perform quantitative RT-PCR on the strains used in this assay, and I pelleted cells with the intention of isolating RNA. Examination of *WOR1* levels in these strains could confirm whether these strains are in the white or opaque state.

DISCUSSION

These data show that *WOR2*, when ectopically expressed, can drive opaque formation in a cells that lack Efg1. This suggests that Wor2 is able to drive opaque expression in switching strains, but only if Efg1's repression of *WOR1* is removed. Figure 4 represents an updated model, including the newly described repression of Wor1 by Efg1. The activity of the network in different cell types is shown in Figure 5.

Though we can be confident in this result because of the number of independent isolates examined, the argument can be strengthened with repeated switching assays. Also, the state of the opaque colonies formed in the *efg1Δ/efgΔ pMET3-WOR2* strains should be verified by RT-qPCR. The cellular morphology of these strains can also be examined more carefully, but this might have limited value because *efg1Δ/efg1Δ* white cells tend to be more elongated than wild type white cells, and the fuzzy appearance of the colonies could be due to filamentation. Both the inherent elongation of *efg1Δ/efg1Δ* strains, and possible filamentation will obscure the cell shape differences usually seen when comparing white and opaque cells.

To further test this model, it is critical that future experiments examine white-opaque switching in an *efg1Δ/efg1Δ wor1Δ/wor1Δ* double mutant. The current model would predict that this strain would be locked in the white phase. I attempted to clone a double mutant that would be isogenic with the other strains used in this study. I tried to delete the *WOR1* alleles in the *efg1Δ/efg1Δ (α1Δα2Δ)* strains (MMY664 and 666) using a modified Ura-blaster method. However, neither the transformation nor the

counterselection on 5-fluororotic acid (5-FOA) to recycle the URA3 marker worked robustly. I did not obtain any *efg1Δ/efg1Δ wor1Δ/wor1Δ* mutants.

Future research can focus on clarifying some characteristics that are not currently represented well in the model, such as the distinction between a gene's role in initiation and maintenance of the opaque state. For instance, *CZF1* was shown to be required to get wild-type levels of white-to-opaque switching, as evidenced by the fact that *czf1Δ/czf1Δ* mutants rarely form opaque colonies. Yet the opaque colonies that arise are heritable, and give rise to white colonies at rates comparable to those seen in wild-type cells. Additionally, Aaron Hernday has invested a tremendous amount of effort in chromatin immunoprecipitation assays, analyzing Czf1, Wor2, and Efg1 binding across the *Candida* genome. This unpublished work does not change or eliminate any of the relationships shown in Figure 1 or 4, but adds many more feedback loops indicating that these transcription factors might be directly regulating themselves and each other.

MATERIALS AND METHODS

Media

For ectopic expression experiments, cells were grown on inducing media (SCD–Met–Cys) or repressing media (SCD+Met+Cys) to control expression of the *MET3* promoter. Previous ectopic expression assays also supplemented uridine to the media [1,2,3]. Uridine was omitted in the experiments described here to ensure that all strains maintained the *pMET3* constructs integrated into their genome.

Strain construction

Both the parental *efg1Δ/efg1Δ (α1Δα2Δ)* strains MMY664 and MMY666, as well as the ectopic expression plasmids have been described before [1]. MMY664 and MMY666 are two independent *efg1Δ/efg1Δ (α1Δα2Δ)* Ura⁻ mutants, generated by Matt Miller. The plasmids pCaEXP (control) or pAJ2230 (*pMET3-WOR2*) were linearized and transformed into the MMY664 and MMY666. Frozen stocks were made from multiple isolates.

White-opaque switching assays with ectopic expression constructs.

White-opaque switching assays were performed as described before, with slight modifications [2]. The primary difference is the use of SD+Met+Cys and SD-Met-Cys (no uridine supplemented) as the “repressing” and “inducing” media. In short, strains are streaked from frozen stock onto repressing media (SD+Met+Cys) and grown at RT for 5 days. At least 5 mostly white (as much as possible in an *efg1Δ/efg1Δ* strain) were replated onto inducing (or repressing, as a control) media and grown at RT for one week. At that time, colonies phenotypes were recorded.

LITERATURE CITED

1. Zordan RE, Miller MG, Galgoczy DJ, Tuch BB, Johnson AD (2007) Interlocking transcriptional feedback loops control white-opaque switching in *Candida albicans*. *PLoS Biol* 5: e256.
2. Zordan RE, Galgoczy DJ, Johnson AD (2006) Epigenetic properties of white-opaque switching in *Candida albicans* are based on a self-sustaining transcriptional feedback loop. *Proc Natl Acad Sci U S A* 103: 12807-12812.
3. Care RS, Trevethick J, Binley KM, Sudbery PE (1999) The MET3 promoter: a new tool for *Candida albicans* molecular genetics. *Mol Microbiol* 34: 792-798.

Figure 1.

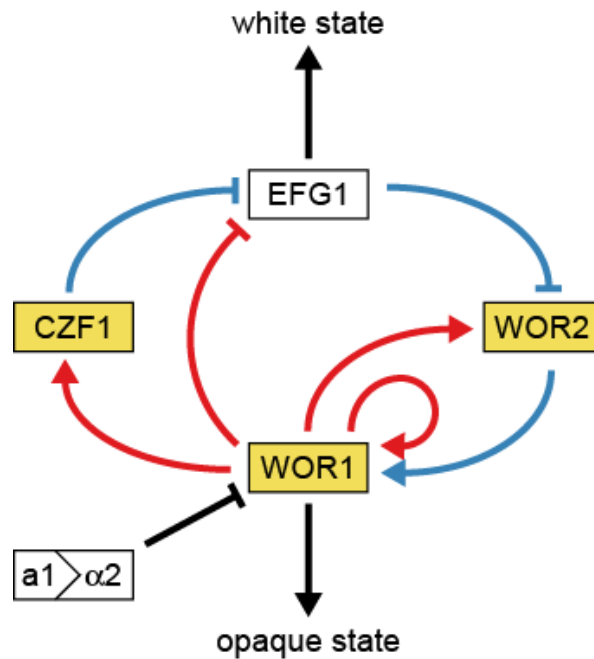


Figure 1. Model of the Genetic Network Regulating the White-Opaque Switch

White and gold boxes represent genes enriched in the white and opaque states, respectively. Blue lines represent relationships based on genetic epistasis. Red lines represent Wor1 control of each gene, based on Wor1 enrichment in chromatin immunoprecipitation experiments. Activation (arrowhead) and repression (bar) are inferred based on white- and opaque-state expression of each gene. Originally published in [1].

Figure 2.

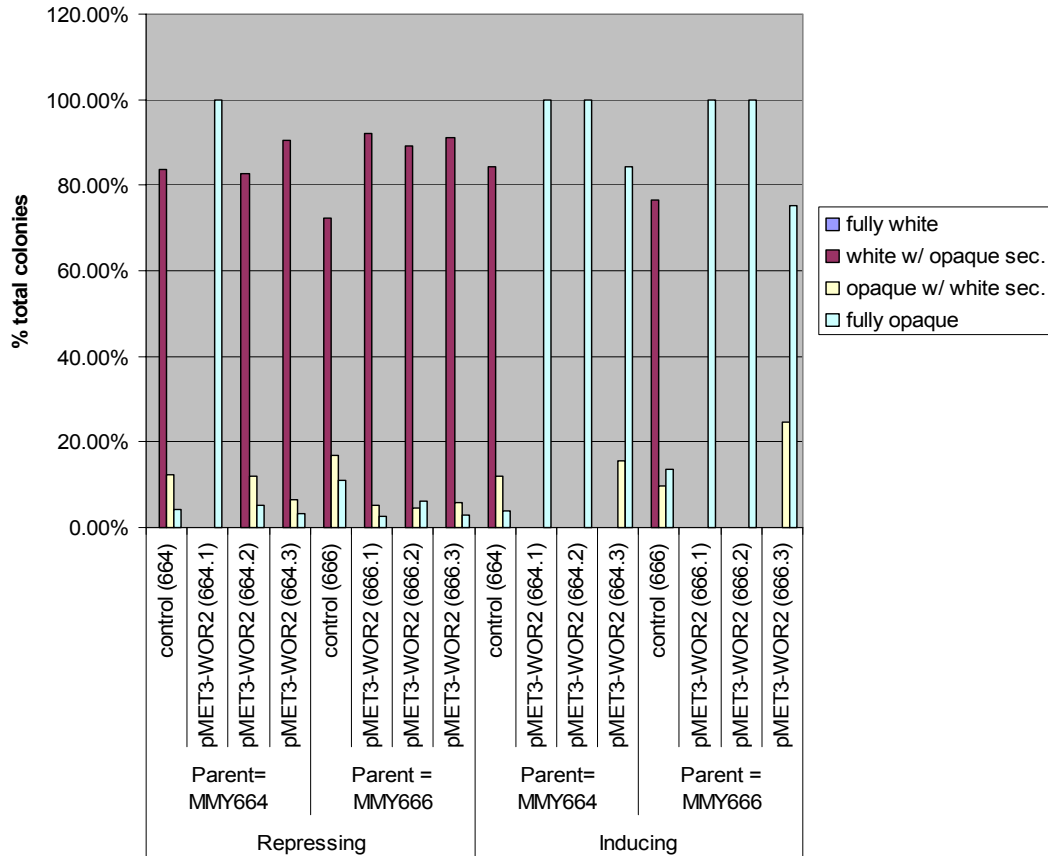


Figure 2. White-to-opaque switching assays with *WOR2* ectopic expression in *efg1Δ/efg1Δ* switching strains

Independent *efg1Δ/efg1Δ* ($\Delta\alpha1\Delta\alpha2$) mutants (MMY664 or 666) were transformed with a control vector (control) or the *pMET3-WOR2* ectopic expression construct. Multiple isolates of the *pMET3-WOR2* derived from each parental *efg1Δ/efg1Δ* strain were tested. Strains were streaked from frozen stock onto repressing media (SD+Met+Cys) and grown at RT for 5 days. The strains were then replated onto either repressing or inducing (SD-Met-Cys) media and grown at RT for one week. Colonies were classified as either fully white, white with opaque sectors, opaque with white sectors, or fully opaque. Data is shown as a percentage of the total colonies counted for each strain.

Figure 3.

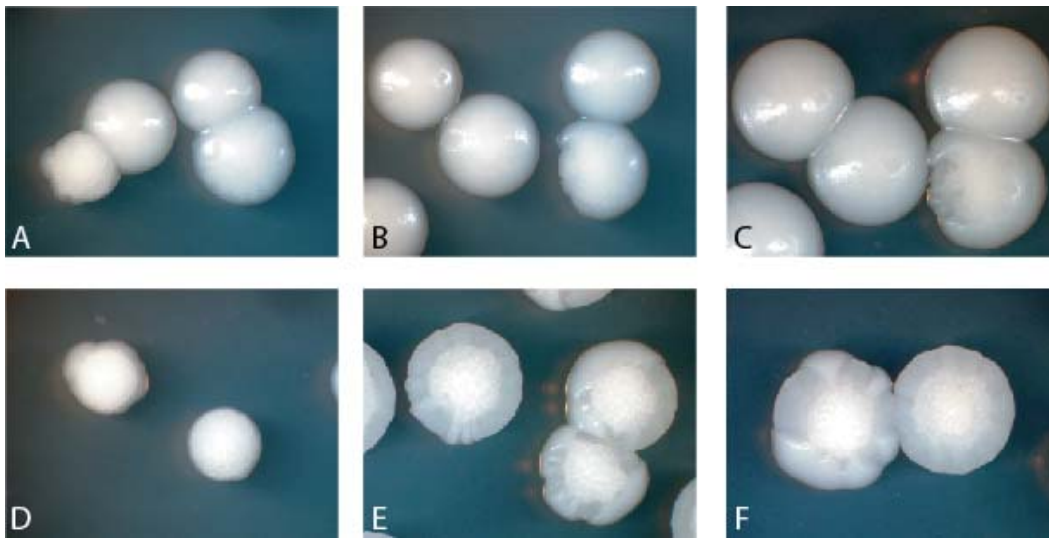


Figure 3. Colony morphology in white-opaque switching assays with *efg1Δ/efg1Δ* strains

A white-opaque switching assay was performed with *efg1Δ/efg1Δ* ($\alpha1\Delta\alpha2\Delta$) strains containing either control or *pMET3-WOR2* constructs. Pictures were taken on both repressing and inducing media after 7 and 12 days of growth at RT. Representative pictures are shown. *Panel A*: Strain 664c (*efg1Δ/efg1Δ* + control), inducing media, 7 days. *Panel B*: Strain 664.1 (*efg1Δ/efg1Δ* + *pMET3-WOR2*), repressing media, 7 days. *Panel C*: Strain 664.3 (*efg1Δ/efg1Δ* + *pMET3-WOR2*), repressing media, 12 days. *Panel D*: Strain 664.3 (*efg1Δ/efg1Δ* + *pMET3-WOR2*), inducing media, 7 days. *Panel E*: Strain 664.3 (*efg1Δ/efg1Δ* + *pMET3-WOR2*), inducing media, 12 days. *Panel F*: Strain 666.3 (*efg1Δ/efg1Δ* + *pMET3-WOR2*), inducing media, 12 days.

Figure 4.

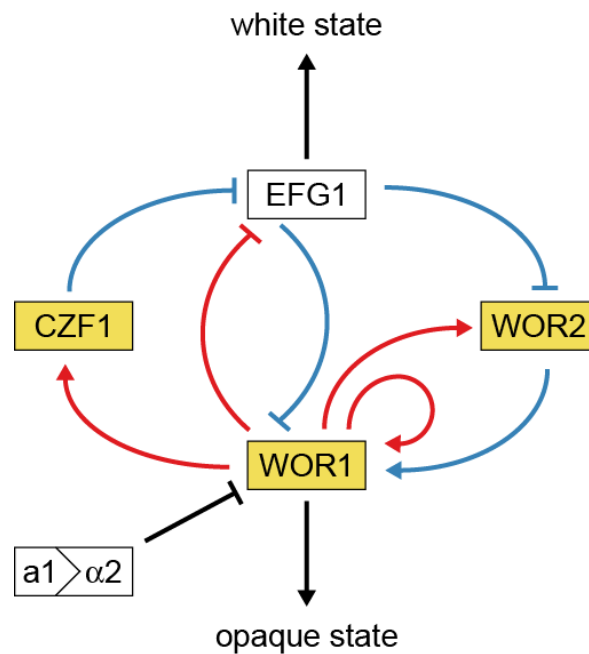


Figure 4. Updated model of the genetic network regulating white-opaque switching

White and gold boxes represent genes enriched in the white and opaque states, respectively. Blue lines represent relationships based on genetic epistasis. Red lines represent Wor1 control of each gene, based on Wor1 enrichment in chromatin immunoprecipitation experiments. Activation (arrowhead) and repression (bar) are inferred based on white- and opaque-state expression of each gene.

Figure 5.

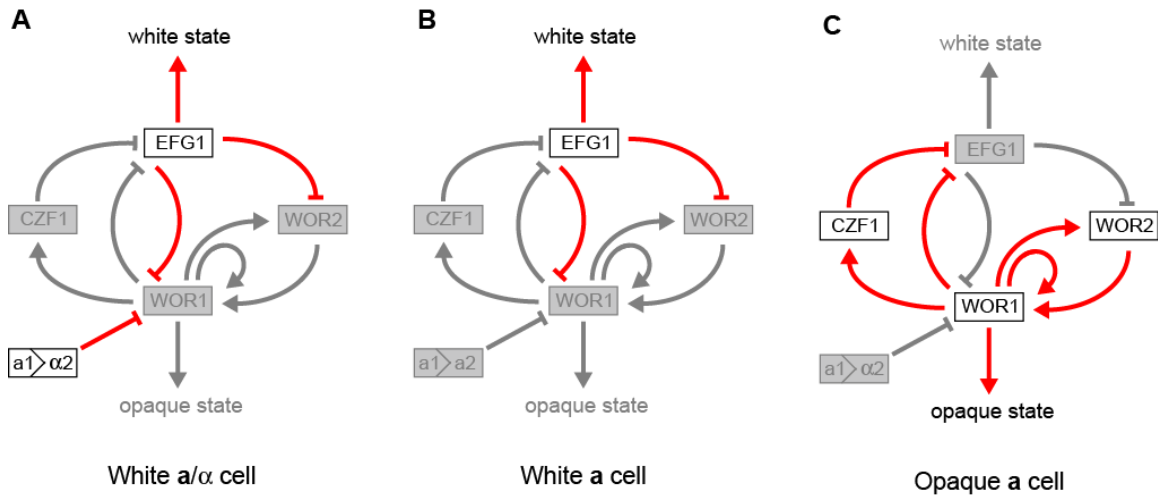


Figure 5. Activity of the white-opaque genetic regulatory network in different cell types

Adapted from [1]. In each scenario, genes indicated by white boxes are up-regulated and genes in gray boxes are down-regulated. Red lines represent active regulatory relationships; gray lines represent relationships that are inactive, due to the down-regulation of the effector gene. (A) In white *a/α* cells, the *a1-α2* heterodimer represses *WOR1*, keeping the *Wor1*-mediated feedback loops inactive. This allows *EFG1* expression and formation of white cells. (B) In white *a* cells, *EFG1* expression contributes to the formation of white cells and down-regulates *WOR2*. This helps keep *Wor1* expression low in white cells, even though the *a1-α2* repression of *WOR1* has been lifted. (C) In opaque *a* cells, *WOR1* expression levels are up-regulated, which in turn activates the represented positive feedback loops, the net effect being increased *CZF1*, *WOR2*, and *WOR1* expression, and decreased *EFG1* expression.

Appendix 2

Strategy for Cloning and Purifying

Wor1 and Wor2

WOR1 is a master regulator of white-opaque switching. It is both necessary and sufficient for opaque formation in *C. albicans*. *wor1* Δ /*wor1* Δ strains are locked in the white phase, and ectopic expression of *WOR1* drives cells to the opaque phase.

Homologs of *WOR1* are found throughout the fungal kingdom, and are identified using BLAST primarily through a region of ~90 amino acids of homology found near the N-terminus of each of these proteins. There is a second region of homology, though this is somewhat less conserved. The total length of each homologous protein varies widely, and there is little conservation throughout the C-terminal portions of the proteins.

Wor1's central role in regulating the white-opaque switch hinted at the possibility that it might be a sequence-specific DNA binding protein, functioning as a transcription factor to regulate large transcriptional changes during white-opaque switching.

Chromatin immunoprecipitation experiments found that Wor1 protein is enriched at a number of intergenic regions throughout the genome, including its own promoter.

However, no functional domains were identified in Wor1 using online protein motif or structure prediction programs, such as Eukaryotic Linear Motif (ELM,

<http://elm.eu.org/about.html>), Protein Homology/Analogy Recognition Engine (Phyre,

<http://www.sbg.bio.ic.ac.uk/phyre/html/index.html>), or PSIPRED's GenThreader

(<http://bioinf.cs.ucl.ac.uk/psipred/>). If Wor1 proves to associate with DNA in a

sequence-specific manner, it would represent a new DNA-binding fold and a new family of fungal transcriptional regulators.

Despite repeated attempts, we have been unable to identify a consensus DNA sequence at sites where Wor1 is bound using the MEME algorithm or other software tools. The difficulty in identifying a DNA sequence that correlates with Wor1 binding could be

a function of the fact that Wor1 is often enriched spread across very large regions of DNA (up to 8kb). Alternatively, the lack of a consensus DNA binding site could be an indication that Wor1 is not, in fact, a sequence-specific DNA binding protein. Instead, Wor1 might associate with DNA upstream of target genes indirectly through contact with Czf1, Efg1, or Wor2. These three factors each have confirmed or predicted sequence-specific DNA binding domains, and genetically interact with Wor1 to control white-opaque switching. Based on chromatin immunoprecipitation experiments performed by David Galgoczy and Aaron Hernday, it appears at least one of these other regulators (Czf1, Efg1, or Wor2) are found at the vast majority of sites bound by Wor1.

To test if Wor1 can bind DNA directly, we plan to express and purify Wor1 from *E. coli* cells, and then use this purified Wor1 in electrophoretic mobility shift assays (EMSAs), though there are some technical hurdles with this approach. In *Candida spp.*, CUG encodes a serine, instead of the standard leucine. Thus, all CUG codons in the *WOR1* gene needed to be changed to code for serine for expression in *E. coli*. Additionally, a mixture of DNA fragments from the *WOR1* promoter will be used as target DNA for the initial EMSA assays since no consensus DNA site has been defined for Wor1 binding.

Cloning full-length and truncated Wor1 alleles

The CUG codons in *WOR1* were changed by Bentley Lim. In short, he designed primers to amplify the *WOR1* coding sequence in fragments, positioning sets of primers over the CUG codon he desired to mutate (Table 1). Note that Bentley amplified *WOR1* from the plasmid pRZ25, which contains a silent point mutation that uses a more common codon, so this was not a concern. To change the six CUG codons in *WOR1*, Bentley amplified seven fragments and then pieced them together by fusion PCR. The resulting PCR product was cloned.

This codon-changed *WOR1* allele was then PCR amplified using Platinum Pfx to add desired restriction sites at each end of the coding region. The full length *WOR1* was cloned (785aa). Two truncated versions of *WOR1* were also cloned. The shortest truncation, Wor1 (1-101aa) contains the first predicted globular domain in the protein, which includes the region of homology amongst the *WOR1* family members. The other truncated allele, Wor1 (1-321aa) includes both predicted globular domains in the protein and eliminates the unstructured region at the C-terminus of the protein.

The shorthand in my notebook and strain notation designates the full-length Wor1 as construct “A”, the Wor1 (1-321aa) truncation as construct “B”, and the Wor1 (1-101aa) truncation as construct “C”. The constructs are also given number designations (1-4), to indicate the restriction sites introduced, and whether there is a STOP codon at the 3’ end of the gene fragment. See Table 2 and Figure 1 for further clarification.

I planned to subclone cloned each *WOR1* allele into two different plasmid backbones for expression in *E. coli*. The first backbone would create a maltose binding

protein (MBP) fusion to the N-terminus of the Wor1 protein. After purification of the fusion protein, the MBP can be cleaved from Wor1 using PreScission protease, leaving a short sequence of amino acids (GPGPSHMAS) at the N-terminus of Wor1. The plasmid pRZ75, containing MBP and a PreScission protease site upstream of a multiple cloning site, was generated from plasmid BHM1092, a generous gift from the Madhani lab. To facilitate cloning into the MBP-fusion expression backbone (pRZ75), I introduced a NheI restriction site at the 5' end of the allele and a XhoI site at the 3' end of the allele during the PCR amplification. These constructs were PCR amplified, cloned into the pCR-BluntII backbone and sequenced (Table 3). When possible, two pCR-BluntII clones of each allele were saved, with the desired construct in each orientation in case subsequent cloning was affected by the gene's orientation with respect to the backbone (Table 3). In my experience, minipreps of plasmids with the pCR-BluntII backbone yielded low amounts of DNA once the cells had been frozen. I compensated by growing 10 mls of culture, monitoring carefully to ensure the overnight cultures did not overgrow, and preparing this on a single Qiagen miniprep column. The Wor1 (1-321aa) and Wor1 (1-101aa) constructs were successfully subcloned into the pRZ75 backbone (Table 4) and transformed into XL1 Blue *E. coli* cells.

The second backbone used for expression was a gift from Aaron Hernday, derived from his work at David Low's lab at UC Santa Barbara. This plasmid puts an N-terminal GST tag on Wor1, which can be cleaved from the GST tag using thrombin. The plasmid pRZ86 corresponds to Aaron's plasmid pDAL649, which has another gene cloned into the GST-fusion backbone. This plasmid was digested SacII with XbaI to remove the

undesired gene and the backbone (containing GST and a thrombin cut site) was gel purified.

To clone the panel of Wor1 alleles into the GST backbone, I introduced a SacII restriction site at the 5' end and an XbaI site at the 3' end of the each Wor1 allele via PCR (Table 1). These constructs were initially cloned into pCR-BluntII backbone and sequenced (Table 3). They were then subcloned into the SacII/XbaI-digested GST backbone (Table 4). However, I made an error designing these primers, and SacII/XbaI digest does not insert the *WOR1* alleles in frame with the GST encoded on the plasmid. To remedy this situation, I cleaved the GST-Wor1 (out of frame) plasmids with SacII to linearize the plasmid and treated them with Klenow exonuclease to remove a two-base overhang created by the SacII digest. These were then re-ligated and resequenced to ensure that the Klenow digest had not removed more than the desired bases. Both the out-of-frame GST-Wor1 fusion plasmids and the Klenow-treated (in-frame) GST-Wor1 plasmids are listed in Table 4. The GST-Wor1 fusion plasmids were transformed into XL1 blue *E. coli* for the initial cloning steps. Once sequence was verified, the correct in-frame plasmids were transformed into BL21(DE3) *E. coli* strains that contain the plasmid pPY1025, containing the *lacI^f* gene to prevent leaky expression from the hybrid *ara-lac* promoter on the GST backbone. After purification, thrombin cleavage will leave the residues GlyArg on the N-terminus of the Wor1 constructs.

Cloning Wor2 for expression in *E. coli*.

While primarily interesting in the ability of Wor1 to bind DNA, I also cloned Wor2 in parallel in so that EMSAs could also be performed to characterize Wor2's DNA binding properties.

I changed the single CUG codon in the full-length *WOR2* using primers designed by Bentley Lim (Table 1). This full length *WOR2* was then PCR amplified to add the desired restriction sites at each end of the coding region. Full length *WOR2* was cloned (446aa), as well as two truncations corresponding to the predicted globular domain (231-343aa) and the predicted ZnII Cys6 cluster (299-343aa) located within the globular domain (Figure 2). These alleles were created by PCR amplification with Platinum Pfx, cloned into the pCR-BluntII backbone, transformed, and sequenced (Table 5). Wor2 clones flanked by NheI and XhoI restriction sites were subcloned into the MBP backbone and transformed into XL1 Blue *E. coli* cells (Table 6). Wor2 clones flanked by SacII and XbaI restriction sites were cloned into the GST backbone and Klenow-treated, as described for Wor1 cloning (Table 6).

Inducing expression of GST-Wor1 (full length)

I attempted to induce expression of GST-*WOR1* (full length) from strain bRZ105. A 3ml culture of LB+Kanamycin(50µg/ml)+Spectinomycin (50µg/ml) was inoculated and grown at 37°C overnight. The overnight culture was diluted 1:50 into 50mls of preheated (to 30°C) LB+Kan(50µg/ml)+Spec(50µg/ml). The 50ml cultures was grown at

30°C for 4 hours, at which point a number of 1.5-ml aliquots of the culture were taken to serve as the “0 hour” time point before induction. IPTG (1mM final concentration) and arabinose (0.2% final concentration) were added to induce expression of GST-Wor1 and the culture was grown at 30°C. Multiple 1.5 ml aliquots were taken at the 1 hour, 2 hour, and 4 hour time points. The cells in each aliquot were pelleted by centrifugation, frozen in liquid nitrogen and stored at -80°C.

I prepared whole cell lysates from one aliquot at each time point. Cell pellets were resuspended in 1x sample buffer and boiled for 5 minutes, and run on a SDS-PAGE gel. Coomassie staining of the gel did not reveal any obvious induction of GST-Wor1 (full) protein expression. Using the same cell lysates, I ran another SDS-PAGE gel and performed a Western Blot using the α -Wor1₇₇₁ peptide antibody, which has been used successfully in Western blots previously. No obvious induction of Wor1 was observed on the Western Blot (not shown), though there was significant cross-hybridization with other proteins in the *E. coli* lysate.

In future attempts to express Wor1, it will be worth optimizing the amounts of arabinose and IPTG used to induce expression. More precautions can be taken to avoid formation of inclusion bodies, on the chance that Wor1 was successfully expressed but was not soluble. Also, a α -GST antibody may more specifically detect the fusion protein in Western blots.

Table 1.

Primer name	Sequence (5' →3')	Description
CUG codon change of Wor1		
wor1.1 Clal	CGGatcgatATGTCTAATTC AAGTATAGTCCCTACATATAATGGG	Wor1 5' for (Clal)
wor1.2 for	GTTTATTGAACAATCTTCGGGAATC	Wor1 CUG#1 for
wor1.2 rev	GATTCCCGAAGATTGTTCAATAAAC	Wor1 CUG#1 rev
wor1.3 for	CAGCTGCTATATCACAAAACGGATTAG	Wor1 CUG#2 for
wor1.3 rev	CTAATCCGTTTTGTGATATAGCAGCTG	Wor1 CUG#2 rev
wor1.4 for	GTTTCTCAACTATCCTATATGTTGCCACCTC	Wor1 CUG#3 for
wor1.4 rev	GAGGTGGCAACATATAGGATAGTTGAGAAAC	Wor1 CUG#3 rev
wor1.5 for	CAATTAATCACTCGCATACTTCATCATATG	Wor1 CUG#4 for
wor1.5 rev	CATATGATGAAGTATGCGAGTGATTAATTG	Wor1 CUG#4 rev
wor1.6 for	GCATCAATACATCTTCCCAACAACAAC	Wor1 CUG#5 for
wor1.6 rev	GTTGTTGTTGGGAAGATGTTGATGC	Wor1 CUG#5 rev
wor1.7 for	CAACAACATCAATCCCAGCAGCAAGTG	Wor1 CUG#6 for
wor1.7 rev	CACTTGCTGCTGGGATTGATGTTGTTG	Wor1 CUG#6 rev
wor1.8 Xho1	CGGctcgagCTAAGTACCGGTGTAATACGACCCAGAAG	Wor1 3' rev (Xho1)
Cloning Wor1		
RZO 373	GgctagcATGTCTAATTC AAGTATAGTCCCTAC	Wor1 full 5' NheI
RZO 374	GctcgagAGTACCGGTGTAATACGACCCAG	Wor1 full 3' XhoI
RZO 375	GctcgagTTAAGTACCGGTGTAATACGACCCAG	Wor1 full 3' XhoI stop
RZO 376	GctcgagACTTCCTGCAACTGAAGAAGAATG	Wor1 (1-321) 3' XhoI
RZO 377	GctcgagTTAACTTCCTGCAACTGAAGAAGAATG	Wor1 (1-321) stop 3' XhoI
RZO 378	GctcgagCTTTTTCTTCTTCTTGTCTTTATCAATTAG	Wor1 (1-101) 3' Xho1
RZO 379	GctcgagTTACTTTTTCTTCTTCTTGTCTTTATCAATTAG	Wor1 (1-101) stop 3' XhoI
RZO 388	AATTAtctagaAGTACCGGTGTAATACGACCCAG	Wor1 full 3' XbaI
RZO 389	AATTAtctagaTTAAGTACCGGTGTAATACGACCCAG	Wor1 full 3' XbaI stop
RZO 390	AATTAtctagaACTTCCTGCAACTGAAGAAGAATG	Wor1 (1-321) 3' XbaI
RZO 391	AATTAtctagaTTAACTTCCTGCAACTGAAGAAGAATG	Wor1 (1-321) stop 3' XbaI
RZO 392	AATTAtctagaCTTTTTCTTCTTCTTGTCTTTATCAATTAG	Wor1 (1-101) 3' Xba1
RZO 393	AATTAtctagaTTACTTTTTCTTCTTGTCTTTATCAATTAG	Wor1 (1-101) stop 3' XbaI
CUG codon change of Wor2		
zcf33.1	CCGatcgatATGACACAATTACCTTCTGTTTCAGAAATTGATCAAC	WOR2 5' for (Clal)
zcf33.2 for	CTTGGGTATCAAGATTTATCCAAATTACCACCAAGG	WOR2 CUG for
zcf33.2 rev	CCTTGGTGGAATTTGGATAAATCTTGATACCCAAG	WOR2 CUG rev
zcf33.3 rev	CCGctcgagTTATTTAAGTAAATCAGCCACTGAAACTCTATTAATTACAG	WOR2 3' rev (Xho1)
Cloning Wor2		
RZO 380	GgctagcATGACACAATTACCTTCTGTTTC	Wor2 full 5' NheI
RZO 381	GgctagcCAGCAAGCACCAATTCATCTTGCC	Wor2 (231-343) 5' NheI
RZO 382	GgctagcCGTCGTACAAGAAGCTGGCTG	Wor2 (299-343) 5' NheI
RZO 383	GctcgagTGGTGGTAATTTGGATAAATCTTGATACCC	Wor2 (-343) 3' XhoI
RZO 384	GctcgagTTATGGTGGTAATTTGGATAAATCTTGATACCC	Wor2 (-343) stop 3' XhoI
RZO 385	GctcgagTTTAAGTAAATCAGCCACTGAAACTC	Wor2 full 3' XhoI
RZO 386	GctcgagTTATTTAAGTAAATCAGCCACTGAAACTC	Wor2 full 3' stop XhoI
RZO 387	ATAATCTTGTccgaggATGTCTAATTC AAGTATAGTCCCTAC	Wor1 full 5' SacII
RZO 394	ATAATCTTGTccgaggATGACACAATTACCTTCTGTTTC	Wor2 full 5' SacII
RZO 395	ATAATCTTGTccgaggCAGCAAGCACCAATTCATCTTGCC	Wor2 (231-343) 5' SacII
RZO 396	ATAATCTTGTccgaggCGTCGTACAAGAAGCTGGCTG	Wor2 (299-343) 5' SacII
RZO 397	AATTAtctagaTGGTGGTAATTTGGATAAATCTTGATACCC	Wor2 (-343) 3' XbaI
RZO 398	AATTAtctagaTTATGGTGGTAATTTGGATAAATCTTGATACCC	Wor2 (-343) stop 3' XbaI
RZO 399	AATTAtctagaTTTAAGTAAATCAGCCACTGAAACTC	Wor2 full 3' XbaI
RZO 400	AATTAtctagaTTATTTAAGTAAATCAGCCACTGAAACTC	Wor2 full 3' stop XbaI

Table 1. Primers used in this study

DNA primers for PCR are listed above. Restriction sites introduced into primers are indicated in lower case.

Table 2.

Code	Protein fragment	Restriction site		STOP codon?	5' primer	3' primer	
		5'	3'				
Wor1	A1	1-785aa (full)	NheI	XhoI	No	RZO373	RZO374
	A2	1-785aa (full)	NheI	XhoI	Yes	RZO373	RZO375
	A3	1-785aa (full)	SacII	XbaI	No	RZO387	RZO388
	A4	1-785aa (full)	SacII	XbaI	Yes	RZO387	RZO389
	B1	1-321aa	NheI	XhoI	No	RZO373	RZO376
	B2	1-321aa	NheI	XhoI	Yes	RZO373	RZO377
	B3	1-321aa	SacII	XbaI	No	RZO387	RZO390
	B4	1-321aa	SacII	XbaI	Yes	RZO387	RZO391
	C1	1-101aa	NheI	XhoI	No	RZO373	RZO378
	C2	1-101aa	NheI	XhoI	Yes	RZO373	RZO379
	C3	1-101aa	SacII	XbaI	No	RZO387	RZO392
	C4	1-101aa	SacII	XbaI	Yes	RZO387	RZO393
Wor2	A1	1-446aa (full)	NheI	XhoI	No	RZO380	RZO385
	A2	1-446aa (full)	NheI	XhoI	Yes	RZO380	RZO386
	A3	1-446aa (full)	SacII	XbaI	No	RZO394	RZO399
	A4	1-446aa (full)	SacII	XbaI	Yes	RZO394	RZO400
	B1	231-343aa	NheI	XhoI	No	RZO381	RZO383
	B2	231-343aa	NheI	XhoI	Yes	RZO381	RZO384
	B3	231-343aa	SacII	XbaI	No	RZO395	RZO397
	B4	231-343aa	SacII	XbaI	Yes	RZO395	RZO398
	C1	299-343aa	NheI	XhoI	No	RZO382	RZO383
	C2	299-343aa	NheI	XhoI	Yes	RZO382	RZO384
	C3	299-343aa	SacII	XbaI	No	RZO396	RZO397
	C4	299-343aa	SacII	XbaI	Yes	RZO396	RZO398

Table 2. Explanation of shorthand code used to identify Wor1 and Wor2 expression constructs

A shorthand code is used in my experimental notebook. Letters indicate the particular protein fragment (A, B, or C), and the numbers refer to the restriction sites and the presence of a STOP codon at the end of the allele. 1= NheI/XhoI, no stop codon, 2 = NheI/XhoI, STOP codon, 3 = SacII/XbaI, no stop codon, 4=SacII/XbaI, STOP codon. The primers used to amplify each construct are indicated in the table.

Figure 1.

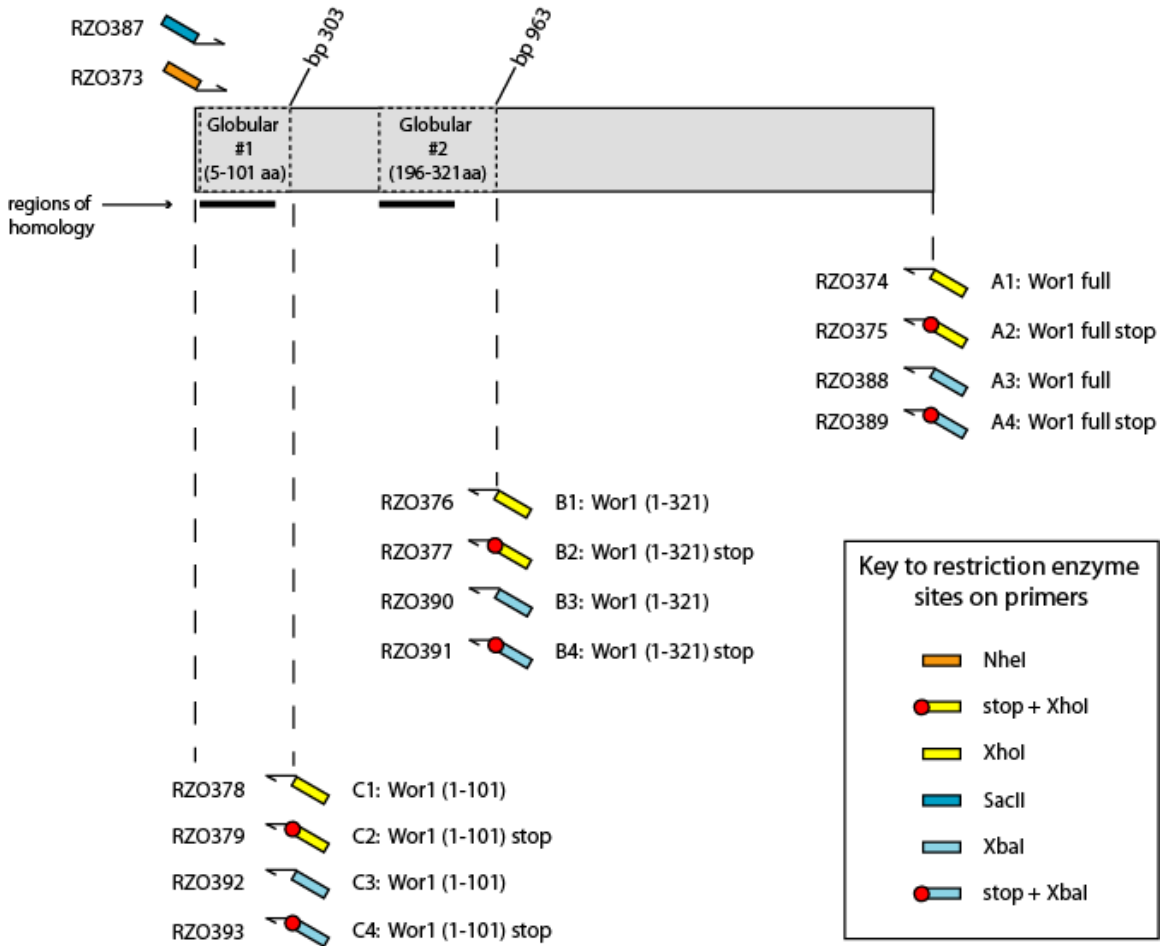


Figure 1. Cloning *WOR1* full-length and truncated alleles for expression in *E. coli*

The gray rectangle represents the full *WOR1* gene, 2355bp, not including the stop codon. Dotted boxes within *WOR1* represent bases that encode the predicted globular domains in the protein. Truncated alleles (constructs B and C) are given coordinates based on the amino acid residues from the full-length protein that will be expressed in the truncated protein. The diagram of the gene and globular domains therein is to scale; the primers are not.

Table 3.

Plasmid	Allele	Description	Orientation	Restriction sites (5'/3')	Mutations	Seq?
pRZ53	A1-5	Wor1 full	forward	NheI/XhoI	none in ORF; 12 bp insert in plasmid backbone	x
pRZ54	B2-1	Wor1 (1-321aa) STOP	reverse	NheI/XhoI	none	x
pRZ55	B2-6	Wor1 (1-321aa) STOP	forward	NheI/XhoI	none	x
pRZ56	C1-1	Wor1 (1-101aa)	reverse	NheI/XhoI	none	x
pRZ57	C1-2	Wor1 (1-101aa)	forward	NheI/XhoI	none	x
pRZ58	C2-1	Wor1 (1-101aa) STOP	reverse	NheI/XhoI	none	x
pRZ59	C2-2	Wor1 (1-101aa) STOP	forward	NheI/XhoI	none	x
pRZ60	A2-4	Wor1 full STOP	forward	NheI/XhoI	none	
pRZ61	A2-7	Wor1 full STOP	reverse	NheI/XhoI	none; gap in seq 1709-1741 in orf	x
pRZ62	A2-10	Wor1 full STOP	reverse	NheI/XhoI	none so far; gap in seq btwn RZO104 and 26 reads	x
pRZ63	B1-1	Wor1 (1-321aa)	forward	NheI/XhoI	none	
pRZ64	B1-4	Wor1 (1-321aa)	reverse	NheI/XhoI	none	x
pRZ65	B1-6	Wor1 (1-321aa)	reverse	NheI/XhoI	silent Q301 to more common codon.	x
pRZ66	A1-2	Wor1 full	forward	NheI/XhoI	none in ORF; 12 bp insert in plasmid backbone	x
pRZ69	B4-1	Wor1 (1-321aa) STOP	reverse	SacII/XbaI	none	x
pRZ70	C4-2	Wor1 (1-101aa) STOP	reverse	SacII/XbaI	none	x
pRZ71	C4-5	Wor1 (1-101aa) STOP	reverse	SacII/XbaI	none in ORF; T insertion in backbone	x
pRZ72	B3-9	Wor1 (1-321aa)	forward	SacII/XbaI	none	x
pRZ73	B3-10	Wor1 (1-321aa)	reverse	SacII/XbaI	none	x
pRZ74	B4-7	Wor1 (1-321aa) STOP	forward	SacII/XbaI	none	x
pRZ76	A3-17	Wor1 full	reverse	SacII/XbaI	none	x
pRZ77	A3-21	Wor1 full	forward	SacII/XbaI	none	x
pRZ78	A4-10	Wor1 full STOP	forward	SacII/XbaI	none	x
pRZ79	A4-14	Wor1 full STOP	reverse	SacII/XbaI	none	X

Table 3. Wor1 constructs in the pCR-BluntII backbone

Wor1 full-length and truncation alleles were PCR amplified from a codon-changed *WOR1* plasmid, using primers indicated in Table 1. The PCR products were TOPO-cloned into Invitrogen's pCR-BluntII backbone and transformed into One Shot cells. Plasmid: Systematic plasmid identification, stored in bacterial strain of the same number (ie, pRZ78 can be miniprep'd from the frozen stock bRZ78). Allele: Shorthand for construct-isolate of each plasmid. Description: Indicates portion of *WOR1* cloned, and whether there is a stop codon at the 3' end. Orientation: forward/reverse with respect to the *lac* promoter in the pCR-BluntII backbone. Restriction sites (5'/3'): indicate the restriction sites introduced at either end of the PCR product. Mutations: any mutations, other than the CUG codon changes intentionally introduced, are listed. Seq: "x" indicates the sequence of the plasmid was verified from the frozen stock. All plasmids were sequenced prior to making the frozen stock.

Table 4.

Bacterial Stock	Description	Out of Frame?	Construct Code	<i>E. coli</i>
bRZ96	MBP-Wor1 (full) stop	N	A2	XL1 Blue
bRZ94	MBP-Wor1 (1-321aa) stop	N	B2	XL1 Blue
bRZ95	MBP-Wor1 (1-101aa) stop	N	C2	XL1 Blue
bRZ88	GST-Wor1 (full) stop	Y	A4	XL1 Blue
bRZ89	GST-Wor1 (1-321aa) stop	Y	B4	XL1 Blue
bRZ90	GST-Wor1 (1-101aa) stop	Y	C4	XL1 Blue
bRZ99	GST-Wor1 (full) stop	N	A4	XL1 Blue
bRZ100	GST-Wor1 (1-321aa) stop	N	B4	XL1 Blue
bRZ101	GST-Wor1 (1-101aa) stop	N	C4	XL1 Blue
bRZ105	GST-Wor1 (full) stop	N	A4	BL21(DE3)*
bRZ106	GST-Wor1 (1-321aa) stop	N	B4	BL21(DE3)*
bRZ107	GST-Wor1 (1-101aa) stop	N	C4	BL21(DE3)*

Table 4. Wor1 constructs in expression backbones

Full and truncated alleles of Wor1 were cloned from the pCR-BluntII backbone into plasmids that would create either MBP or GST N-terminal fusions to Wor1. Note that *WOR1* is out of frame in certain GST-backbones. BL32(DE3)* indicates that the *E. coli* strain BL21(DE3) was also transformed with the plasmid pPY1025 (Spec^R), which contains *lacI^f*.

Figure 2.

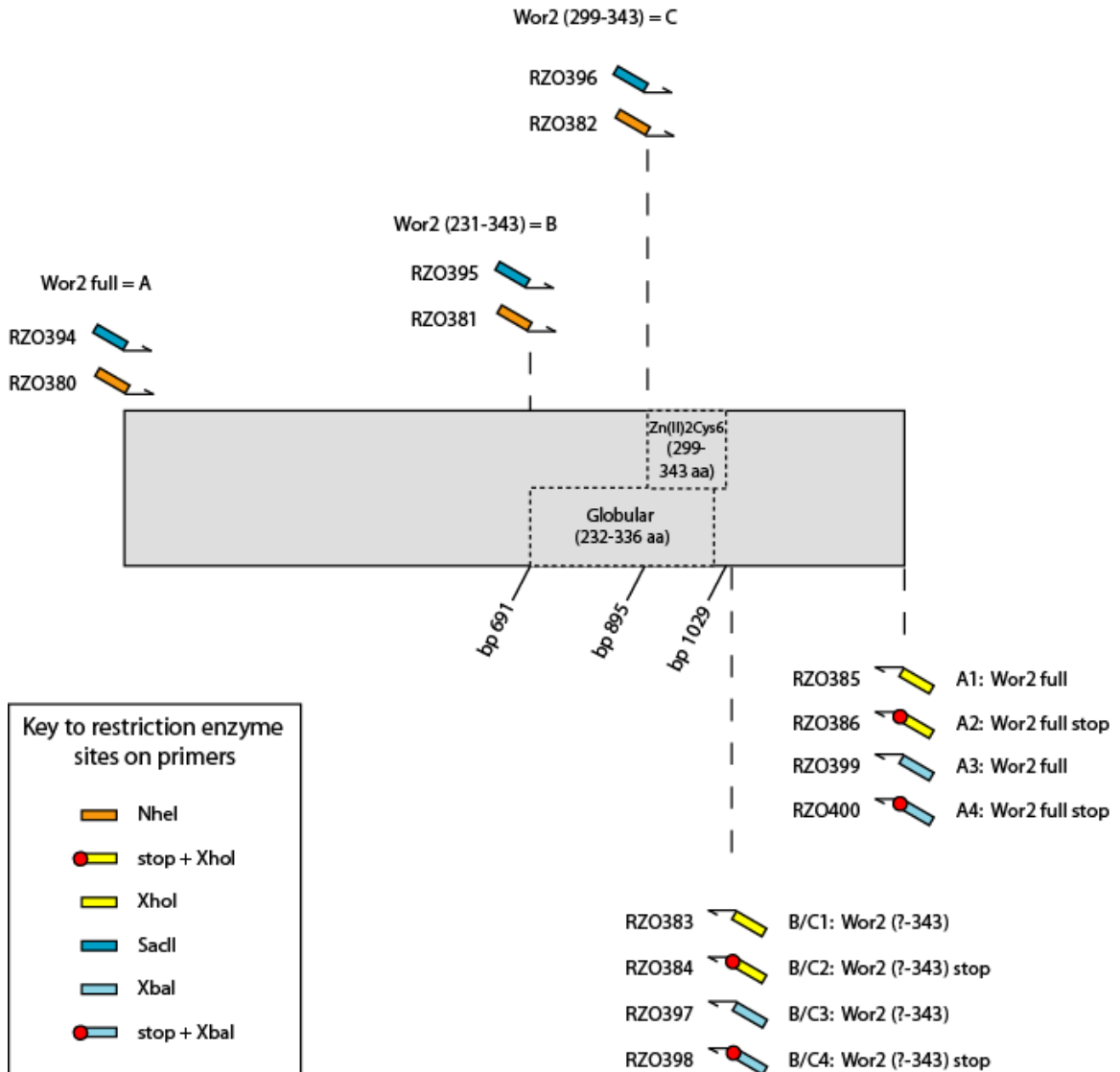


Figure 2. Cloning *WOR2* full-length and truncated alleles for expression in *E. coli*

The gray rectangle represents the full *WOR2* gene, 1338bp, not including the stop codon.

Dotted boxes within *WOR2* represent bases that encode the predicted globular domain and the predicted DNA binding domain (Zn(II)Cys6) in the protein. Truncated alleles

(constructs B and C) are given coordinates based on the amino acid residues from the full-length protein that will be expressed in the truncated protein. The diagram of the gene and domains therein is to scale; the primers are not.

Table 5.

Plasmid	Allele	Description	Orientation	Restriction sites	Mutations	Seq.
pRZ67	A2-8	Wor2 full STOP		NheI/XhoI	none	
pRZ68	A2-9	Wor2 full STOP		NheI/XhoI	none	
pRZ80	B2-1	Wor2 (231-343) STOP	reverse	NheI/XhoI	none	x
pRZ81	B4-2	Wor2 (231-343) STOP	reverse	SacII/XbaI	none	x
pRZ82	B4-3	Wor2 (231-343) STOP	forward	SacII/XbaI	none	x
pRZ83	C2-1	Wor2 (299-343) STOP	reverse	NheI/XhoI	none	x
pRZ84	C4-1	Wor2 (299-343) STOP	forward	SacII/XbaI	none	x
pRZ85	C4-2	Wor2 (299-343) STOP	reverse	SacII/XbaI	none	x

Table 5. Wor2 constructs in the pCR-BluntII backbone

Wor2 full-length and truncation alleles were PCR amplified from a codon-changed *WOR2* plasmid, using primers indicated in Table 1. The PCR products were TOPO-cloned into Invitrogen's pCR-BluntII backbone and transformed into One Shot cells. Plasmid: Systematic plasmid identification, stored in bacterial strain of the same number (ie, pRZ78 can be miniprep'd from the frozen stock bRZ78). Allele: Shorthand for construct-isolate of each plasmid. Description: Indicates portion of *WOR2* cloned, and whether there is a stop codon at the 3' end. Orientation: forward/reverse with respect to the *lac* promoter in the pCR-BluntII backbone. Restriction sites (5'/3'): indicate the restriction sites introduced at either end of the PCR product. Mutations: any mutations, other than the CUG codon changes intentionally introduced, are listed. Seq: "x" indicates the sequence of the plasmid was verified from the frozen stock. All plasmids were sequenced prior to making the frozen stock.

Table 6.

Bacterial Stock	Description	Out of Frame?	Construct Code	<i>E. coli</i>
bRZ96	MBP-Wor2 (full) stop	N	A2	XL1 Blue
bRZ97	MBP-Wor2 (231-343aa) stop	N	B2	XL1 Blue
bRZ98	MBP-Wor2 (299-343aa) stop	N	C2	XL1 Blue
bRZ91	GST-Wor2 (full) stop	Y	A4	XL1 Blue
bRZ92	GST-Wor2 (231-343aa) stop	Y	B4	XL1 Blue
bRZ93	GST-Wor2 (299-343aa) stop	Y	C4	XL1 Blue
bRZ102	GST-Wor2 (full) stop	N	A4	XL1 Blue
bRZ103	GST-Wor2 (231-343aa) stop	N	B4	XL1 Blue
bRZ104	GST-Wor2 (299-343aa) stop	N	C4	XL1 Blue
bRZ108	GST-Wor2 (full) stop	N	A4	BL21(DE3)*
bRZ109	GST-Wor2 (231-343aa) stop	N	B4	BL21(DE3)*
bRZ110	GST-Wor2 (299-343aa) stop	N	C4	BL21(DE3)*

Table 6. Wor2 constructs in expression backbones

Full and truncated alleles of Wor2 were cloned from the pCR-BluntII backbone into plasmids that would create either MBP or GST N-terminal fusions to Wor1. Note that *WOR2* is out of frame in certain GST-backbones. BL32(DE3)* indicates that the *E. coli* strain BL21(DE3) was also transformed with the plasmid pPY1025 (Spec^R), which contains *lacI^q*.

Publishing Agreement

It is the policy of the University to encourage the distribution of all theses and dissertations. Copies of all UCSF theses and dissertations will be routed to the library via the Graduate Division. The library will make all theses and dissertations accessible to the public and will preserve these to the best of their abilities, in perpetuity.

Please sign the following statement:

I hereby grant permission to the Graduate Division of the University of California, San Francisco to release copies of my thesis or dissertation to the Campus Library to provide access and preservation, in whole or in part, in perpetuity.

Rebecca E Jordan Sept. 4, 2008
Author Signature Date